

UCLA

UCLA Electronic Theses and Dissertations

Title

Characterization of Cellular Signaling in Ewing Sarcoma Family of Tumors

Permalink

<https://escholarship.org/uc/item/3xd2j7zj>

Author

Anderson, Jennifer Lynn

Publication Date

2012

Peer reviewed|Thesis/dissertation

UNIVERSITY OF CALIFORNIA

Los Angeles

Characterization of Cellular Signaling in Ewing Sarcoma Family of Tumors

A dissertation submitted in partial satisfaction of the
requirements for the degree Doctor of Philosophy
in Molecular Biology

by

Jennifer Lynn Anderson

2012

ABSTRACT OF THE DISSERTATION

Characterization of Cellular Signaling in Ewing Sarcoma Family of Tumors

by

Jennifer Lynn Anderson

Doctor of Philosophy in Molecular Biology

University of California, Los Angeles, 2012

Professor Christopher Denny, Chair

Aberrant cellular signaling networks lie at the heart of cancer pathogenesis. Whether stimulated by a dominant oncogene or activated receptor tyrosine kinase, these signals affect biological processes such as proliferation and apoptosis. In the Ewing sarcoma family of tumors (EFST), a group of pediatric bone and soft tissue malignancies, EWS/FLI1 transcriptional modulation and insulin-like growth factor 1 (IGF1) signaling are the two main forces that drive tumorigenesis. In order to obtain a comprehensive view of signaling, we applied a mass spectrometry-based phosphoproteomic approach to quantify global changes in phosphorylation after IGF1 stimulation, IGF1 receptor inhibition, and EWS/FLI1 knock down. Our analyses identified hundreds unique phosphopeptides enriched in processes such as regulation of cell cycle and cytoskeleton organization. In particular, examination of tyrosine phosphopeptides downstream of IGF1 identified potential roles for Src family kinases and members of the Eph family of receptor tyrosine kinases in ESFT pathogenesis. Additionally, phosphotyrosine profiling revealed a large up regulation of Stat3 phosphorylation upon EWS/FLI1 knock down. Further investigation revealed this activation occurs through a paracrine mechanism. Overall,

phosphoproteomic profiling has uncovered novel regulators and mechanisms for ESFT signaling, allowing for the development of new therapeutic strategies.

The dissertation of Jennifer Lynn Anderson is approved.

Thomas Graeber

Matteo Pellegrini

Ren Sun

Michael Teitell

Christopher Denny, Committee Chair

University of California, Los Angeles

2012

To Kathy,
for inspiring my journey

and to Daniel,
for motivating me to complete it

TABLE OF CONTENTS

Abstract		ii
Committee Page		iv
Dedication		v
List of Figures		xi
List of Tables		xiii
Acknowledgements		xiv
Vita		xvi
Publications and Presentations		xvii
Chapter 1	INTRODUCTION	1
	Signal transduction	2
	Insulin-like growth factor signaling	4
	Eph-ephrin signaling	6
	JAK/STAT signaling	7
	Stat3	9
	Phosphoproteomics	10
	Workflow	11
	Quantitation	13
	Applications to signal transduction research	14
	Ewing sarcoma family of tumors	15
	References	17
Chapter 2	PEDIATRIC SARCOMAS	22
	Abstract	23
	Introduction	24
	Ewing sarcoma family of tumors	26

	Cell of origin of Ewing sarcoma family of tumors	27
	Molecular genetics	27
	Target genes and targeted therapies	29
	Alveolar rhabdomyosarcoma	31
	Cell of origin of alveolar rhabdomyosarcoma	32
	Molecular genetics	32
	Target genes and targeted therapies	34
	Synovial sarcoma	36
	Cell of origin of synovial sarcoma	36
	Molecular genetics	37
	Target genes and targeted therapies	39
	Dermatofibrosarcoma protuberans	41
	Cell of origin of DFSP	42
	Molecular genetics	42
	Signaling pathways and targeted therapies	44
	Congenital fibrosarcoma	45
	Molecular genetics	45
	Signaling pathways and targeted therapies	46
	Alveolar soft-part sarcoma	48
	Molecular genetics	49
	Target genes and targeted therapies	50
	Conclusions	51
	References	52
Chapter 3	MATERIALS AND METHODS	63
	Cells	64
	Plasmids and viruses	64

	BACs and bacterial strains used for recombineering	64
	Recombineering	65
	Reagents	66
	Quantitative real time PCR	66
	Immunoblot	67
	Phosphotyrosine enrichment	68
	Phosphoserine/threonine enrichment	69
	Mass spectrometry and phosphopeptide quantitation	70
	Growth assays	71
	Immunoprecipitation	72
	Immunofluorescence	72
	Flow cytometry	73
	Conditioned media	73
	Cytokine array	74
	ELISA	74
	IL-6 immunodepletion and gp130 neutralization	74
	References	75
Chapter 4	IGF1 SIGNALING IN EWING SARCOMA FAMILY OF TUMORS	76
	Introduction	77
	Results	78
	ESFT cells respond to IGF1 stimulation	78
	Phosphotyrosine profiling identifies known IGF system components as well as novel regulators of ESFT signaling	80
	Expression of Eph receptors in ESFTs suggests Eph-ephrin signaling may play a role in tumorigenesis	85
	Phosphotyrosine profiling of ESFT cells that vary in sensitivity to AMG-479 treatment identifies potential candidates involved in drug resistance	90

	Discussion	90
	References	96
Chapter 5	EWS/FLI1-MEDIATED SIGNALING IN EWING SARCOMA FAMILY OF TUMORS	100
	Introduction	101
	Results	102
	Phosphoproteomic profiling identifies up regulation of Stat3 phosphorylation at residue 705 upon EWS/FLI1 knock down	102
	Phospho-Stat3 up regulation primarily occurs in a subset of cells untransduced by lentiviral shRNA	107
	Soluble factors secreted upon EWS/FLI1 knock down are sufficient to induce Stat3 phosphorylation	112
	IL-6, GM-CSF, and CXCL1 are secreted by ESFT cells after EWS/FLI1 knock down	115
	Blocking IL-6 or gp130 inhibits up-regulation of phospho-Stat3	115
	Discussion	117
	References	121
Chapter 6	EWS/FLI1 MECHANISMS OF GENE REGULATION	124
	Introduction	125
	Results	126
	BAC EWS/ETS target gene reporters only reflect two-fold modulation	126
	Intact EWS and ETS domains are required for EWS/FLI1 repression of IGFBP3	131
	EWS/FLI1(TPM) mutant acts in a dominant negative fashion	133
	Discussion	135
	References	138
Chapter 7	CONCLUSIONS AND FUTURE DIRECTIONS	140
	Summary	141

Conclusions and Future Directions	142
References	146

LIST OF FIGURES

Figure 2-1.	Molecular genetics and targeted therapies in ESFT.	28
Figure 2-2.	Molecular genetics and targeted therapies in SS.	38
Figure 2-3.	Molecular genetics and targeted therapies in DFSP.	43
Figure 2-4.	Molecular genetics of CFS.	47
Figure 4-1.	IGF1 stimulates activation of downstream components and cell growth in ESFTs.	79
Figure 4-2.	ESFT cells display an increase in tyrosine phosphorylation upon IGF1 treatment and decrease with IGF1R inhibitor.	81
Figure 4-3.	Initial IGF1 phosphotyrosine profiling results.	83
Figure 4-4.	IGF1/AMG-479 phosphotyrosine profiling results.	84
Figure 4-5.	Eph receptor and ephrin ligand transcript levels in ESFT cells.	87
Figure 4-6.	EphA2 and EphB4 are expressed and phosphorylated in ESFT cell lines.	88
Figure 4-7.	EphA2 is expressed on the surface of ESFT cells at sites of cell-to-cell contact.	89
Figure 4-8.	Comparison of IGF1 modulation between anti-IGF1R sensitive and resistant ESFT cell lines.	91
Figure 4-9.	Motif and immunoblot analysis suggest a role for SFKs in IGF signaling in ESFT.	94
Figure 5-1.	Phosphoproteomic profiling identifies proteins whose phosphorylation status is modulated downstream of EWS/FLI1.	103
Figure 5-2.	Phosphotyrosine profiling identifies up regulation of Stat3 phosphorylation at residue 705 upon EWS/FLI1 knock down.	108
Figure 5-3.	Immunofluorescence displays nearly mutually exclusive phospho-Stat3 and GFP expression.	109
Figure 5-4.	Phospho-specific flow cytometry confirms difference in phospho-Stat3 levels between transduced and untransduced populations of ESFT cells after EWS/FLI1 knock down.	111
Figure 5-5.	ESFT cells secrete a factor capable of stimulating Stat3 phosphorylation.	113
Figure 5-6.	EWS/FLI1 knock down modulates levels of secreted factors.	114

Figure 5-7.	Stat3 phosphorylation after EWS/FLI1 down appears to be mediated primarily by IL-6 secretion.	116
Figure 5-8.	Stat3 small molecular inhibitor and dominant negative Stat3 decrease ESFT growth.	118
Figure 6-1.	Schematic of recombination-mediated genetic engineering methods used to generate BAC reporter constructs.	127
Figure 6-2.	Schematic of BAC reporter constructs.	129
Figure 6-3.	Upp reporters show approximately two-fold induction by EWS/FLI1.	130
Figure 6-4.	Re-expression of wild-type EWS/FLI1 and EWS mutant suppresses IGFBP3 expression, whereas introduction of the ETS domain mutant increases mRNA levels.	132
Figure 6-5.	EWS/FLI1(TPM) elevates IGFBP3 transcript levels in the presence of the endogenous fusion.	134

LIST OF TABLES

Table 2-1.	Sarcomas with defined chromosomal translocations.	25
Table 2-2.	Targeted agents undergoing clinical testing for pediatric sarcomas.	33
Table 3-1.	Primers used for quantitative real time PCR.	67
Table 4-1.	List of Eph receptor phosphopeptides identified by phosphotyrosine profiling.	86
Table 5-1.	Over represented Gene Ontology biological processes.	105
Table 5-2.	Over represented pathways.	106

ACKNOWLEDGEMENTS

First of all, I must thank my thesis advisor and mentor, Christopher Denny. Chris has been an incredibly patient and understanding mentor whose encouragement and guidance have allowed me to develop as a scientist. I truly appreciate his ability to focus on my strengths while helping me work to improve my weaknesses. Additionally, his intelligence and excitement about science have kept me motivated while working in his lab.

I am also very fortunate to have worked with all of the members of my committee: Thomas Graeber, Matteo Pellegrini, Ren Sun, and Michael Teitell. They have gone above and beyond their duties to assist me by taking time out their busy schedules to consult with me on my project outside of annual committee meetings. Tom and Matteo have in particular have aided me on the systems biology parts of my project: Tom, for initiating the collaboration with his lab that created my project and continual support throughout, and Matteo, for providing me with basic computational skills and assistance whenever I needed to process a large data set.

I must also thank all of the members of my lab, past and present, who cheered me up when none of my experiments were working and shared in my enthusiasm when I received exciting data. Gary, Kelly, and Rupert were responsible for the majority of my training early on and taught me many valuable lab skills. Kelly, thank you not only for teaching me experimental techniques, but also for guiding me through each stage of grad school and being a constant source of support in the lab. Also, your editing of numerous proposals, abstracts, and parts of my dissertation has helped me to become a better writer. Noah, thank you for helping to develop my career by encouraging me to attend conferences and write review articles, and also for treating my injuries and illnesses as a physician of the Denny Lab Urgent Care Clinic. Ann, thank you for you for your assistance with the Ephrin part of my project and being an amazing lab manager. I would also like to thank Jason for always keeping me entertained and Neha for giving me an opportunity to interact with patients in clinic and reminding me why I chose to do cancer research. Additionally, I would like to thank all of the undergraduate and high school

students that have worked on my project: Thi Nguyen, Raquel Hernandez-Solis, and especially Ryan Akiyama, who kept my project going while I was writing my dissertation. And lastly, thank you to Paul, for taking care of all my administrative issues and sharing my passion for Apple products.

I would also like to thank all the members of the Graeber lab. Without their assistance, I would never have completed any phosphoproteomics experiments. In particular, I would like to thank Björn Titz, who taught me the majority of the techniques and has helped me troubleshoot multiple aspects of the protocols.

I could not have made it through graduate school without the love and support from all my friends and family. Thank you to my parents for always believing in me and making an effort to understand my project. To Jody, for being a sister, roommate, best friend, lab mate, chef, and most importantly someone I could talk to my day about, whether it was science-related or not. I have also been lucky to make great friends during grad school (ACCESS 13, Gias) while maintaining relationships with those that extend as far back as elementary school. And thank you to my ballet teachers Angelina and Charlotte, who gave me an outlet from science, encouraged my quest for a PhD, and trained me to be better a dancer.

I would also like to acknowledge the Cellular and Molecular Biology Training Grant (Ruth L. Kirschstein National Research Service Award GM007185) and the UCLA Graduate Division Dissertation Year Fellowship for providing financial support.

Chapter 2 of this dissertation is a version of the following paper: Pediatric sarcomas: translating molecular pathogenesis of disease to novel therapeutic possibilities by JL Anderson, CT Denny, WD Tap, and N Federman, published in *Pediatric Research* in 2012. Part of Chapter 6 is included in the following paper: Oncogenic fusion protein EWS/FLI1 down-regulates gene expression by both transcriptional and posttranscriptional mechanisms by KA France, JL Anderson, A Park, and CT Denny, published in the *Journal of Biological Chemistry* in 2011.

VITA

- 2005
B.S., Microbiology, Immunology, and Molecular Genetics
B.S., Mathematics
University of California, Los Angeles
Los Angeles, California
- 2006-2012
Graduate Student Researcher
Laboratory of Dr. Christopher Denny
Department of Pediatrics
University of California, Los Angeles
Los Angeles, California
- 2007-2008
Teaching Assistant
Department of Molecular, Cell, and Developmental Biology
University of California, Los Angeles
Los Angeles, California
- 2007-2010
Cellular and Molecular Biology Training Grant
University of California, Los Angeles
Los Angeles, California
- 2008
Advancement to Candidacy for Ph.D.
University of California, Los Angeles
Los Angeles, California
- 2011-2012
Dissertation Year Fellowship
Graduate Division
University of California, Los Angeles
Los Angeles, California

PUBLICATIONS AND PRESENTATIONS

Anderson JL, Low T, Titz B, Tap WD, Graeber TG, Denny CT. (May 2010) Using phosphoproteomics to define cell signaling networks modulated by EWS/FLI1 and IGF-I in Ewing's family tumors. Poster, Days of Molecular Medicine 2010: Systems Biology Approaches to Cancer and Metabolic Disease, Stockholm, Sweden.

Anderson JL, Low T, Titz B, Tap WD, Graeber TG, Denny CT. (June 2011) Characterization of cellular signaling in Ewing's family tumors using a phosphoproteomic approach. Poster, Cancer Proteomics 2011, Dublin, Ireland.

Anderson JL, Denny CT, Tap WD, Federman N. (2012) Pediatric sarcomas: translating molecular pathogenesis of disease to novel therapeutic possibilities. *Pediatr Res.* **72**(2):112-121. doi:10.1038/pr.2012.54.

Call GB, Olson JM, Chen J, Anderson J, URFCFG, Banerjee U. (2007) Genomewide clonal analysis of lethal mutations in the *Drosophila melanogaster* eye: comparison of the X chromosome and autosomes. *Genetics.* **177**(2):689-697. doi:10.1534/genetics.107.077735.

Chen J, Call GB, Anderson J, URFCFG, Banerjee U. (2005) Discovery-based science education: functional genomic dissection in *Drosophila* by undergraduate researchers. *PLoS Biol.* **3**(2):e59. doi:10.1371/journal.pbio.0030059.

France KA, Anderson JL, Park A, Denny CT (2011) Oncogenic fusion protein EWS/FLI1 down-regulates gene expression by both transcriptional and posttranscriptional mechanisms. *J Biol Chem.* **286**(26):22750-22757. doi:10.1074/jbc.M111.225433.

Xia Y, Babitt JL, Bouley R, Zhang Y, Da Silva N, Chen S, Zhuang Z, Samad TA, Brenner GJ, Anderson JL, Hong CC, Schneyer AL, Brown DG, Lin HY. (2010) Dragon enhances BMP signaling and increases transepithelial resistance in kidney epithelial cells. *J Am Soc Nephrol.* **21**(4):666-677. doi:10.1681/ASN.2009050511.

CHAPTER 1
INTRODUCTION

Cancer is a complex disease with over 100 discrete subgroups that originate from nearly every cell type in the human body. The malignant phenotype is caused by a series of somatic mutations that lead to proto-oncogene activation or loss of function of a tumor suppressor [1,2]. Although various neoplasms host a multitude of diverse genetic aberrations, they are united in their ability to sustain growth as a consequence of defects in cellular regulatory circuits.

Signal Transduction

Cells rely on a complex network of interacting proteins to translate an external stimulus into a physiological response. A signal is transduced once an extracellular ligand binds to a receptor on the cell surface, initiating a cascade of post-translational modifications that ultimately results in changes in gene expression [3]. This process is carefully regulated in normal tissues to control cell proliferation and survival. Perturbation can cause a shift in the balance between cell cycle progression and programmed cell death, leading to autonomous cell growth [4].

Reversible protein phosphorylation is one of the central processes for transmitting cellular signals. It was previously estimated that approximately one third of mammalian proteins are phosphorylated [5,6], although a recent study suggests this number is closer to 70% [7]. Proteins can be phosphorylated at serine, threonine, and tyrosine residues, though the abundance of phosphorylation at these residues varies. Phosphoserine, phosphothreonine, and phosphotyrosine follow a distribution of 86.4-90%, 10-11.8%, and 0.05-1.8%, respectively [8,9]. These transient modifications function as a molecular switch, either activating or deactivating protein activity.

Protein phosphorylation states are controlled by the opposing functions of kinases and phosphatases. Humans possess 518 kinases, which provide a high degree of specificity during signal transduction [10]. In contrast, there are fewer phosphatases (~130), some of which can recognize thousands of substrates. Kinases and phosphatases are subdivided into groups based on their catalytic specificity as well as whether they are membrane bound or cytoplasmic.

They typically modulate either tyrosine or serine/threonine, although there are a few dual specificity kinases and phosphatases that recognize all three residues. Ninety of the 518 human kinases phosphorylate tyrosine [10]. While the number of putative protein tyrosine phosphatases is comparable to the number of kinases [11], there are only about 30 serine/threonine phosphatases.

One of the key mechanisms of signal transduction occurs through growth factor activation of receptor tyrosine kinases (RTKs). RTKs contain an extracellular ligand-binding domain linked by a transmembrane helix to a cytoplasmic region containing a tyrosine kinase domain. In most cases, the dormant receptor exists as a monomer on the cell surface. Growth factor binding induces dimerization of the receptor, which triggers autophosphorylation and activation of the kinase domains. Phosphorylated tyrosine residues on activated RTKs create docking sites for downstream signaling molecules. Proteins are recruited to these sites either directly through SH2 (SRC homology 2) or PTB (phospho-tyrosine binding) domain-mediated recognition of phosphorylated tyrosine residues or indirectly through adapter proteins. These nodes at the cell surface propagate the signal through common downstream pathways, leading to activation of transcription factors and subsequent changes in gene expression [12].

Growth factor signaling is tightly controlled in normal cells to regulate entry into and progression through the cell cycle. Cancer cells are able to de-regulate these signals to obtain growth factor independence and sustain chronic proliferation, one of the hallmarks of cancer. This can be achieved either at the ligand level, by autonomous growth factor production, or at the receptor level, through mutations that result in constitutive activation or overexpression. Modifications of downstream components can also lead to increased signaling via activating mutations in the mitogen-activated protein kinase (MAPK) and phosphatidylinositol-3-kinase (PI3K) pathways or removal of negative feedback regulators, as in the case of PTEN (phosphatase and tensin homolog). To compound sustained growth, malignant cells also evade negative regulators of cell proliferation by inactivating tumor suppressors such as RB

(retinoblastoma) and TP53 (tumor protein p53) and resist cell death by altering expression of anti- or pro-apoptotic regulators or survival signals [13,14]. The following sections discuss three signaling pathways with which dysregulation has been implicated in cancer.

Insulin-like growth factor signaling

Insulin-like growth factor (IGF) signaling is involved in the regulation of cellular processes such as proliferation and apoptosis. The IGF system is composed of ligands, receptors, and binding proteins. The ligands are comprised of two growth factors, IGF1 and IGF2, which are both able to bind to the IGF1 receptor (IGF1R). They can act as both hormones and growth factors by stimulating local and distant cell populations. IGFs are predominantly produced in the liver, but can be secreted by other organs through autocrine or paracrine mechanisms involving interactions between populations of stromal and epithelial cells. In particular, hepatic IGF1 is produced as a response to growth hormone secretion. IGFs exist primarily as protein bound ligands. The bioavailability of these growth factors is regulated by IGF binding proteins (IGFBPs), whose similar binding affinity provides competition with IGF receptors. Of the six characterized binding proteins, IGFBP3 has the highest IGF-binding capacity [15].

Since the IGF2 receptor does not contain a kinase domain, the IGF1R is primarily responsible for transmitting signals across the cell membrane. The IGF1R exists as a dimeric receptor, with each monomer consisting of an extracellular alpha chain covalently bound to a transmembrane beta chain containing a tyrosine kinase domain [16]. This is a notable exception to most RTKs that are expressed as monomers on the cell surface. In addition to homodimeric receptors, IGF1R monomers can combine with insulin receptor monomers to form hybrid receptors. Receptor activation occurs when ligand binding induces a conformational change that triggers autophosphorylation [12]. Modulation of key tyrosine residues within the kinase domain leads to additional phosphorylation events in the juxtamembrane and C-terminal regions to create docking sites for adapter proteins. This leads to recruitment of insulin receptor

substrate (IRS) family members and Src homology and collagen domain protein (SHC), which link IGF signaling to the PI3K and MAPK pathways [17].

PI3K signaling is initiated through IRS mediated phosphorylation of the p85 regulatory subunit of PI3K. The p110 catalytic subunit then phosphorylates phosphatidylinositol 4,5-bisphosphate (PIP₂) to generate phosphatidylinositol (3,4,5)-triphosphate (PIP₃), which is recognized by the pleckstrin-homology (PH) domain within Akt. This action is antagonized by PIP₃ phosphatases such as PTEN. Recruitment of Akt to the plasma membrane coordinates its phosphorylation, first at threonine 308 by phosphoinositide-dependent protein kinase 1 (PDK1) and then at serine 473 by mTORC2 (mechanistic target of rapamycin (mTOR) complex 2), which results in maximal activation. Akt subsequently modulates several downstream components, including mTORC1 (mTOR complex 1), BCL-2 family members, forkhead transcription factors, and glycogen synthase kinase 3 (GSK3), to facilitate cell survival and entry into the cell cycle [18,19].

Progression through the extracellular signal-related kinase (ERK) arm of the MAPK pathway begins with SHC-GRB2-SOS complex formation. SHC mediates receptor interaction with the adapter protein GRB2 (growth factor receptor-bound protein 2), which binds the guanine nucleotide exchange factor SOS (son of sevenless) through its Src homology 3 (SH3) domain. This recruitment of SOS to the plasma membrane increases its proximity to RAS, allowing for exchange of GDP for GTP, resulting in RAS activation. This begins a cascade starting with activation of RAF, which phosphorylates MEK (mitogen-activated protein kinase kinase), which in turn phosphorylates ERK. ERK is then able to modulate transcription factors such as ELK1 to regulate cellular proliferation [20,21].

Due to the role of IGF signaling in promotion of cell survival and proliferation, deregulation of this pathway is involved in tumorigenesis. Although IGF1R is not mutated in malignant cells, neoplasms can display strong surface expression of the receptor. Autocrine production of IGF1 has been observed and high levels have been associated with increased

cancer risk. Moreover, the presence of a functional IGF1R is necessary for oncogene-mediated cellular transformation. The relevance to IGF signaling has been described for multiple carcinomas, but is of particular interest in sarcomas due to their response to anti-IGF1R therapy. The role of IGF signaling in sarcomagenesis is further described in the next chapter [15,22].

Eph-ephrin signaling

Eph receptors and ephrin (*Eph receptor interacting*) ligands are part of a bidirectional signaling network involved in a myriad of roles in development and physiology. Their ubiquitous expression during early development links them to processes such as cardiovascular and skeletal development, axon guidance, and tissue patterning [23]. Since both receptors and ligands are membrane bound, this signaling pathway represents a principle mechanism for contact-dependent communication between cells. Activities such as regulation of the actin cytoskeleton, cell adhesion and migration, angiogenesis, and intercellular junctions are all mediated by Eph signaling [23,24]. In addition to their involvement in normal physiology, increasing evidence has been presented on the role of Eph receptors and ephrins in cancer.

Both receptors and ligands are divided into two classes, A and B, based on their structure and sequence similarity. In humans, the nine EphA and five EphB receptors together comprise the largest family of RTKs. EphA receptors predominantly interact with the five glycosylphosphatidylinositol (GPI)-linked ephrin-A ligands. Similarly, EphB receptors bind the three transmembrane ephrin-B ligands. Receptor-ligand interaction occurs with a high degree of promiscuity within each class, though certain receptors display a preference for only one ligand. Additionally, inter-class interactions, such as EphB2 binding to ephrin-A5, have been observed [25,26].

Eph signaling is unique in its ability to transmit signals from both the receptor and ligand. Forward signaling is propelled by the kinase activity of the Eph receptor while reverse signals are propagated by tyrosine kinases that interact with the cytoplasmic region of ephrins. Eph

receptors are activated by transphosphorylation of tyrosine residues upon ephrin binding as well as through interaction with Src family kinases (SFKs). SFKs also mediate the conformation change of the ephrin-B cytoplasmic domain to promote signaling. In addition to the employment of common effectors such as SFKs, Eph and ephrins utilize selective interactions with kinases and phosphatases for receptor/ligand specific signal propagation. Furthermore, they can function independently of each other through crosstalk with other signaling systems, such as the epidermal growth factor (EGF) and fibroblast growth factor (FGF) pathways [24,27].

Altered Eph receptor expression, most commonly up regulation of EphA2 and EphB4, has been observed in many cancers. Despite their high expression, Eph receptors are poorly activated by ephrins and display low levels of phosphorylation. In fact, Eph forward signaling can result in tumor suppression. However, siRNA-mediated down regulation of EphA2 and EphB4 decreases malignancy and inhibits tumor growth. This suggests that Eph signaling does play a role in tumorigenesis, possibly through crosstalk with other pathways. Less is known about ephrin-mediated reverse signaling, though there is some evidence of ephrin-B involvement in cell migration and invasion. Additionally, Eph-ephrin promotion of tumor angiogenesis and active signaling in the tumor microenvironment adds to the complex role this pathway plays in cancer [24,26].

JAK/STAT signaling

The Janus kinase (JAK)/signal transducer and activator of transcription (STAT) pathway is comprised of non-receptor tyrosine kinases whose phosphorylation of downstream transcription factors leads to their dimerization and activation of transcriptional activity. Canonical pathway activation is initiated upon cytokine binding to a transmembrane receptor that lacks intrinsic kinase activity. Receptor dimerization leads to activation of receptor-associated tyrosine kinases, which are most often members of the JAK family. The JAK kinases, JAK1-3 and tyrosine kinase 2 (TYK2), then phosphorylate tyrosine residues within the cytokine receptor cytoplasmic

domains to provide binding sites for SH2 domain-containing STAT proteins (STAT1-4, 5A, 5B, and 6). Subsequent recruitment of STATs to the plasma membrane gives rise to JAK-mediated phosphorylation at a specific C-terminal tyrosine residue. Following tyrosine phosphorylation, STAT proteins dissociate from the cytokine receptor, dimerize via reciprocal SH2 domain-phosphotyrosine interactions, and then translocate to the nucleus to initiate gene transcription [28-30]. STAT activation can also be mediated by growth factor receptors either through their own intrinsic kinase activity or in concert with non-receptor tyrosine kinases such as SFKs or ABL (Abelson leukemia protein). SFKs can furthermore modulate STATs downstream of cytokine signaling or independently of activated receptors [31,32].

The biological activity of the JAK/STAT pathway is distinguished by its quick and transient signal transmission. To achieve this sensitivity, kinase activity is balanced by a series of negative regulators. This group consists of tyrosine phosphatases, suppressors of cytokine signaling (SOCS), and protein inhibitors of activated STAT (PIAS).

Multiple types of protein tyrosine phosphatases (PTPs) are involved in inhibition of JAK and STAT proteins. The first is a group of cytoplasmic, SH2 domain-containing tyrosine phosphatases that includes SHP1 (protein tyrosine phosphatase, non-receptor type 6 (PTPN6)) and SHP2 (PTPN11). Their SH2 domain recognizes and binds activated receptors and JAKs, which leads to dephosphorylation and removal of STAT docking sites. Transmembrane PTPs such as CD45 and PTPRT are implicated in negative regulation of JAKs and STAT3, respectively [33,34]. Additionally, low molecular weight PTPs including PTP1B (phosphotyrosine phosphatase 1B) and TC-PTP (T cell protein tyrosine phosphatase) modulate JAK/STAT signaling by dephosphorylating JAKs [35,36]. A few of these phosphatases such as SHP2 and PTP1B that were initially shown to modulate JAKs have been shown to dephosphorylate STATs as well [33,37].

The negative regulatory activity of PTPs is supplemented by SOCS and PIAS. SOCS are transcriptionally up regulated as part of a feedback loop in response to a variety of cellular

activators, including cytokines. These proteins antagonize STAT activation by competing for cytokine receptor binding sites and inhibiting JAK activity. PIAS interact with STATs directly. This interaction inhibits the ability of STATs to bind DNA, thus decreasing their transcriptional activity.

Stat3

Due to its roles in immunity and cancer, STAT3 is one of the most studied of the STAT proteins. In the context of cytokine signaling, STAT3 is induced by interleukin-6 (IL-6) as well other members of the IL-6 family of cytokines. IL-6 first binds to the IL-6 receptor (IL-6R), which exists in both membrane-bound and soluble forms. This complex then associates with the ubiquitously expressed glycoprotein 130 (gp130). This membrane-bound receptor is not specific to IL-6 and can be utilized by multiple IL-6 family members. IL-6R binding leads to ligand-induced dimerization of gp130 and subsequent JAK activation [38,39]. JAKs, and in some cases Src, then phosphorylate STAT3 at tyrosine 705, allowing for homodimerization and nuclear translocation. STAT3 is furthermore phosphorylated at serine 727, which augments its transcriptional activity [40]. STAT3 activation can also be mediated by growth factor receptors, including EGFR, HER2 (human epidermal growth factor receptor 2, also known as ERBB2), FGFR, IGFR, HGFR (hepatocyte growth factor receptor, also known as MET), PDGFR (platelet-derived growth factor receptor), and VEGFR (vascular endothelial growth factor receptor) [32].

Activation of STAT3 results in the transcriptional up regulation of cell proliferation and survival factors. STAT3 target genes include the anti-apoptotic proteins BCL-X_L (B-cell lymphoma-2-like 1), BCL-2 (B-cell CLL/lymphoma 2), survivin, and MCL1 (myeloid cell leukemia sequence 1), which promote resistance of cell death. STAT3 also confers a mitogenic response by increasing the expression of the cell cycle protein cyclin D1 and the transcription factor MYC [31,32,41]. In continuation with this pro-survival response, STAT3 controls the transcription of

growth factors and cytokines, including its own activators IL-6 and VEGF, which generates a feedforward loop to maintain activation of this pathway [41].

Owing to its control of these processes, persistent activation of STAT3 in malignant cells drives tumor progression. STAT3 was first characterized as an oncogene when a constitutively active form was shown to transform immortalized fibroblasts [42]. Sustained STAT3 activity is associated with multiple neoplasms and can occur through various mechanisms. Increased autocrine and paracrine production of cytokines can up regulate STAT3. STAT3 phosphorylation in tumor cells results in the secretion of factors that promote immunosuppression and STAT3 activation in immune cells in the tumor microenvironment. This contributes to the aforementioned feedforward loop as immune cells in turn secrete STAT3 stimulating factors to maintain signaling in the tumor. Decreased expression of negative regulators such as SOCS or phosphatases can also lead to constitutive STAT3 phosphorylation. Additionally, many tumors display overexpression of growth factor receptors and non-receptor tyrosine kinases such as Src, which regulate STAT3. STAT3 further contributes to cancer development by inducing tumor angiogenesis [32,41,43].

Phosphoproteomics

Given the importance of signal transduction to normal physiology and cancer, appropriate biochemical techniques are needed to delineate these pathways. Traditionally, antibody-based approaches have been utilized to measure protein levels and detect specific post-translational modifications. Protein-protein interactions can also be studied through the combination of immunoprecipitation and immunoblot analysis. These methods are sufficient when investigating a single protein, but fall short when it comes to system-wide analysis. Commercially available antibodies recognize only a subset of signaling molecules and even fewer in the context of post-translational modifications, restricting the scope of pathway analysis.

Recent advances in mass spectrometry (MS) have allowed for application of this technology to signal transduction studies. Increased instrument sensitivity, speed of analysis, and enhanced sample preparation methods now enable the identification of up to thousands of proteins and/or phosphorylation sites in a single experiment [44,45]. The facility for whole proteome analysis permits an unbiased, global perspective that was not possible with antibody driven techniques. MS-based methods are also able to localize phosphorylation sites and quantitate phosphoproteins, which add to their value in system-wide analysis of protein phosphorylation, or phosphoproteomics.

Workflow

The phosphoproteomic workflow begins with isolation of protein from cells or tissues, followed by tryptic digestion into peptides. Despite the developments in MS technology, fractionation or enrichment must be applied to reduce the complexity of the sample prior to entering the mass spectrometer. This is especially important for phosphoproteomics studies since phosphopeptides can be masked by unmodified peptides with higher signal intensities due to their low abundance and ionization efficiency [46]. Phosphopeptides are generally enriched via a combination of antibody- and affinity-based methods.

Affinity-based techniques include immobilized metal affinity chromatography (IMAC), titanium dioxide (TiO₂) enrichment, and strong cation exchange (SCX) chromatography. IMAC utilizes the high affinity of phosphate groups for trivalent metal ions. Metal ions such as Fe³⁺ are immobilized on a column through chelation to nitrilotriacetic acid (NTA) or iminodiacetic acid (IDA) beads and phosphopeptides are captured by complex formation with the bound metal ion [46,47]. However, the specificity of this process is hindered by peptides with negatively charged carboxylic acid groups that compete with phosphate groups for metal binding. Due to the selectivity complications of the IMAC protocol, TiO₂ enrichment has become a preferred method for phosphopeptide enrichment. The Lewis acid-base interactions employed by TiO₂ can also

attract acidic peptides as in IMAC, but the use of organic acids to outcompete carboxylic acid groups from binding to TiO_2 greatly enhances the selectivity for phosphopeptides [46,47].

The final method, SCX, enriches phosphopeptides through their difference in net charge from nonphosphorylated peptides. SCX particles contain negatively charged functional groups that interact with positively charged peptides. The protocol uses buffers with a pH of 2.7, in which most tryptic peptides possess a net charge of +2 due to the N-terminal amino group and protonated C-terminal lysine or arginine. Monophosphorylated peptides, in contrast, have a net charge of +1 due to the presence of the negatively charged phosphate group, resulting in decreased affinity for the SCX column. Peptides are eluted with a linear salt gradient, which causes the low affinity phosphopeptides to be abundant in early fractions. Multi-phosphorylated peptides contain a net zero or negative charge and therefore will not bind to the SCX column and are present in the flow-through. [44,46,47].

Performing IMAC or TiO_2 enrichment in combination with SCX chromatography has proven to be a robust strategy for phosphopeptide enrichment [47]. However, this protocol leads to the identification of mainly phosphoserine and phosphothreonine containing peptides due to the high abundance of phosphorylation at these residues. To effectively identify tyrosine phosphopeptides, antibody-based methods are required. The quality of available antibodies that recognize phosphotyrosine allows for efficient immunoprecipitation of tyrosine phosphorylated peptides, yielding suitable enrichment and discovery of these species [48,49].

To further reduce sample complexity, phosphopeptides are next separated on a reversed-phase (C_{18}) capillary liquid chromatography (nanoLC) column. Column elution is coupled to electrospray ionization, which transfers the ionized peptides to a high-resolution mass spectrometer for subsequent analysis. An initial MS scan (MS1) records the mass-to-charge ratio (m/z) and intensity of the intact peptide. The most abundant peptides from each column retention time are selected for sequencing by tandem MS (MS/MS) based on their intensity values. These peptides are fragmented, most commonly by collision-induced

dissociation (CID), and subjected to a second MS scan (MS/MS or MS²). MS² fragmentation spectra are then compared to protein sequence databases to determine the identity of each peptide.

Quantitation

Analysis of signal transduction networks requires comparison of components in response to various stimuli or at multiple time points, which necessitates peptide quantification. In addition to being able to identify thousands of proteins and phosphorylation sites, mass spectrometric technology can also be used to accurately ascertain phosphopeptide levels. MS-based quantitation methods include metabolic labeling, chemical labeling, and label-free quantitation.

Metabolic labeling utilizes stable isotopes such as ¹⁵N or ¹³C that are incorporated into proteins during cell growth. The most common technique, SILAC (stable isotope labeling by amino acids in cell culture), uses heavy arginine and lysine to generate C-terminally labeled tryptic peptides [50]. Treatment of cells with differentially labeled amino acids generates proteomes that can be distinguished by molecular weight differences imposed by the introduction of heavy isotopes. This allows for samples to be combined prior to fractionation and enrichment, thus eliminating quantitation errors that can arise during sample manipulation [3].

Chemical labeling involves tagging of proteins or peptides without the necessity of growing cells in culture. ICAT (isotope-coded affinity tag) and iTRAQ (isobaric tag for relative and absolute quantitation) are two of the most regularly used methods. ICAT uses a reagent that combines a thiol-specific reactive group conjugated to biotin with a linker that can incorporate heavy isotopes [51]. Peptides are modified at cysteine residues and purified by avidin affinity chromatography. As with SILAC, differentially labeled peptides can be discriminated by mass differences observed in the MS¹ spectrum. iTRAQ, on the other hand, is unique in its ability to apply differential labeling to MS² spectra [52]. This technique employs

amine-specific tags consisting of a reporter and balance group that are indistinguishable in the MS1 spectra. However, fragmentation of the balance group releases unique reporters whose MS2 intensities can be compared for protein quantitation [47].

Finally, the robustness and reproducibility of MS-based phosphoproteomic protocols now permit label-free quantitation. In this method, MS data for each peptide can be compared across experimental conditions by using retention time, mass, and ion intensity. The advantage of label-free quantitation is that no additional sample manipulation is required. However, the level of quantitative precision achieved by isotopic labeling is not obtained due to inherent signal differences between runs [3,45].

Applications to signal transduction research

The first global, dynamic study of mammalian cellular signaling examined phosphorylation downstream of EGFR [9]. Quantitation of phosphopeptides at various time points after EGF stimulation was accomplished through differential SILAC labeling. SCX and TiO₂ enrichment prior to high-accuracy MS identified 6,600 phosphosites corresponding to 2,244 proteins. This high yield demonstrated the capability of MS-based studies for system-wide pathway analysis.

Applications of SILAC have also been used to discriminate phosphoproteomes of distinct cell populations. One example is a study that defined phosphotyrosine signaling networks in Eph receptor- and ephrin-expressing cells [53]. Because both the receptor and ligand are membrane bound, mixing of cell populations is required to activate bi-directional signaling. Phosphorylation events specific to forwarding and reverse signaling were distinguished by differentially labeling EphB2 and ephrin-B1-expressing cells by SILAC. Phosphotyrosine immunoprecipitation followed by MS analysis uncovered 442 tyrosine phosphorylation sites on 304 proteins whose levels changed significantly upon EphB2-ephrin-B1 contact.

Additionally, large-scale phosphotyrosine profiling was performed to survey oncogenic kinases in non-small cell lung cancer (NSCLC) [48]. As in the Eph-ephrin study, immunoaffinity

purification was used to enrich for phosphotyrosine prior to tandem MS. More than 50 tyrosine kinases and 2,500 downstream substrates were identified through the analysis of 41 cell lines and over 150 tumor samples. This data set included kinases known to play a role in NSCLC pathogenesis as well as novel regulators, reinforcing the utility of MS-based approaches for characterization of signaling in cancer.

These examples showcase the benefits of applying MS to study signal transduction, and more specifically, oncogenic signaling. As deregulated signaling is the manifestation of the underlying genetic anomalies in cancer, directing therapeutic agents toward these uncontrolled pathways presents a logical avenue for the development of new treatments. Success has already been attained through the use of specific kinase inhibitors, most famously by targeting BCR-ABL in chronic myelogenous leukemia [54,55]. Combination of MS-derived pathway data with the current arsenal of drugs has the potential to extend this achievement to other malignancies.

Ewing sarcoma family of tumors

The Ewing sarcoma family of tumors (ESFT) is a group of bone and soft tissue malignancies that primarily afflict children and young adults within the first two decades of life. The unifying factor within this collection of neoplasms is the presence of a chromosomal translocation that generates an aberrant transcription factor, most commonly EWS/FLI1 [56]. Sarcomagenesis occurs primarily through EWS/FLI1-mediated modulation of gene expression and dysregulation of IGF1 signaling. As a transcriptional regulator, EWS/FLI1 both up and down regulates a network of direct target genes. Contained in this set are components of signal transduction pathways, including members of the IGF1 system [57,58], which links EWS/FLI1 to cellular signaling.

Although current therapies have increased the ESFT five-year survival rate to almost 70%, this number drops to approximately 30% when considering patients with metastatic,

refractory, and/or recurrent disease [59]. The clinical use of agents directed against signal transducers such as IGF1R [60-65] and mTOR [66] represent the shift in focus towards targeted therapies. By taking advantage of mass spectrometry-based phosphoproteomics techniques, this dissertation aims to characterize cellular signaling downstream of IGF1 and EWS/FLI1 in ESFT. The increased knowledge of these signal transduction networks may lead to novel therapeutic targets in these malignancies.

References

1. Christoffersen T, Guren TK, Spindler K-LG, Dahl O, Lønning PE, Gjertsen BT. (2009) Cancer therapy targeted at cellular signal transduction mechanisms: strategies, clinical results, and unresolved issues. *Eur J Pharmacol.* **625**:6-22.
2. Stratton MR, Campbell PJ, Futreal PA. (2009) The cancer genome. *Nature.* **458**:719-724.
3. Choudhary C, Mann M. (2010) Decoding signalling networks by mass spectrometry-based proteomics. *Nat Rev Mol Cell Biol.* **11**:427-439.
4. Blume-Jensen P, Hunter T. (2001) Oncogenic kinase signalling. *Nature.* **411**:355-365.
5. Cohen P. The Croonian Lecture 1998. Identification of a protein kinase cascade of major importance in insulin signal transduction.; 1999 Mar 28. pp. 485-495.
6. Cohen P. The role of protein phosphorylation in human health and disease. The Sir Hans Krebs Medal Lecture.; 2001 Oct. pp. 5001-5010.
7. Olsen JV, Vermeulen M, Santamaria A, Kumar C, Miller ML, Jensen LJ, Gnad F, Cox J, Jensen TS, Nigg EA, Brunak S, Mann M. (2010) Quantitative phosphoproteomics reveals widespread full phosphorylation site occupancy during mitosis. *Sci Signal.* **3**:ra3.
8. Hunter T, Sefton BM. (1980) Transforming gene product of Rous sarcoma virus phosphorylates tyrosine. *Proc Natl Acad Sci U S A.* **77**:1311-1315.
9. Olsen JV, Blagoev B, Gnad F, Macek B, Kumar C, Mortensen P, Mann M. (2006) Global, In Vivo, and Site-Specific Phosphorylation Dynamics in Signaling Networks. *Cell.* **127**:635-648.
10. Manning G, Whyte DB, Martinez R, Hunter T, Sudarsanam S. (2002) The protein kinase complement of the human genome. *Science.* **298**:1912-1934.
11. Alonso A, Sasin J, Bottini N, Friedberg I, Friedberg I, Osterman A, Godzik A, Hunter T, Dixon J, Mustelin T. (2004) Protein tyrosine phosphatases in the human genome. *Cell.* **117**:699-711.
12. Lemmon MA, Schlessinger J. (2010) Cell signaling by receptor tyrosine kinases. *Cell.* **141**:1117-1134.
13. Hanahan D, Weinberg RA. (2000) The hallmarks of cancer. *Cell.* **100**:57-70.
14. Hanahan D, Weinberg RA. (2011) Hallmarks of Cancer: The Next Generation. *Cell.* **144**:646-674.
15. Pollak MN, Schernhammer ES, Hankinson SE. (2004) Insulin-like growth factors and neoplasia. *Nat Rev Cancer.* **4**:505-518.
16. de Meyts P, Whittaker J. (2002) Structural biology of insulin and IGF1 receptors: implications for drug design. *Nat Rev Drug Discov.* **1**:769-783.

17. Chitnis MM, Yuen JSP, Protheroe AS, Pollak M, Macaulay VM. (2008) The type 1 insulin-like growth factor receptor pathway. *Clin Cancer Res.* **14**:6364-6370.
18. Vivanco I, Sawyers CL. (2002) The phosphatidylinositol 3-Kinase AKT pathway in human cancer. *Nat Rev Cancer.* **2**:489-501.
19. Engelman JA. (2009) Targeting PI3K signalling in cancer: opportunities, challenges and limitations. *Nat Rev Cancer.* **9**:550-562.
20. Downward J. (2003) Targeting RAS signalling pathways in cancer therapy. *Nat Rev Cancer.* **3**:11-22.
21. Shaul YD, Seger R. (2007) The MEK/ERK cascade: from signaling specificity to diverse functions. *Biochim Biophys Acta.* **1773**:1213-1226.
22. Maki RG. (2010) Small is beautiful: insulin-like growth factors and their role in growth, development, and cancer. *J Clin Oncol.* **28**:4985-4995.
23. Arvanitis D, Davy A. (2008) Eph/ephrin signaling: networks. *Genes Dev.* **22**:416-429.
24. Pasquale EB. (2008) Eph-ephrin bidirectional signaling in physiology and disease. *Cell.* **133**:38-52.
25. Branco-Price C, Johnson RS. (2010) Tumor Vessels Are Eph-ing Complicated. *Cancer Cell.* **17**:533-534.
26. Pasquale EB. (2010) Eph receptors and ephrins in cancer: bidirectional signalling and beyond. *Nat Rev Cancer.* **10**:165-180.
27. Pasquale EB. (2005) Eph receptor signalling casts a wide net on cell behaviour. *Nat Rev Mol Cell Biol.* **6**:462-475.
28. Levy DE, Darnell JE. (2002) Stats: transcriptional control and biological impact. *Nat Rev Mol Cell Biol.* **3**:651-662.
29. Li WX. (2008) Canonical and non-canonical JAK-STAT signaling. *Trends Cell Biol.* **18**:545-551.
30. Vera J, Rateitschak K, Lange F, Kossow C, Wolkenhauer O, Jaster R. (2011) Systems biology of JAK-STAT signalling in human malignancies. *Prog Biophys Mol Biol.* **106**:426-434.
31. Yu H, Jove R. (2004) The STATs of cancer — new molecular targets come of age. *Nat Rev Cancer.* **4**:97-105.
32. Yu H, Kortylewski M, Pardoll D. (2007) Crosstalk between cancer and immune cells: role of STAT3 in the tumour microenvironment. *Nat Rev Immunol.* **7**:41-51.
33. Xu D, Qu CK. (2008) Protein tyrosine phosphatases in the JAK/STAT pathway. *Front Biosci.* **13**:4925-4932.

34. Zhang X, Guo A, Yu J, Possemato A, Chen Y, Zheng W, Polakiewicz RD, Kinzler KW, Vogelstein B, Velculescu VE, Wang ZJ. (2007) Identification of STAT3 as a substrate of receptor protein tyrosine phosphatase T. *Proc Natl Acad Sci U S A.* **104**:4060-4064.
35. Chen W, Daines MO, Khurana Hershey GK. (2004) Turning off signal transducer and activator of transcription (STAT): the negative regulation of STAT signaling. *J Allergy Clin Immunol.* **114**:476-489; quiz 490.
36. Valentino L, Pierre J. (2006) JAK/STAT signal transduction: regulators and implication in hematological malignancies. *Biochem Pharmacol.* **71**:713-721.
37. Zhang W, Chan RJ, Chen H, Yang Z, He Y, Zhang X, Luo Y, Yin F, Moh A, Miller LC, Payne RM, Zhang Z-Y, Fu X-Y, Shou W. (2009) Negative regulation of Stat3 by activating PTPN11 mutants contributes to the pathogenesis of Noonan syndrome and juvenile myelomonocytic leukemia. *J Biol Chem.* **284**:22353-22363.
38. Blanchard F, Duplomb L, Baud'huin M, Brounais B. (2009) The dual role of IL-6-type cytokines on bone remodeling and bone tumors. *Cytokine Growth Factor Rev.* **20**:19-28.
39. Taga T, Kishimoto T. (1997) Gp130 and the interleukin-6 family of cytokines. *Annu Rev Immunol.* **15**:797-819.
40. Schindler C, Levy DE, Decker T. (2007) JAK-STAT signaling: from interferons to cytokines. *J Biol Chem.* **282**:20059-20063.
41. Yu H, Pardoll D, Jove R. (2009) STATs in cancer inflammation and immunity: a leading role for STAT3. *Nat Rev Cancer.* **9**:798-809.
42. Bromberg JF, Wrzeszczynska MH, Devgan G, Zhao Y, Pestell RG, Albanese C, Darnell JE. (1999) Stat3 as an oncogene. *Cell.* **98**:295-303.
43. Sansone P, Bromberg J. (2012) Targeting the interleukin-6/Jak/stat pathway in human malignancies. *J Clin Oncol.* **30**:1005-1014.
44. Grimsrud PA, Swaney DL, Wenger CD, Beauchene NA, Coon JJ. (2010) Phosphoproteomics for the masses. *ACS Chem Biol.* **5**:105-119.
45. Kolch W, Pitt A. (2010) Functional proteomics to dissect tyrosine kinase signalling pathways in cancer. *Nat Rev Cancer.* **10**:618-629.
46. Thingholm TE, Jensen ON, Larsen MR. (2009) Analytical strategies for phosphoproteomics. *Proteomics.* **9**:1451-1468.
47. Macek B, Mann M, Olsen JV. (2009) Global and site-specific quantitative phosphoproteomics: principles and applications. *Annu Rev Pharmacol Toxicol.* **49**:199-221.
48. Rikova K, Guo A, Zeng Q, Possemato A, Yu J, et al. (2007) Global survey of phosphotyrosine signaling identifies oncogenic kinases in lung cancer. *Cell.* **131**:1190-1203.

49. Rush J, Moritz A, Lee KA, Guo A, Goss VL, Spek EJ, Zhang H, Zha X-M, Polakiewicz RD, Comb MJ. (2005) Immunoaffinity profiling of tyrosine phosphorylation in cancer cells. *Nat Biotechnol.* **23**:94-101.
50. Ong SE, Blagoev B, Kratchmarova I, Kristensen DB, Steen H, Pandey A, Mann M. (2002) Stable isotope labeling by amino acids in cell culture, SILAC, as a simple and accurate approach to expression proteomics. *Mol Cell Proteomics.* **1**:376-386.
51. Gygi SP, Rist B, Gerber SA, Turecek F, Gelb MH, Aebersold R. (1999) Quantitative analysis of complex protein mixtures using isotope-coded affinity tags. *Nat Biotechnol.* **17**:994-999.
52. Ross PL, Huang YN, Marchese JN, Williamson B, Parker K, et al. (2004) Multiplexed protein quantitation in *Saccharomyces cerevisiae* using amine-reactive isobaric tagging reagents. *Mol Cell Proteomics.* **3**:1154-1169.
53. Jørgensen C, Sherman A, Chen GI, Pasculescu A, Poliakov A, Hsiung M, Larsen B, Wilkinson DG, Linding R, Pawson T. (2009) Cell-specific information processing in segregating populations of Eph receptor ephrin-expressing cells. *Science.* **326**:1502-1509.
54. Druker BJ, Talpaz M, Resta DJ, Peng B, Buchdunger E, Ford JM, Lydon NB, Kantarjian H, Capdeville R, Ohno-Jones S, Sawyers CL. (2001) Efficacy and safety of a specific inhibitor of the BCR-ABL tyrosine kinase in chronic myeloid leukemia. *N Engl J Med.* **344**:1031-1037.
55. Druker BJ, Tamura S, Buchdunger E, Ohno S, Segal GM, Fanning S, Zimmermann J, Lydon NB. (1996) Effects of a selective inhibitor of the Abl tyrosine kinase on the growth of Bcr-Abl positive cells. *Nat Med.* **2**:561-566.
56. Arvand A, Denny CT. (2001) Biology of EWS/ETS fusions in Ewing's family tumors. *Oncogene.* **20**:5747-5754.
57. Prieur A, Tirode F, Cohen P, Delattre O. (2004) EWS/FLI-1 silencing and gene profiling of Ewing cells reveal downstream oncogenic pathways and a crucial role for repression of insulin-like growth factor binding protein 3. *Mol Cell Biol.* **24**:7275-7283.
58. Riggi N, Cironi L, Provero P, Suva ML, Kaloulis K, Garcia-Echeverria C, Hoffmann F, Trumpp A, Stamenkovic I. (2005) Development of Ewing's sarcoma from primary bone marrow-derived mesenchymal progenitor cells. *Cancer Res.* **65**:11459-11468.
59. Rodriguez-Galindo C, Navid F, Khoury J, Krasin M (2006) Ewing sarcoma family of tumors. In: Pappo A, editor. *Pediatric Bone and Soft Tissue Sarcomas.* Berlin/Heidelberg: Springer-Verlag. pp. 181-217.
60. Tolcher AW, Sarantopoulos J, Patnaik A, Papadopoulos K, Lin C-C, et al. (2009) Phase I, pharmacokinetic, and pharmacodynamic study of AMG 479, a fully human monoclonal antibody to insulin-like growth factor receptor 1. *J Clin Oncol.* **27**:5800-5807.
61. Olmos D, Postel-Vinay S, Molife LR, Okuno SH, Schuetze SM, et al. (2010) Safety, pharmacokinetics, and preliminary activity of the anti-IGF-1R antibody figitumumab (CP-

- 751,871) in patients with sarcoma and Ewing's sarcoma: a phase 1 expansion cohort study. *Lancet Oncol.* **11**:129-135.
62. Juergens H, Daw NC, Geoerger B, Ferrari S, Villarroel M, Aerts I, Whelan J, Dirksen U, Hixon ML, Yin D, Wang T, Green S, Paccagnella L, Gualberto A. (2011) Preliminary Efficacy of the Anti-Insulin-Like Growth Factor Type 1 Receptor Antibody Figitumumab in Patients With Refractory Ewing Sarcoma. *J Clin Oncol.*
 63. Pappo AS, Patel SR, Crowley J, Reinke DK, Kuenkele KP, et al. (2011) R1507, a monoclonal antibody to the insulin-like growth factor 1 receptor, in patients with recurrent or refractory Ewing sarcoma family of tumors: results of a phase II Sarcoma Alliance for Research through Collaboration study. *J Clin Oncol.* **29**:4541-4547.
 64. Malempati S, Weigel B, Ingle AM, Ahern CH, Carroll JM, Roberts CT, Reid JM, Schmechel S, Voss SD, Cho SY, Chen HX, Krailo MD, Adamson PC, Blaney SM. (2012) Phase I/II trial and pharmacokinetic study of cixutumumab in pediatric patients with refractory solid tumors and Ewing sarcoma: a report from the Children's Oncology Group. *J Clin Oncol.* **30**:256-262.
 65. Tap WD, Demetri G, Barnette P, Desai J, Kavan P, et al. (2012) Phase II study of ganitumab, a fully human anti-type-1 insulin-like growth factor receptor antibody, in patients with metastatic Ewing family tumors or desmoplastic small round cell tumors. *J Clin Oncol.* **30**:1849-1856.
 66. Mita MM, Mita AC, Chu QS, Rowinsky EK, Fetterly GJ, et al. (2008) Phase I trial of the novel mammalian target of rapamycin inhibitor deforolimus (AP23573; MK-8669) administered intravenously daily for 5 days every 2 weeks to patients with advanced malignancies. *J Clin Oncol.* **26**:361-367.

CHAPTER 2
PEDIATRIC SARCOMAS

Abstract

Pediatric sarcomas represent a diverse group of rare bone and soft tissue malignancies.

Though the molecular mechanisms that propel the development of these cancers are not well understood, identification of tumor-specific translocations in many sarcomas has provided

significant insight into their tumorigenesis. Each fusion protein resulting from these

chromosomal translocations is thought to act as a driving force in the tumor, either as an

aberrant transcription factor, constitutively active growth factor, or ligand-independent receptor

tyrosine kinase. Identification of transcriptional targets or signaling pathways modulated by

these oncogenic fusions has led to the discovery of potential therapeutic targets. Some of these

targets have shown considerable promise in pre-clinical models and are currently being tested

in clinical trials. This review summarizes the molecular pathology of a subset of pediatric

sarcomas with tumor-associated translocations and how increased understanding at the

molecular level is being translated to novel therapeutic advances.

Introduction

Sarcomas are a rare, heterogeneous group of neoplasms presumed to be of mesenchymal origin. Tumors can arise in bone or soft tissues such as muscle and fat and can develop anywhere in the body. They account for only 1% of all malignancies, and although the incidence is higher in adults, sarcomas occur with higher frequency in children. Each year, between 1500 and 1600 children and young adults in the United States develop these malignant bone and soft tissue tumors comprising approximately 13% of cancers afflicting patients below the age of 20 [1,2]. The overall five-year survival rate for pediatric cancers is 82% for U.S. patients diagnosed between 1999 and 2006 . However, this statistic for sarcomas is approximately 60% and falls closer to 20-30% for recurrent and metastatic cases. Current treatment consists of surgery, multi-agent chemotherapy, and/or radiation. Unfortunately, complete surgical resection is not always possible and chemotherapy is often ineffective, especially for metastatic cases or chemoresistant tumors.

Sarcomas can be divided into two groups based on the underlying molecular events that initiate tumorigenesis. The first group is characterized by the presence of specific chromosomal translocations (Table 2-1) or activating mutations while the second is more cytogenetically complex. Sarcomas with complex karyotypes predominantly afflict older patients and translocations tend to be observed with higher frequency in pediatric cases. Pediatric sarcomas with tumor-associated translocations include the Ewing sarcoma family of tumors (ESFT), rhabdomyosarcoma (RMS), synovial sarcoma (SS), dermatofibrosarcoma protuberans (DFSP), congenital fibrosarcoma (CFS), and alveolar soft part sarcoma (ASPS).

The genetic aberrations in these neoplasms produce defined fusions that are critical for sarcomagenesis. Depending on the genes involved in the fusion, the resulting protein can promote tumor progression through transcriptional modulation, epigenetic modifications, or activation of oncogenic signaling pathways. For example, EWS-ETS fusions in ESFT transcriptionally up- and down-regulate target genes that promote tumor development. The

Table 2-1. Sarcomas with defined chromosomal translocations

Tumor type	Translocation	Fusion
Ewing sarcoma family of tumors	t(11;22)(q24;q12)	EWS-FLI1
	t(21;22)(q22;q12)	EWS-ERG
	t(7;22)(p22;q12)	EWS-ETV1
	t(17;22)(q21;q12)	EWS-ETV4
	t(2;22)(q33;q12)	EWS-FEV
	t(16;21)(p11;q22)	FUS-ERG
	t(2;16)(q35;p11)	FUS-FEV
	(t(1;22)(p36.1;q12)	EWS-ZSG
ES-like tumors (CD-99 negative)	t(20;22)(q13;q12)	EWS-NFATc2
	t(6;22)(p21;q12)	EWS-POU5F1
	t(1;22)(q36.1;q12)	EWS-PATZI
	t(2;22)(q31;q12)	EWS-SP3
Clear-cell sarcoma	t(4;19)(q35;q13)	CIC-DUX4
	t(12;22)(p13;q12)	EWS-ATF1
Desmoplastic small round-cell tumor	t(2;22)(q33;q12)	EWS-BREB1
	t(11;22)(p13;q12)	EWS-WT1
Myxoid liposarcoma	t(21;22)(q22;q12)	EWS-ERG
	t(12;16)(q13;q11)	FUS-DDIT3
Extraskelatal myxoid chondrosarcoma	t(12;22)(q13;q12)	EWS-DDIT3
	t(9;22)(q22-31;q11-12)	EWS-NR4A3
Low grade fibromyxoid sarcoma	t(9;17)(q22;q11)	TAF15-NR4A3
	t(9;15)(q22;q21)	TCF12-NR4A3
	t(9;22)(q22;q15)	TFG-NR4A3
Angiomatoid fibrous histiocytoma	t(7;16)(q33;p11)	FUS-CREB3L2
	t(11;16)(p11;p11)	FUS-CREB3L1
Alveolar rhabdomyosarcoma	t(12;16)(q13;p11)	FUS-ATF1
	t(12;22)(q13;q12)	EWS-ATF1
	t(2;22)(q33;q12)	EWS-CREB1
Alveolar soft part sarcoma	t(2;13)(q35;q14)	PAX3-FOXO1
	t(1;13)(q36;q14)	PAX7-FOXO1
	t(2;2)(p23;q35)	PAX3-NCOA1
	t(2;8)(q35;q13)	PAX3-NCOA2
Congenital fibrosarcoma	t(8;13;9)(p11.2;q14;9q32)	FGFR1-FOXO1
	t(X;17)(p11;q25)	ASPSL-TFE3
Congenital mesoblastic nephroma	t(12;15)(p13;q25)	ETV6-NTRK3
	t(12;15)(p13;q25)	ETV6-NTRK3
Inflammatory myofibroblastic tumor	t(1;2)(q25;q23)	TPM3-ALK
	t(2;19)(q23;q13)	TPM4-ALK
	t(2;17)(q23;q23)	CLTC-ALK
Synovial sarcoma	t(2;2)(p23;q13)	RANBP2-ALK
	t(X;18)(p11;q11)	SS18-SSX1
	t(X;18)(p11;q11)	SS18-SSX2
	t(X;18)(p11;q13)	SS18-SSX4
Endometrial sarcoma	t(X;20)(p11;q13)	SS18L1-SSX1
	t(7;17)(p15;q21)	JAZF1-SUZ12
	t(6;7)(p21;p15)	JAZF1-PHF1
Dermatofibrosarcoma protuberans	t(6;10)(p21;p11)	EPC1-PHF1
	t(17;22)(q22;q13)	COL1A1-PDGFB
Giant cell fibroblastoma	t(17;22)(q22;q13)	COL1A1-PDGFB

SYT-SSX fusions found in synovial sarcoma mediate chromatin remodeling through interactions with polycomb group proteins and components of the SWI/SNF complex. Additionally, growth factors pathways are constitutively activated by the COL1A1-PDGFB and ETV6-NTRK3 fusions in DFSP and CFS.

Due to the rarity of sarcomas, especially when considering the prevalence of individual subtypes, they are understudied cancers. As the fusion proteins present within translocation-associated sarcomas are inherent to tumor development, they provide an avenue of research for development of improved treatment. Additionally, increased understanding of these neoplasms at the molecular level can allow for therapies to be tailored to distinct subtypes. This review focuses on six pediatric sarcomas with tumor-associated translocations and will discuss the molecular genetics of these malignancies, potential therapeutic targets, and the status of agents directed against these targets in clinical trials.

Ewing sarcoma family of tumors

The Ewing sarcoma family of tumors (ESFT) is a group of bone and soft tissue small round blue cell malignancies that predominantly occur within the second decade of life. ESFT occurs primarily as tumors of the bone, with less than 15% of cases arising in extraosseous locations, such as soft tissues [3]. ESFT primary osseous sites are split between the extremities and the central axis, with an increased tendency for incidence in the shaft of long tubular bones, pelvis, and rib. Histologically, ESFT is comprised of sheets of homogeneous small round cells that express CD 99, a cell surface glycoprotein encoded by the MIC2 gene [4]. ESFT is the second most common bone malignancy in children and adolescents, with an annual incidence of 2.93 per million in the United States [5], and accounts for 3% of pediatric cancers. There is a slight male predominance (1.3:1) [4] and these tumors primarily afflict Caucasians, being extremely rare in Africans and African-Americans. The 5-year survival rate for ESFT is nearing 70%, although this number shrinks to approximately 20-30% in patients with metastatic, refractory

and/or recurrent disease [6]. The current treatment is multimodal consisting of intensive multi-agent chemotherapy, surgery and/or high dose radiation therapy. Systemic chemotherapeutic agents include alternating cycles of vincristine (vinca alkaloid), cyclophosphamide (nitrogen mustard), and doxorubicin (anthracycline) with ifosfamide (nitrogen mustard alkylator) and etoposide (topo-isomerase II inhibitor).

Cell of origin of Ewing sarcoma family of tumors

The histogenesis of ESFT has long been disputed. Although early reports suggested a neural crest origin, more recent evidence implies tumors originate from mesenchymal stem cells (MSCs). Support for a neural origin is provided by the presence of neural markers and ultrastructural features, as well as the ability of ESFT cell lines to undergo neural differentiation *in vitro* [7,8]. A mesenchymal histogenesis is suggested by the resemblance of gene expression profiles of ESFT cell lines subsequent to knock down of the most common ESFT fusion gene EWS-FLI1 to cells that are mesenchymal in origin [9]. Additionally, expression of EWS-FLI1 in murine primary bone marrow-derived mesenchymal progenitor cells resulted in transformation and growth of ESFT-like tumors *in vivo* [10].

Molecular genetics

The pathognomonic genetic aberration in ESFT fuses the EWS gene (also known as EWSR1, Ewing sarcoma breakpoint region 1) to one of five ETS transcription factors: FLI1, ERG, ETV1, ETV4, or FEV (Table 2-1). FLI1 (Friend leukemia virus integration 1) is the fusion partner in approximately 85% of cases and ERG in about 10%, while ETV1, ETV4, and FEV each account for less than 1% [4]. In very rare cases, FUS combines with ERG or FEV and EWS is juxtaposed to non-ETS genes [11] (Table 2-1). Adding to the complexity of multiple translocations, variation in the location of the chromosomal breakpoint results in numerous types of each fusion. For example, breakpoints can occur between exons 7 and 11 in EWS and

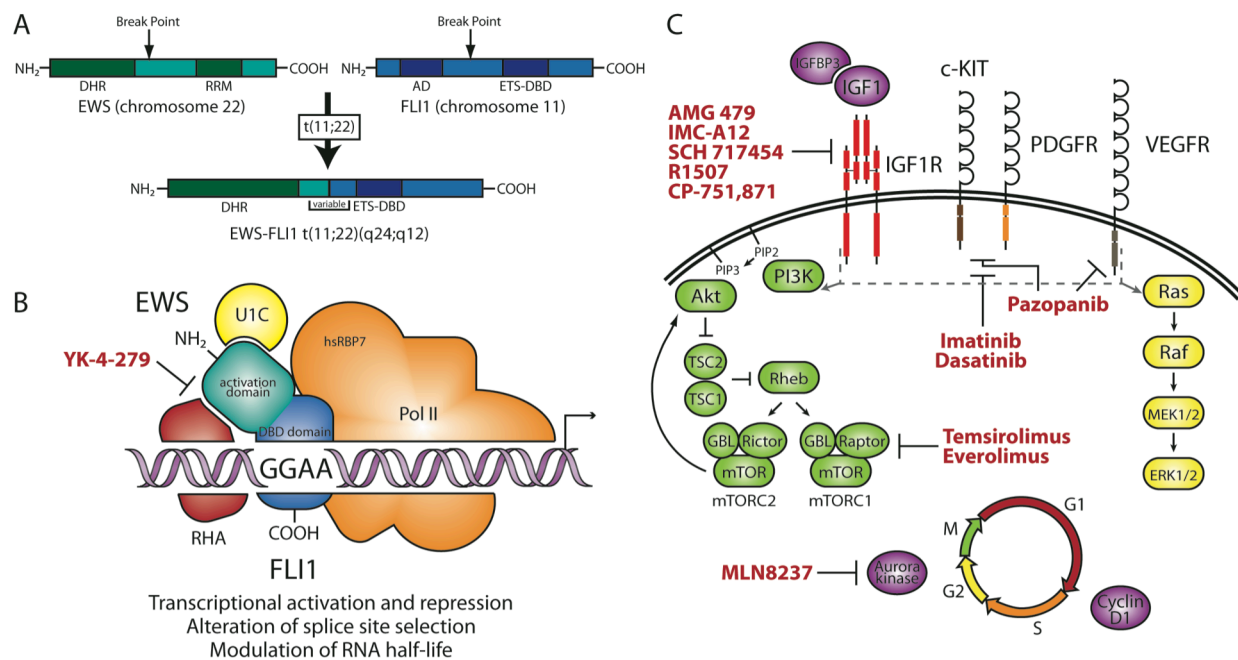


Figure 2-1. Molecular genetics and targeted therapies in ESFT. (A) Schematic of EWS-FLI1 t(11;22)(q24;q12) translocation. The EWS-FLI1 fusion includes the N-terminal activation domain of EWS, which contains multiple degenerate hexapeptide repeats (consensus SYGQQS), and the C-terminal ETS DNA-binding domain (ETS-DBD) of FLI1. The RNA recognition motif (RRM) of EWS and the activation domain (AD) of FLI1 are not retained in the fusion. Variation in the sites of chromosomal break points leads to multiple fusion types (bracketed region). (B) Putative molecular function of the EWS-FLI1 protein and selected protein–protein interactions. As an aberrant transcription factor, EWS-FLI1 regulates genes in part by binding to GGAA microsatellites upstream of target genes. EWS-FLI1 has been shown to interact with the splicing factor U1C (also known as SNRPC, small nuclear ribonucleoprotein polypeptide C), RNA helicase A (RHA), and the hRBP7 subunit of RNA polymerase II (Pol II), which links the protein to splicing and transcription. The small molecule that blocks the EWS-FLI1–RHA interaction is indicated in red. (C) Signaling pathways and targeted therapies in ESFT. EWS-FLI1 modulation of IGFBP3 and IGF1 and overexpression of IGF1R promote increased IGF1 signaling. ESFT cells also express PDGFR, c-KIT, and VEGFR. Activation of IGF1R, PDGFR, c-KIT, and VEGFR leads to downstream signaling through the PI3K and MAPK pathways (indicated by gray dashed line and arrows). EWS-FLI1 upregulates Aurora kinase A and cyclin D1, promoting progression through the cell cycle. Targeted therapeutic agents used in recent clinical trials for ES are indicated in bold red. Genes modulated by EWS-FLI1 are indicated in purple. Receptors overexpressed in ES are indicated in red. ESFT, Ewing sarcoma family of tumors; ETS, erythroblast transformation-specific; FLI1, Friend leukemia virus integration 1; IGFBP, insulin-like growth factor binding protein; IGF1, insulin-like growth factor 1; IGF1R, IGF1 receptor; MAPK, mitogen-activated protein kinase; PDGF, platelet-derived growth factor; PDGFR, PDGF receptor; PI3K, phosphoinositide-3-kinase; VEGFR, vascular endothelial growth factor receptor.

within introns 3 to 7 in FLI1, generating 18 possible in-frame EWS-FLI1 fusions [12]. Most of these have been observed in patient tumors, though type 1 and 2 fusions, which join EWS exon 7 to FLI1 exon 6 or 5, are present in the majority of cases. Initial reports suggested type 1 fusions confer a prognostic advantage to patients with localized disease, but more recent studies have demonstrated there is no difference in clinical outcome based on fusion type [13,14].

The most common EWS-ETS fusion, EWS-FLI1, is generated from the t(11;22)(q24;q12) reciprocal translocation that combines the N-terminal EWS activation domain and the C-terminal ETS DNA-binding domain of FLI1 [15] (Figure 2-1A). EWS is a member of the FET (FUS, EWS, and TAF15) family of proteins, which may be involved in transcription and mRNA splicing as they contain both an activation and RNA-binding domain [16]. The ETS family constitutes a group of 30 transcription factors characterized by the presence of a highly conserved ETS domain that mediates site-specific DNA binding. They also contain either an activation or a repression domain and are involved in various cellular processes such as cell proliferation and differentiation [17]. Because the more potent EWS activation domain replaces that of FLI1 while the FLI1 DNA-binding domain remains intact, EWS-FLI1 is thought to primarily act as an aberrant transcription factor. As most ETS transcription factors bind to a core consensus (GGAA/T), EWS-FLI1 has also been shown to interact with DNA in a site-specific manner through association with GGAA microsatellites [18]. Interactions with splicing factors and the ability to alter splice site selection suggest EWS-FLI1 also plays a role in RNA splicing [19,20]. The capacity of EWS-FLI1 to function post-transcriptionally is further demonstrated by modulation of target gene RNA half-life [21] (Figure 2-1B).

Target genes and targeted therapies

Ectopic expression of EWS-FLI1 in heterologous cell types or siRNA-mediated knock down of the fusion in ESFT cell lines have both been used to discover potential target genes. These

studies have identified both up and down regulated genes, demonstrating the function of EWS-FLI1 as both a transcriptional activator and repressor. Multiple direct targets have been confirmed through demonstration of EWS-FLI1 binding to their promoters including IGFBP3 (insulin-like growth factor binding protein 3) [22] and the Aurora A and B kinases [23].

IGFBP3 repression by EWS-FLI1 is one of the multiple connections between the insulin-like growth factor (IGF) pathway and ESFT pathogenesis. In addition to targeting IGFBP3, EWS-FLI1 has been shown to up-regulate IGF1 in mesenchymal progenitor cells [24]. The decrease in IGFBP3, which sequesters free IGF1 from binding to its receptor, combined with an increase in IGF1 levels promotes increased IGF signaling. Additionally, ESFT cell lines ubiquitously express the IGF1 receptor (IGF1R) and display autocrine production of IGF1 [25]. Moreover, IGF1R is necessary for EWS-FLI1-mediated cellular transformation [26] and inhibition of IGF1R suppresses tumor growth *in vitro* and *in vivo* [27]. In the clinic, phase I trials of monoclonal antibodies targeting IGF1R (Figure 2-1C) have shown partial and complete responses in ESFT patients [28]. Although these early results were promising, recent phase II studies showed limited response rates of approximately 10% for patients with recurrent or refractory Ewing sarcoma. To improve the efficacy of anti-IGF1R therapies, future work is being directed toward identification of predictive biomarkers associated with patients with Ewing sarcoma who benefit from treatment or combination therapy with other targeted agents [29-32] (Table 2-2). Additionally, resistance to therapy has been a common problem. One mechanism of resistance involves increased IGF2 signaling through the insulin receptor (IR), suggesting a combination of IGF1R and IR-targeting may be required for effective therapy [33].

Though the IGF pathway has received the most attention, other EWS-FLI1 target genes or interacting proteins provide potential therapeutic targets. EWS-FLI1 up-regulates both Aurora A and Aurora B, cell cycle-regulated serine/threonine kinases that are overexpressed in multiple cancers [23]. Preclinical testing revealed a maintained complete clinical response for an Aurora kinase A inhibitor (Figure 2-1C) in an ESFT xenograft model [34]. A phase II trial

evaluating the effects of this drug in pediatric leukemias and solid tumors, including ESFT, is currently underway (NCT01154816, Table 2-2). It has also been shown that RNA helicase A (RHA), a protein involved in the regulation of transcription and splicing, binds to EWS-FLI1 and enhances its transcriptional activity [35]. Utilization of a small molecule inhibitor to block the RHA-EWS-FLI1 interaction (Figure 2-1B) induces apoptosis in ESFT cells and reduces tumor growth in xenografts [36]. This promising preclinical evidence suggests these agents may be effective in clinical trials. Additionally, siRNA targeting of EWS-FLI1 itself results in decreased tumor growth [37]; however lack of efficient delivery methods render translation to patient therapy difficult.

Alveolar rhabdomyosarcoma

Rhabdomyosarcoma (RMS) is the most common pediatric soft tissue sarcoma, accounting for 5-7% of all malignancies in children and adolescents less than 20 years of age. RMS is the third most common extracranial solid tumor in children, surpassed only by neuroblastoma and Wilms' tumor. The overall five-year survival rate is 60%, rising to 80% when only considering cases with localized disease and dropping to 33% for those with metastatic disease [38]. Current therapy for RMS is similar to ESFT, employing a combination of adjuvant intensive chemotherapy with surgery and/or radiation to the primary and metastatic sites of disease.

RMS is divided into histologic subtypes. Embryonal RMS (ERMS) and alveolar RMS (ARMS) are the two major subtypes, accounting for approximately 60% and 20% of cases, respectively [2]. These tumors are differentiated both by histology and the presence of PAX-FOXO1 fusions in ARMS. RMS tumors can arise anywhere in the body, though frequency of primary sites varies with subtype and age of diagnosis. ERMS neoplasms tend to arise most often in the head and neck region, genitourinary tract, and retroperitoneum and occur in young children. Extremity tumors are more common in ARMS, which predominantly afflicts adolescents and young adults [39]. Additionally, ERMS has a superior prognosis, with a 69%

five-year survival compared to 49% for ARMS [38]. For patients that have refractory, recurrent and/or metastatic ARMS long-term survival is truly the exception rather than the rule.

Cell of origin of alveolar rhabdomyosarcoma

Though the expression of skeletal muscle markers and location of tumors in skeletal muscle suggest a myogenic origin, the exact cell of origin for ARMS remains uncertain. Mouse models and *in vitro* cell culture systems have provided evidence for both a skeletal muscle and mesenchymal stem cell origin. In a mouse model of ARMS, the most common ARMS fusion PAX3-FOXO1 was conditionally knocked in at the endogenous PAX3 locus in terminally differentiating Myf6-expressing skeletal muscle [40]. Mice expressing the fusion developed tumors that histologically and immunohistochemically resembled ARMS, albeit at very low frequency. Additional mouse studies restricting PAX3-FOXO1 expression to Pax7-expressing muscle satellite cells or unconditional knock-in have not resulted in tumors [41,42]. These results imply the ARMS cell of origin may be a differentiated skeletal muscle cell, though additional mutations may be necessary to facilitate the PAX3-FOXO1 fusion to drive tumorigenesis.

Molecular genetics

In addition to histologic differences, ARMS is distinguished from ERMS by the presence of specific chromosomal translocations present in the majority of ARMS tumors. The predominant translocation, t(2;13)(q35;q14), fuses PAX3 (paired box 3) to FOXO1 (forkhead box O1, also known as FKHR) [43]. Less commonly, the t(1;13)(p36;q14) translocation fuses another PAX gene, PAX7, to FOXO1 [44]. A recent study also identified rare, noncanonical t(2;2)(p23;35) and t(2;8)(q35;q13) translocations that unite PAX3 with the nuclear receptor transcriptional coactivators NCOA1 or NCOA2 [45] (Table 2-1).

Table 2-2. Targeted agents undergoing clinical testing for pediatric sarcomas.

Target	Drug	Phase	NCT Number	Eligible Sarcoma Types	Status
ALK, c-MET	Crizotinib (PF-02341066)	I/II	NCT01182896	Sarcoma, OS	Recruiting
Aurora kinase A	Alisertib (MLN8237)	II	NCT01154816	RMS, OS, EWS, NRSTS	Recruiting
BCL-2	Oblimersen (G3139)	I	NCT00039481	EWS, OS, SS, DSRCT	Completed
c-MET	Tivantinib (ARQ 197)	II	NCT00557609	CCS, ASPS	Completed
Death Receptor-5	Conatumumab (AMG 655)	I/II	NCT00626704	Locally advanced, unresectable or metastatic STS	Active
EGFR	Cetuximab (IMC-C225)	II	NCT00148109	EGFR positive bone and STS	Active
HDACs	PCI-24781	I/II	NCT01027910	Metastatic or unresectable sarcoma	Recruiting
HDACs	SB939	II	NCT01112384	Translocation-associated, metastatic sarcomas	Recruiting
IGF1R	Cixutumumab (IMC-A12)	II	NCT00668148	EWS, RMS, LMS, LS, SS	Active
IGF1R	Cixutumumab (IMC-A12)	II	NCT00831844	OS, EWS, RMS, SS	Recruiting
IGF1R	Figitumumab (CP-751,871)	I/II	NCT00560235	EWS	Active
IGF1R	Ganitumab (AMG 479)	II	NCT00563680	EWS, DSRCT	Active
IGF1R	Teprotumumab (R1507)	II	NCT00642941	EWS, OS, SS, RMS, ASPS, DSRCT, EMC, CCS, MLS	Active
IGF1R; mTOR	Cixutumumab; Temsirolimus	I	NCT00880282	Childhood solid tumor	Recruiting
IGF1R; mTOR	Cixutumumab; Temsirolimus	II	NCT01016015	Metastatic, locally advanced, or locally recurring bone and STS	Recruiting
IGF1R; mTOR	Figitumumab; Everolimus	I	NCT00927966	Advanced sarcoma	Active
mTOR	Everolimus (RAD001)	II	NCT01048723	Soft tissue extremity and/or retroperitoneal sarcomas	Recruiting
mTOR	Everolimus (RAD001)	II	NCT01216839	RMS and other STS (children and adolescents)	Recruiting
PDGFR- α	Olaratumab (IMC-3G3)	I/II	NCT01185964	STS	Recruiting
PDGFR, c-Kit	Imatinib (Gleevec)	II	NCT00031915	EWS, OS, SS, RMS, LS, MPNST, FS, AS	Completed
PDGFR, c-Kit	Imatinib (Gleevec)	II	NCT00085475	DFSP, GCF	Recruiting
RAF, VEGFR, PDGFR, c-Kit	Sorafenib	II	NCT00837148	SS, LMS, MPNST	Recruiting
RAF, VEGFR, PDGFR, c-Kit	Sorafenib	II	NCT00330421	Bone and STS	Completed
PDGFR, c-Kit, Src kinases, Eph kinases	Dasatinib	II	NCT00464620	RMS, MPNST, CS, EWS, ASPS, C, ES, GCTB, HPC, GIST	Active
VEGF	Bevacizumab	I/II	NCT01106872	Locally advanced, unresectable or metastatic STS	Recruiting
VEGF	Bevacizumab	II	NCT00643565	RMS and NRSTS (children and adolescents)	Recruiting
VEGF; HDACs	Bevacizumab; Valproic Acid	I/II	NCT01106872	Locally advanced, unresectable, or metastatic STS	Recruiting
VEGFR	Cediranib	II	NCT00942877	ASPS	Recruiting
VEGFR, PDGFR, c-Kit	Sunitinib	II	NCT00400569	LS, LMS, FS	Active
VEGFR, PDGFR, c-Kit; VEGFR	Sunitinib; Cediranib	II	NCT01391962	ASPS	Recruiting
VEGFR, PDGFR, c-Kit	Axitinib	II	NCT01140737	AS, LMS, SS, RMS, MPNST, fibroblastic, fibrohistiocytic	Recruiting
VEGFR, PDGFR, c-Kit	Pazopanib	I	NCT00929903	STS, DSRCT, extraosseous EWS	Recruiting
VEGFR, PDGFR, c-Kit	Pazopanib	II	NCT00297258	STS (LMS, SS, adipocytic tumors)	Active
VEGFR, PDGFR, c-Kit	Pazopanib	II	NCT01059656	DFSP	Not yet recruiting
VEGFR, PDGFR, c-Kit	Pazopanib	III	NCT00753688	Metastatic STS	Active

Abbreviations: AS, angiosarcoma; ASPS, alveolar soft part sarcoma; C, chordoma; CCS, clear cell sarcoma; CS, chondrosarcoma, DFSP, dermatofibrosarcoma protuberans; DSRCT, desmoplastic small round cell tumor; EMC, extraskeletal myxoid chondrosarcoma; ES, epithelioid sarcoma; EWS, Ewing sarcoma; FS, fibrosarcoma; GCF, giant cell fibrosarcoma; GCTB, giant cell tumor of bone; GIST, gastrointestinal stromal tumor; HPC, hemangiopericytoma; LMS, leiomyosarcoma; LS, liposarcoma; MLS, myxoid liposarcoma; MPNST, malignant peripheral nerve sheath tumor; NRSTS, non-rhabdomyosarcoma soft tissue sarcoma; OS, osteosarcoma; RMS, rhabdomyosarcoma; SS, synovial sarcoma; STS, soft tissue sarcoma.

PAX3 and PAX7 are part of the paired box family of transcription factors, which are involved in embryonic development and myogenesis [46]. FOXO1 is a member of a subfamily of forkhead transcription factors regulated by the PI3K (phosphoinositide-3-kinase) pathway and believed to play a role in myogenic growth and differentiation [47]. Both translocation breakpoints consistently occur within the seventh intron of the PAX gene and the first intron of FOXO1, resulting in a chimeric transcription factor that contains the PAX DNA-binding domain and transcriptional activation domain of FOXO1. Fusion type has been found to correlate with clinical outcome, as patients with PAX7-FOXO1-positive tumors had better overall survival rates than those with tumors containing the PAX3-FOXO1 fusion [48]. More recently, clinical characteristics and prognosis of fusion-negative ARMS were found to be more similar to ERMS than fusion-positive ARMS, implying the presence of the PAX-FOXO1 fusion is more crucial than histology to the underlying biology of the tumor [49].

Target genes and targeted therapies

Initial PAX3-FOXO1 target genes were identified by evaluating the expression of known PAX3 target genes in ERMS cells transduced with PAX3-FOXO1. Up regulation of MET (met proto-oncogene/hepatocyte growth factor receptor) upon PAX3-FOXO1 expression and an observed correlation between MET and PAX3-FOXO1 in tumor samples suggested MET is a downstream target [50]. The role of MET in ARMS tumorigenesis was further characterized by experiments that demonstrated MET is required for PAX3-FOXO1-mediated transformation of mouse embryonal fibroblasts and shRNA knock down of MET results in decreased tumor growth *in vitro* and *in vivo* [51]. More recently, studies have shown that MET is post-transcriptionally regulated, as low levels of the microRNAs miR-1 and miR-206 result in de-repression and up regulation of MET in RMS cells [52]. Furthermore, overexpression of these miRNAs promoted myogenic differentiation and inhibited tumor growth *in vivo* [52,53]. Additionally, a preclinical study

demonstrated the ability of a c-MET small molecule inhibitor to hinder growth of ARMS cell lines [54]. All this data intimates that targeting MET could be an effective therapy in ARMS.

Components of the IGF system are also potential therapeutic targets in ARMS. Heterologous expression of the PAX3-FOXO1 fusion results in an increase in IGF1R levels and overexpression of IGF2 and IGF1R has been observed in ARMS and ERMS tumors and cell lines [55,56]. Elevated IGF2 levels in ERMS result from loss of heterozygosity at the 11p15.5 locus while in ARMS it may be transcriptionally up regulated. Introduction of PAX3-FOXO1 into NIH-3T3 cells identified a myogenic transcriptional signature distinct from PAX3 alone that included genes such as MyoD, myogenin, and IGF2 [57]. Multiple studies have demonstrated suppression of tumor growth *in vivo* and *in vitro* with small molecular inhibitors and monoclonal antibodies targeting IGF1R. This has led to both phase I and II clinical trials to evaluate anti-IGF1R therapy in RMS. In phase I trials involving multiple tumor types, responses were only observed in Ewing sarcoma patients. However, preliminary phase II data have shown three objective radiological responses for RMS patients [58].

The platelet-derived growth factor alpha receptor (PDGFR α) is another gene that has shown to be transcriptionally up regulated by PAX3-FOXO1 [59]. PDGFR α is overexpressed in human ARMS and ERMS tumors as well as in mouse models of ARMS. SiRNA down regulation of PDGFR α resulted in decreased cell growth *in vitro* and PDGFR α inhibition in mouse models using imatinib mesylate (Gleevec or STI-571) or a PDGFR α neutralizing antibody led to disease stabilization and in some cases resistance to therapy [60]. Resistance has also been observed with anti-IGF1R therapy, which may be due to activation of other growth factor receptors such as HER-2 (ERBB2) and PDGFR α [61,62]. Because both IGF1R and PDGFR α are potential therapeutic targets that have shown resistance as single agents, combination therapy may enhance patient response. Combination of anti-IGF1R therapy with mTOR (mechanistic target of rapamycin) inhibitors is currently being evaluated in a phase I trial for pediatric solid tumors (NCT00880282) and in combination with cytotoxic chemotherapy in a

Children's Oncology Group study (ARST08P1) for patients with high-risk rhabdomyosarcoma (Table 2-2).

Synovial sarcoma

Synovial sarcoma (SS) is the most common non-rhabdomyosarcoma soft tissue sarcoma in adolescents and young adults, accounting for approximately 8% of all soft tissue sarcomas. The overall five-year survival rate is between 70 and 80%, but as with most sarcomas, this number drops sharply for those patients with metastatic and recurrent disease. Other than complete surgical resection of localized synovial sarcomas, there is no standard of care for treatment and approach to these tumors may vary from center to center. Radiation therapy may be used as an adjuvant therapy to improve local control and chemotherapy is generally reserved for larger tumors or in patients with metastatic disease.

Cell of origin of synovial sarcoma

Synovial sarcoma is histologically unique, displaying both biphasic and monophasic tumors. Monophasic tumors are mesenchymal in origin, exhibiting a spindle cell morphology that is difficult to distinguish from fibrosarcoma. Biphasic tumors furthermore contain cells of epithelial differentiation that form a glandular component within the mesenchymal spindle cells [39]. The designation of synovial sarcoma originated from tumor proximity to large joints, as most tumors arise in the extremities, and microscopic resemblance to synovial tissue. However, this is a misnomer as the histogenesis is not of synovial origin [63]. The presence of both epithelial and mesenchymal components of tumors suggests the cell of origin may be a stem or progenitor cell. This is supported by the presence of stemness genes in SS cell lines and the ability of SS cells to be terminally differentiated along the mesenchymal lineage after knock down of the fusion gene SS18-SSX [64]. SS tumor proximity to skeletal muscle also alludes to a myogenic origin. In a mouse model where the expression of SS18-SSX2 was driven by the myogenic regulatory

factor Myf5, tumors developed that were histologically similar to human synovial sarcoma. Myf5 is expressed early in the skeletal muscle developmental lineage within immature myoblasts. Myf6-driven SS18-SSX2, which is restricted to further differentiated myocytes and myofibers, did not result in tumors, suggesting SS arises shortly after differentiation from a muscle stem cell [65].

Molecular genetics

The underlying genetic aberration in SS results from a specific t(X;18)(p11.2;q11.2) translocation that fuses SS18 (synovial sarcoma translocation, chromosome 18, also known as SYT) to either SSX1, SSX2, or SSX4 (synovial sarcoma, X breakpoint 1, 2, or 4) [66-69] (Figure 2-2A). SS18 is a ubiquitously expressed, nuclear protein that contains a novel SNH (SYT N-terminal homology) domain that allows for interaction with chromatin remodeling factors and a C-terminal QPGY domain that resembles the transactivation domain within the FET family of proteins. Despite the absence of a DNA-binding domain, SS18 is thought to function as a transcriptional activator and may play a role in signal transduction via its SH2 and SH3-binding motifs. The SSX genes constitute a family of highly homologous proteins located on the X chromosome. They are believed to act as transcription repressors due to the presence of a Kruppel-associated box (KRAB) domain and SSX repression domain (SSXRD). The SSX proteins also lack a DNA-binding domain so must rely on protein-protein interactions to mediate transcriptional repression [70].

The t(X;18) translocation fuses the C-terminus of SSX to all but the last eight amino acids of SS18, generating a chimeric protein that contains both transcriptional activation (QPGY) and repression (SSXRD) domains (Figure 2-2A). The SSXRD allows SS18-SSX proteins to co-localize with components of the polycomb group (PcG) chromatin remodeling repressor complex while the SS18 SNH domain facilitates interaction with members of the SWI/SNF complex [71,72] (Figure 2-2B). This suggests the fusion drives tumor progression

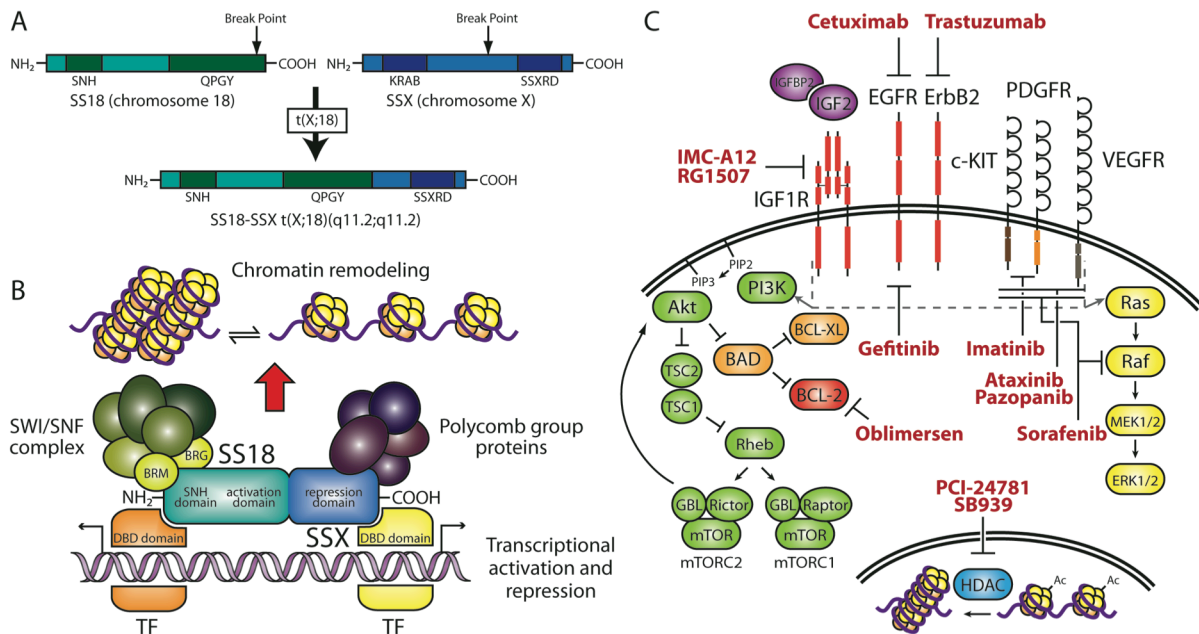


Figure 2-2. Molecular genetics and targeted therapies in SS. (A) Schematic of the SS18-SSX t(X;18)(q11.2;q11.2) translocation. The SS18-SSX fusion contains both the SNH (SYT N-terminal homology) and QPGY activation domains of SS18 as well as the SSXR. The SSX KRAB domain is not retained in the fusion. (B) Putative molecular function of SS18-SSX and selected protein-protein interactions. The SNH domain facilitates binding to components of the SWI/SNF complex while the SSXR interacts with polycomb group proteins, which results in chromatin remodeling. Interactions with transcription factors (TFs) may also lead to transcriptional activation and repression. (C) Signaling pathways and targeted therapies in SS. Activation of growth factor receptors leads to downstream signaling through the PI3K and MAPK pathways (indicated by gray dashed box and arrows). Histone deacetylases (HDACs) remove acetyl groups (Ac) from histones, resulting in condensed chromatin. Targeted therapeutic agents used in recent clinical trials for SS are indicated in bold red. EGFR, epidermal growth factor receptor; IGF1, insulin-like growth factor 1; KRAB; Kruppel-associated box; MAPK, mitogen-activated protein kinase; PDGFR, platelet-derived growth factor receptor; PI3K, phosphoinositide-3-kinase; SNH, SYT N-terminal homology; SS, synovial sarcoma; SSXR, SSX repression domain; SWI/SNF, switch/sucrose nonfermentable; SYT, synovial sarcoma translocation; VEGFR, vascular endothelial growth factor receptor.

though epigenetic chromatin remodeling. The SS18-SSX1 fusion protein is able to transform rat fibroblasts and association the hBRM/hSNF2 α chromatin remodeling factor is required for transformation [73]. Its presence is required for sarcomagenesis as siRNA down regulation of SS18-SSX expression inhibits tumor growth *in vitro* and *in vivo* [74].

SS18 is fused to either SSX1 or SSX2 over in over 90% of SS cases and is only rarely observed bound to SSX4. Although initial studies showed patients with SS18-SSX2 fusions had improved survival rates, an expanded study performed more recently concluded there was no correlation between fusion variant and survival [75]. While fusion type may not determine survival, it is strongly associated with histology as biphasic and monophasic tumors contain the SS18-SSX1 and SS18-SSX2 transcripts, respectively [76]. Determining the presence of the SS18-SSX fusion is crucial in the suspected diagnosis of SS, as monophasic SS can be a diagnostic dilemma. Like ESFT, SS can express CD99 and BCL-2 (B-cell CLL/lymphoma 2).

Target genes and targeted therapies

Expression profiling has uncovered several genes modulated by the SS18-SSX fusion. cDNA microarray analysis of synovial sarcoma and closely related spindle cell tumors revealed a set of 153 genes that distinguished SS from the other neoplasms as well as 21 genes that were differentially expressed between biphasic and monophasic tumors. Genes such as insulin-like growth factor binding protein 2 (IGFBP2), ERBB2, and insulin-like growth factor II (IGF2) were up regulated in SS and those encoding keratins and the ETS transcription factor ELF3 were overexpressed in biphasic tumors [77]. Evidence for the role of IGF2 in SS pathogenesis is further supported by studies in which SS18-SSX fusions were exogenously expressed in heterologous cell systems. Gene expression profiling determined IGF2 to be the most highly up regulated gene upon SS18-SSX2 expression in 293T cells [78] and SS18-SSX1 expression in human primary lung fibroblasts [79].

SS18-SSX2 was shown to interact with BRG1, a component of the SWI/SNF complex, and BRG1 was found to bind to the IGF2 promoter. This data combined with active chromatin marks observed upon induction of SS18-SSX2 suggests the fusion interacts with BRG1 to epigenetically modulate IGF2 expression [78]. Additionally, SS18-SSX2 is necessary for maintenance of IGF2 expression and IGF2 is required for SS18-SSX1 mediated tumor formation [79]. IGF2 expression results in activation of the IGF1R and phosphorylation of the downstream proteins Akt and MAPK (mitogen-activated protein kinase). Providing evidence the IGF pathway could be a therapeutic target, treatment of SS cell lines with the IGF1R inhibitor NVP-AEW541 resulted in impaired cell growth and increased apoptosis [80].

Immunohistochemical and molecular studies have demonstrated high expression levels of the anti-apoptotic protein BCL-2 in the majority of SS tumors [81]. Due to the absence of genomic amplifications or rearrangements, overexpression of BCL-2 may result from transcriptional activation [82]. Though BCL-2 has not been shown to be a direct target of SS18-SSX, lower mRNA and protein levels in SS tumors and cell lines lacking the t(X,18) translocation suggests an association does exist [83]. Furthermore, BCL-2 antisense oligonucleotide treatment of a translocation positive SS cell line resulted in increased sensitivity to doxorubicin treatment, implying BCL-2 may be a promising therapeutic target [84]. In a phase I trial assessing the effectiveness of BCL-2 antisense therapy (Figure 2-2C) in combination with chemotherapy in childhood solid tumors, two synovial sarcoma patients displayed prolonged stable disease [85].

EGFR (epidermal growth factor receptor) is also overexpressed in SS. Microarray analysis of a set of 41 soft tissue tumors and subsequent clustering analysis identified EGFR as part of cluster that showed SS specific expression [86]. Immunohistochemical studies and molecular characterization have confirmed the presence of EGFR in SS [87,88]. This data led to a phase II trial to establish the efficacy of the EGFR inhibitor gefitinib (Figure 2-2C) in EGFR-positive, chemoresistant synovial sarcoma. In this trial, stable disease was the best observed

response, suggesting EGFR is not required for tumorigenesis [89]. Gene expression profiling and immunohistochemical studies have identified another member of the EGFR family, HER-2 (ERBB2), that is up regulated in SS that may provide an alternate target for the treatment of this disease [77,88] (Figure 2-2C).

Dermatofibrosarcoma protuberans

Dermatofibrosarcoma protuberans (DFSP) is a relatively rare cutaneous malignancy, accounting for approximately 0.1% of all cancers and 1% of soft tissue sarcomas. DFSP has an annual incidence rate of 4.2 per million and primarily afflicts adults between the ages of 30 and 50 years [90]. Pediatric cases, both congenital and in young children, do occur, but with much less frequency than adult cases. The annual incidence drops to 0.3 per million in children younger than nine, resulting in only a small number of reported cases [90,91]. DFSP is described as a neoplasm of intermediate malignancy due to its slow growth rate but high frequency of recurrence. Owing to metastases occurring in less than 5% of patients, the five-year survival rate exceeds 95% [90,91].

Treatment of DFSP, like other soft tissue sarcomas, centers around achieving a complete surgical resection. Radiation is used when surgical margins are positive and a re-resection is not feasible. Chemotherapy is only used in metastatic cases, but there is increasing evidence that imatinib therapy can be used in an adjuvant setting in patients with recurrent, refractory, and/or metastatic disease. The mechanism for this activity is discussed later.

As suggested by its name, DFSP tumors arise in the dermis, infiltrating the dermal stroma and often breaching the subcutaneous fat. Primary site locations can occur throughout the body, though the trunk, proximal extremities, and head and neck are the most common [90]. Closely related giant cell fibroblastoma (GCF) is a low grade pediatric soft tissue neoplasm occurring within the first two decades of life that shares many clinical, morphological, and

molecular genetic facets with DFSP, but has a distinct histological pattern. Due to its similarities to DFSP, GCF is described by several investigators as a pediatric form of this disease [92].

Cell of origin of DFSP

The histogenesis of DFSP remains uncertain. Initial studies suggested a fibroblastic origin, based on ultrastructural evidence and the cells' ability to synthesize collagen. CD34 expression, which is observed in neural tumors, combined with a spindle shape similar to endoneurial cells implied a neural origin. The expression of histiocytic enzymes, histologic similarity to benign and malignant histiocytomas, and ultrastructural characteristics similar to dendritic dermal cells lead to the proposition of a histiocytic origin for DFSP. Another theory that has been presented is that DFSP tumors arise from an undifferentiated mesenchymal stem cell [93].

Molecular genetics

DFSP tumors contain either the t(17;22)(q22;q13.1) reciprocal chromosomal translocation or a supernumerary ring chromosome derived from t(17;22). Both of these karyotypic aberrations result in a fusion of the genes COL1A1 (encoding the pro-alpha1 chain of type I collagen) on 17q21-22 and PDGFB (encoding the platelet-derived growth factor B chain) on 22q13.1 [94] (Figure 2-3A). Rings are predominantly found in adult cases, though occasionally translocations are identified. In contrast, all pediatric tumors contain translocations. DFSP variants and related malignancies such as GCF have also been found to contain the COL1A1-PDGFB fusion.

The t(17;22) breakpoint occurs upstream of the second exon of PDGFB gene and within the alpha-helical region of COL1A1. This results in the removal of the both the PDGFB inhibitory regulatory elements and signal peptide in the COL1A1-PDGFB fusion and placement of remainder of PDGF locus, beginning with exon 2, under the control of the COL1A1 promoter. Although the PDGFB breakpoint is invariably located in the first intron, the one in the COL1A1

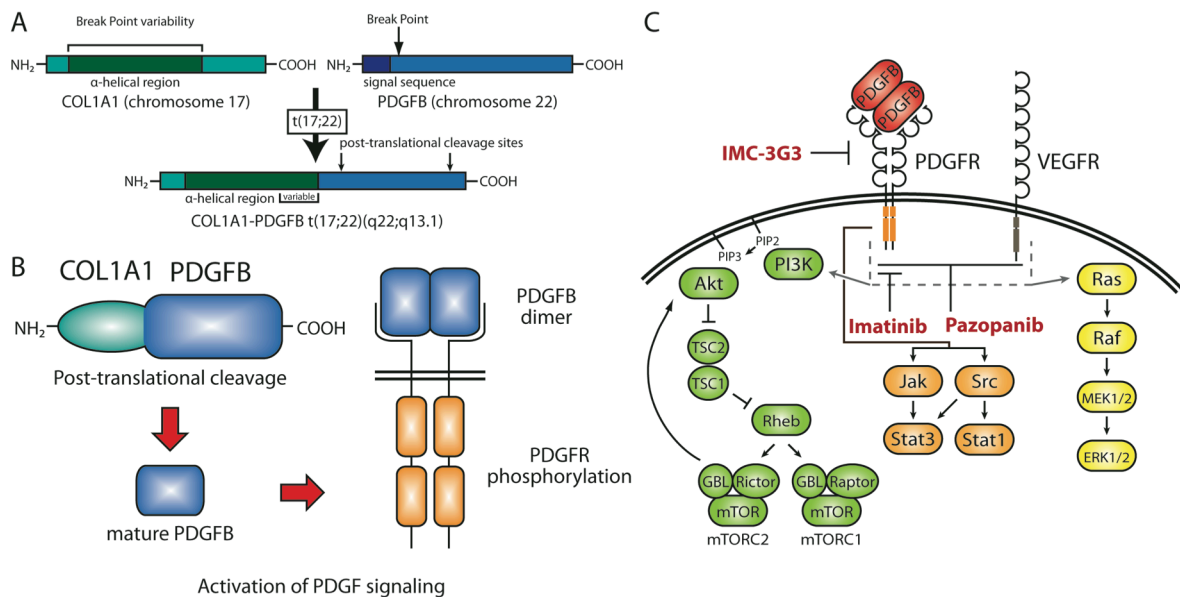


Figure 2-3. Molecular genetics and targeted therapies in DFSP. (A) Schematic of the COL1A1-PDGFB t(17;22)(q22;q13.1) translocation. The COL1A1-PDGFB fusion joins the α -helical region of COL1A1 to PDGFB lacking its signal sequence. The COL1A1 N-terminal signal sequence replaces that of PDGFB. Break points throughout the α -helical region in COL1A1, but only occur within the first intron of PDGFB. PDGFB post-translational cleavage sites are retained in the fusion. (B) Putative molecular function of the COL1A1-PDGFB fusion. The COL1A1 signal sequence allows for protein export and post-translational cleavage results in the generation of mature PDGFB. Ligand binding of the PDGF-BB dimer results in receptor dimerization, autophosphorylation, and activation. (C) Signaling pathways and targeted therapies in DFSP. Activation of PDGFR by the PDGFB dimer results in downstream signaling through the PI3K, MAPK, and Jak/Stat (Janus kinase/signal transducer and activator of transcription) pathways. VEGFR is also activated in DFSP and signals through the PI3K and MAPK pathways. Targeted therapeutic agents in current clinical trials for DFSP (imatinib and dasatinib) and soft tissue sarcomas expressing PDGFR- α (IMC-3G3) are indicated in bold red. DFSP, dermatofibrosarcoma protuberans; MAPK, mitogen-activated protein kinase; PDGFB, platelet-derived growth factor B chain; PDGFR, platelet-derived growth factor receptor; PI3K, phosphoinositide-3-kinase; VEGFR, vascular endothelial growth factor receptor.

locus can occur within multiple exons, probably due to the repetitive nature of the alpha-helical region. Most of the COL1A1 coding sequence is postulated to be functionally irrelevant as PDGFB is post-translationally cleaved at sites retained in the fusion to generate the mature growth factor. In contrast, the replacement of the PDGF repressor elements with the COL1A1 promoter allows for aberrant expression of the protein. The COL1A1 N-terminal signal sequence, also retained in the fusion, permits PDGFB secretion, resulting in constitutive activation of the PDGF β pathway [95] (Figure 2-3B). The finding that there is no correlation between COL1A1-PDGFB fusion type and clinical response or histology supports the theory that the COL1A1 portion of the fusion only provides a mechanism for PDGFB overexpression [96].

Signaling pathways and targeted therapies

The COL1A1-PDGFB fusion has been shown to transform NIH3T3 cells and its transforming activity is dependent on active PDGF signaling [97]. Additionally, stable transfection of the fusion in a Chinese hamster lung fibroblastic line led to growth factor independent growth and tumor formation in nude mice [95]. Both of these studies demonstrated activation of the PDGF- β receptor as a result of constitutive PDGFB expression, indicating the involvement of PDGF signaling in DFSP tumorigenesis. In order to block this pathway, NIH-3T3 cells transformed with COL1A1-PDGFB and DFSP tumor-derived primary cultures were treated with imatinib mesylate, which inhibits the PDGF receptor [98] (Figure 2-3C). Growth inhibitory effects were observed *in vitro* and *in vivo*, suggesting imatinib could be an effective therapy in the treatment of DFSP.

Initial case reports demonstrating patient response to imatinib led to a study of its activity in 10 patients with locally advanced or metastatic DFSP. Despite low levels of PDGFR phosphorylation in patient tumors, imatinib was shown to be an effective therapy as four patients with locally advanced disease displayed a complete clinical response [99]. On a larger

scale, the efficacy of imanitib treatment is currently being evaluated in a phase II trial for DFSP and GCF (NCT00085475, Table 2-2). In addition to imanitib, another tyrosine kinase inhibitor pazopanib, which targets VEGFR in addition to PDGFR (Figure 2-3C), has just begun phase II testing for DFSP (NCT01059656, Table 2-2).

Congenital fibrosarcoma

Congenital (or infantile) fibrosarcoma (CFS) is a malignant tumor of fibroblastic spindle cells that occurs almost exclusively within the first two years of life, generally within the first 3 months. The annual incidence is only 0.2 per million, but CFS is one of the most common pediatric non-rhabdomyosarcoma soft tissue sarcomas [2]. Despite a 30% recurrence rate, very few tumors metastasize and the 5-year survival rate can exceed 90%. This is in contrast to adult-type fibrosarcoma, which, though histologically similar to CFS, is a more aggressive tumor with a higher rate of metastasis and poorer outcome. Tumors develop in deep soft tissues, occurring most often in the distal limbs and less frequently in the trunk and head and neck region. Myoblastic differentiation markers have been observed in some CFS cases, suggesting the cell of origin could be a fibroblastic or myofibroblastic precursor [100].

Treatment for CFS involves complete surgical resection with negative margins. Radiation can be used, though because these patients are generally quite young this therapeutic modality is avoided. Systemic neoadjuvant chemotherapy is currently under investigation in clinical trials for this disease.

Molecular Genetics

The main karyotypic aberration associated with CFS is the t(12;15)(p13;q25) rearrangement that fuses the transcription factor ETV6 (ets variant 6, also known as TEL) to the receptor tyrosine kinase NTRK3 (neurotrophic tyrosine kinase receptor type 3, also known as TRKC) [101] (Figure 2-4A). Though first identified in CFS, the ETV6-NTRK3 fusion is not unique to this

malignancy. Expression has also been observed in congenital mesoblastic nephroma [102], secretory breast carcinoma [103], and acute myelogenous leukemia [104]. The fusion links the sterile alpha motif (also known as pointed or helix-loop-helix) oligomerization domain of ETV6 to the kinase domain of NTRK3. This allows the protein to self-associate independent of ligand binding, resulting in an auto-phosphorylated, constitutively active kinase (Figure 2-4B).

ETV6-NTRK3 is able to transform NIH-3T3 cells, which requires both the ETV6 oligomerization domain and NTRK3 kinase domain [105]. ETV6-NTRK3 mediated cellular transformation is also dependent on IGF1R signaling as the absence of IGF1R or inhibition of the downstream PI3K and MAPK pathways prevented anchorage-independent growth in soft agar [106,107]. Analogous experiments have been performed in breast epithelial cells, yielding similar results. Blocking the IGF1R pathway also inhibits ETV6-NTRK3 transformation of breast epithelial cells and treatment of transformed cells with a dual specificity IGF1R/IR (insulin receptor) inhibitor results in decreased tumor growth *in vivo* [108]. Additionally, expressing the fusion in the Eph4 mammary epithelial line resulted in tumors that retained epithelial markers [103]. This contrasts to transformations of NIH-3T3 and Scg6 mammary myoepithelial cells that display mesenchymal features, which show little or no evidence of differentiation [103,107]. These results suggest the ETV6-NTRK3 fusion does not drive differentiation, but activates lineage-independent oncogenic pathways [109].

Signaling pathways and targeted therapies

In addition to dependence on IGF1R for cellular transformation, ETV6-NTRK3 is linked to the IGF1 pathway through its interaction with IRS-1 (insulin receptor substrate 1). IRS-1 is an adaptor protein that recognizes the phosphorylated IGF1R or IR and facilitates signaling through downstream pathways such as PI3K and MAPK. IRS-1 is constitutively phosphorylated in ETV6-NTRK3 transformed cells and binds to the C-terminus of the fusion at its phosphotyrosine binding domain [110]. This interaction with IRS-1 is likely the cause of the constitutive activation

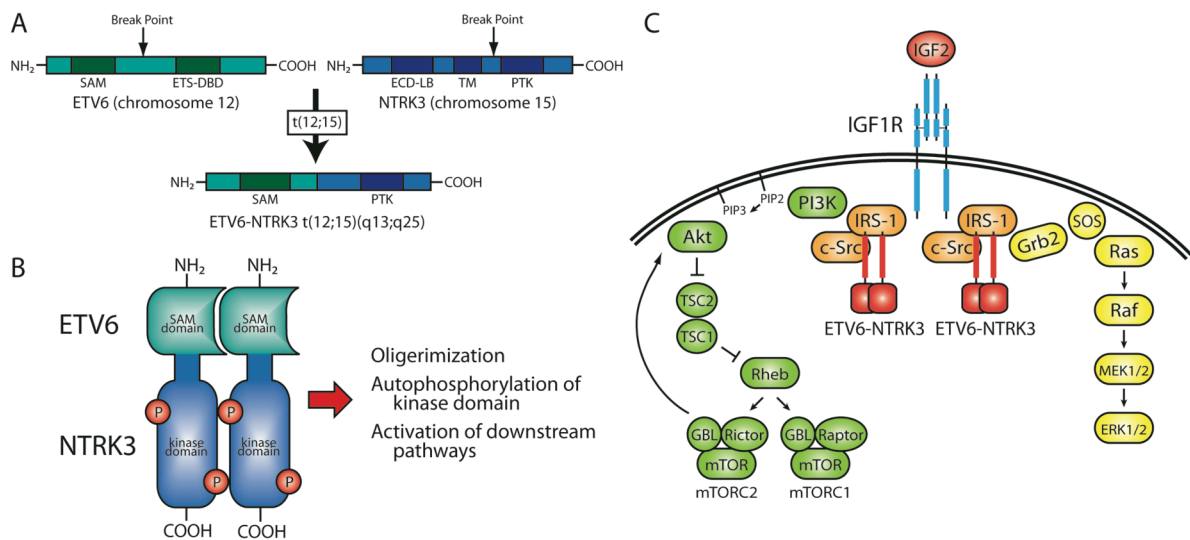


Figure 2-4. Molecular genetics of CFS. (A) Schematic of ETV6-NTRK3 t(12;15) translocation. The ETV6-NTRK3 fusion contains the SAM (sterile alpha motif) oligomerization domain of ETV6 and the protein tyrosine kinase (PTK) domain of NTRK3. The DNA binding domain (ETS-DBD) of ETV6 and the extracellular ligand binding (ECD-LB) and transmembrane (TM) domains of NTRK3 are not retained in the fusion. (B) Putative molecular function of the ETV6-NTRK3 fusion. The SAM domain causes protein oligomerization, allowing for autophosphorylation of the NTRK3 kinase domain and activation of downstream signaling pathways. (C) Signaling pathways in CFS. C-Src facilitated binding of the C-terminus of ETV6-NTRK3 to IRS-1 leads to signaling through the PI3K and MAPK pathways. IGF1R, which is required for ETV6-NTRK3 mediated cellular transformation, likely serves to localize the ETV6-NTRK3-IRS-1-c-Src complex to the cell membrane. Overexpression of the IGF1R ligand IGF2 (insulin-like growth factor 2) has been observed in primary CFS tumors and may also contribute to dependence on IGF1 signaling. Overexpressed proteins are indicated in red.

of the PI3K and MAPK pathways observed in ETV6-NTRK3 expressing cells [107]. Additionally, the ETV6-NTRK3-IRS-1 interaction is mediated by c-Src, which is required for induction of the PI3K-Akt cascade [111].

ETV6-NTRK3 has also been shown to suppress TGF- β (transforming growth factor beta) signaling. The fusion binds to TGF- β receptor II and inhibits its ability to phosphorylate and activate TGF- β receptor I, blocking activation of downstream signaling. This suggests that growth of ETV6-NTRK3 transformed cells requires inhibition of TGF- β signaling [112]. Overall, the elucidation of signaling molecules downstream of ETV6-NTRK3 provide potential therapeutic targets such as IGF1R and Src for which agents are already in use for the treatment of other cancers.

Alveolar soft-part sarcoma

Alveolar soft-part sarcoma (ASPS) is an indolent but malignant soft tissue tumor of uncertain histogenesis. ASPS is a rare neoplasm, accounting for less than 1% of all soft tissue sarcomas, that primarily affects adolescents and young adults between the ages of 15 and 35 years. There is predilection for females, with up to 60% of cases occurring in women. ASPS is characterized by compartments of polygonal tumor cells that form a distinguishing alveolar pattern that gives the malignancy its name [113].

ASPS is a slow-growing tumor with a prolonged clinical course and frequent metastases, often in the lung [39]. As a result, survival rates drop from approximately 80% at two years to 15% at 20 years. Tumors arise in muscle and deep soft tissues, with the incidence of primary sites varying between adults and children. In adults, common sites include the extremities, trunk, head and neck, and retroperitoneum while in children and adolescents, a higher number of tumors develop in the head and neck region [113].

Treatment of ASPS involves an attempt at complete surgical resection of the primary site and metastatic sites. Unfortunately, these patients frequently develop diffuse pulmonary

metastatic disease making surgical resection nearly impossible. There is no standard treatment for this indolent STS, and ASPS is generally not sensitive to the current armamentarium of cytotoxic chemotherapeutics.

Molecular Genetics

ASPS is characterized by a der(17)t(X;17)(p11.2;q25.3) non-reciprocal translocation that fuses the ASPL (also known as ASPSCR1) gene located at 17q25.3 to the transcription factor TFE3 present at Xp11.22 [114]. ASPSCR1 (alveolar soft part sarcoma chromosome region, candidate 1) is a ubiquitously expressed gene originally identified in context of the fusion. Protein motif analysis detected a C-terminal UBX (ubiquitin regulatory X) domain, which is structurally homologous to ubiquitin and interacts with the Cdc48/p97 AAA ATPase [115]. Though there is little functional information about the ASPL protein, its murine homolog has been shown to regulate trafficking of the GLUT4 glucose transporter [116]. TFE3 (transcription factor binding to IGHM enhancer 3) is a member of the MiTF-TFE (microphthalmia transcription factor-transcription factor E) family of basic/helix-loop-helix/leucine zipper transcription factor family [117]. It interacts synergistically with Smad3 to mediate TGF- β -induced transcription and plays a role in osteoclast development [118,119].

The breakpoints on chromosomes X and 17 result in a fusion that loses the UBX domain within ASPL, but retains the DNA-binding domain, dimerization domain, nuclear localization signal, and C-terminal activation domain of TFE3. Variable breakpoints have been reported for TFE3, resulting in two types of ASPL-TFE3 fusions. The type 1 breakpoint within intron 3 results in the loss of the TFE3 N-terminal activation domain and fusion of ASPSCR1 to exon 4. ASPL is fused to TFE3 exon 3 in the type 2 fusion, which includes the N-terminal activation domain [113,114]. Both type 1 and type 2 ASPL-TFE3 fusions have also been detected in pediatric renal neoplasms [120].

Target genes and targeted therapies

ASPS is a frustrating disease for patients, parents, and oncologists because of its frequent metastatic presentation and general resistance to standard cytotoxic chemotherapies. Novel therapeutic approaches for this disease are needed. Because ASPL-TFE3 is a chimeric transcription factor, target genes provide potential therapeutic targets. MET was found to be a direct target gene and transcriptional up regulation by ASPL-TFE3 leads to autophosphorylation and activation of downstream signaling pathways. Furthermore, treatment of ASPL-TFE3 containing cell lines with an siRNA or small molecular inhibitor targeting MET resulted in a decrease in cell viability and reduces phosphorylation of downstream proteins [121]. The treatment of ASPS with the selective MET inhibitor ARQ 197 is currently undergoing analysis in phase II clinical trials (NCT00557609, Table 2-2). Stable disease was observed in ASPS patients based on preliminary data, which is promising given the chemoresistant nature of the tumor [122].

The vascularity of ASPS has prompted molecular analysis of angiogenesis genes and clinical use of anti-angiogenic therapies in the treatment of the disease. An angiogenic gene oligoarray identified a unique signature of 18 up regulated angiogenesis genes in ASPS [123]. Genome-wide microarray analysis also confirmed elevated levels of angiogenesis transcripts, including c-MET and VEGF (vascular endothelial growth factor), in addition to identifying genes involved in processes such as cell proliferation and metastasis [124]. In one case report, a highly vascular, chemoresistant ASPS with VEGF expression was treated with bevacizumab, a monoclonal antibody against VEGF- α , in combination with interferon α 2b, resulting in stability of disease [125].

The vascular pattern of ASPS also provoked the use of the tyrosine kinase inhibitor sunitinib malate (SM), which targets PDGFR, VEGFR, KIT, and RET, in a cohort of five patients with metastatic disease. Two patients displayed a partial response and one maintained stable disease, providing preliminary evidence that SM may be an effective therapy for ASPS [126]. A

subsequent study with nine patients also showed response to SM therapy and biochemical studies performed on tumor samples revealed that the antitumor activity is mediated by PDGFR- β , VEGFR-2, and RET inhibition [127]. Another VEGFR inhibitor, cediranib, is currently undergoing phase II testing for ASPS in three clinical trials (Table 2-2).

Conclusions

Current treatment involving surgery and multi-agent chemotherapy has resulted in a plateau in the survival rate of pediatric sarcomas. Although the molecular genetics of these tumors reveal they are distinct entities, they are often treated as a homogeneous group when it comes to standard therapy. Fusion gene transcriptional targets, downstream signaling pathways, and over-expressed growth factor receptors provide novel therapeutic targets that are currently being investigated in clinical trials. Certain targets have shown promise, but tumor resistance is a common problem, suggesting combination therapy may be required for effective treatment. Although initial trials and *in vitro* studies have paved the way for advances in targeted therapy in sarcoma, further work is needed to better characterize tumors at the molecular genetic level to tailor therapies to individual tumors.

References

1. Gurney JG, Swensen AR, Bulterys M (1999) Malignant Bone Tumors. In: Ries LAG, Smith MA, Gurney JG, Linet M, Tamra T et al., editors. *Cancer Incidence and Survival among Children and Adolescents: United States SEER Program 1975-1995*. Bethesda, MD: National Cancer Institute, SEER Program. pp. 99-110.
2. Gurney JG, Young JL, Jr., Roffers SD, Smith MA, Bunin GR (1999) Soft Tissue Sarcomas. In: Ries LAG, Smith MA, Gurney JG, Linet M, Tamra T et al., editors. *Cancer Incidence and Survival among Children and Adolescents: United States SEER Program 1975-1995*. Bethesda, MD: National Cancer Institute, SEER Program. pp. 111-124.
3. Applebaum MA, Worch J, Matthay KK, Goldsby R, Neuhaus J, West DC, DuBois SG. (2011) Clinical features and outcomes in patients with extraskkeletal ewing sarcoma. *Cancer*. **117**:3027-3032.
4. Ludwig JA. (2008) Ewing sarcoma: historical perspectives, current state-of-the-art, and opportunities for targeted therapy in the future. *Curr Opin Oncol*. **20**:412-418.
5. Balamuth NJ, Womer RB. (2010) Ewing's sarcoma. *Lancet Oncol*. **11**:184-192.
6. Rodriguez-Galindo C, Navid F, Khoury J, Krasin M (2006) Ewing sarcoma family of tumors. In: Pappo A, editor. *Pediatric Bone and Soft Tissue Sarcomas*. Berlin/Heidelberg: Springer-Verlag. pp. 181-217.
7. Cavazzana AO, Miser JS, Jefferson J, Triche TJ. (1987) Experimental evidence for a neural origin of Ewing's sarcoma of bone. *Am J Pathol*. **127**:507-518.
8. Franchi A, Pasquinelli G, Cenacchi G, Della Rocca C, Gambini C, Bisceglia M, Martinelli GN, Santucci M. (2001) Immunohistochemical and ultrastructural investigation of neural differentiation in Ewing sarcoma/PNET of bone and soft tissues. *Ultrastruct Pathol*. **25**:219-225.
9. Tirode F, Laud-Duval K, Prieur A, Delorme B, Charbord P, Delattre O. (2007) Mesenchymal stem cell features of Ewing tumors. *Cancer Cell*. **11**:421-429.
10. Riggi N, Cironi L, Provero P, Suvà M-L, Kaloulis K, Garcia-Echeverria C, Hoffmann F, Trumpp A, Stamenkovic I. (2005) Development of Ewing's sarcoma from primary bone marrow-derived mesenchymal progenitor cells. *Cancer Res*. **65**:11459-11468.
11. Pinto A, Dickman P, Parham D. (2011) Pathobiologic markers of the Ewing sarcoma family of tumors: state of the art and prediction of behaviour. *Sarcoma*. **2011**:1-15.
12. Zucman J, Melot T, Desmaze C, Ghysdael J, Plougastel B, Peter M, Zucker JM, Triche TJ, Sheer D, Turc-Carel C. (1993) Combinatorial generation of variable fusion proteins in the Ewing family of tumours. *EMBO J*. **12**:4481-4487.
13. Le Deley M-C, Delattre O, Schaefer K-L, Burchill SA, Koehler G, et al. (2010) Impact of EWS-ETS fusion type on disease progression in Ewing's sarcoma/peripheral primitive neuroectodermal tumor: prospective results from the cooperative Euro-E.W.I.N.G. 99 trial. *J Clin Oncol*. **28**:1982-1988.

14. van Doorninck JA, Ji L, Schaub B, Shimada H, Wing MR, Krailo MD, Lessnick SL, Marina N, Triche TJ, Sposto R, Womer RB, Lawlor ER. (2010) Current treatment protocols have eliminated the prognostic advantage of type 1 fusions in Ewing sarcoma: a report from the Children's Oncology Group. *J Clin Oncol.* **28**:1989-1994.
15. Delattre O, Zucman J, Plougastel B, Desmaze C, Melot T, Peter M, Kovar H, Joubert I, de Jong P, Rouleau G. (1992) Gene fusion with an ETS DNA-binding domain caused by chromosome translocation in human tumours. *Nature.* **359**:162-165.
16. Kovar H. (2011) Dr. Jekyll and Mr. Hyde: the two faces of the FUS/EWS/TAF15 protein family. *Sarcoma.* **2011**:837474.
17. Sharrocks AD. (2001) The ETS-domain transcription factor family. *Nat Rev Mol Cell Biol.* **2**:827-837.
18. Gangwal K, Sankar S, Hollenhorst P, Kinsey M, Haroldsen S, Shah A, Boucher K, Watkins W, Jorde L, Graves B, Lessnick S. (2008) Microsatellites as EWS/FLI response elements in Ewing's sarcoma. *Proc Natl Acad Sci U S A.*
19. Knoop LL, Baker SJ. (2000) The splicing factor U1C represses EWS/FLI-mediated transactivation. *J Biol Chem.* **275**:24865-24871.
20. Knoop LL, Baker SJ. (2001) EWS/FLI alters 5'-splice site selection. *J Biol Chem.* **276**:22317-22322.
21. France KA, Anderson JL, Park A, Denny CT. (2011) Oncogenic fusion protein EWS/FLI1 down-regulates gene expression by both transcriptional and posttranscriptional mechanisms. *J Biol Chem.* **286**:22750-22757.
22. Prieur A, Tirode F, Cohen P, Delattre O. (2004) EWS/FLI-1 silencing and gene profiling of Ewing cells reveal downstream oncogenic pathways and a crucial role for repression of insulin-like growth factor binding protein 3. *Mol Cell Biol.* **24**:7275-7283.
23. Wakahara K, Ohno T, Kimura M, Masuda T, Nozawa S, Dohjima T, Yamamoto T, Nagano A, Kawai G, Matsushashi A, Saitoh M, Takigami I, Okano Y, Shimizu K. (2008) EWS-Fli1 up-regulates expression of the Aurora A and Aurora B kinases. *Mol Cancer Res.* **6**:1937-1945.
24. Cironi L, Riggi N, Provero P, Wolf N, Suvà M-L, Suvà D, Kindler V, Stamenkovic I. (2008) IGF1 is a common target gene of Ewing's sarcoma fusion proteins in mesenchymal progenitor cells. *PLoS ONE.* **3**:e2634.
25. Scotlandi K, Benini S, Sarti M, Serra M, Lollini PL, Maurici D, Picci P, Manara MC, Baldini N. (1996) Insulin-like growth factor I receptor-mediated circuit in Ewing's sarcoma/peripheral neuroectodermal tumor: a possible therapeutic target. *Cancer Res.* **56**:4570-4574.
26. Toretsky JA, Kalebic T, Blakesley V, LeRoith D, Helman LJ. (1997) The insulin-like growth factor-I receptor is required for EWS/FLI-1 transformation of fibroblasts. *J Biol Chem.* **272**:30822-30827.

27. Scotlandi K, Maini C, Manara MC, Benini S, Serra M, Cerisano V, Strammiello R, Baldini N, Lollini P-L, Nanni P, Nicoletti G, Picci P. (2002) Effectiveness of insulin-like growth factor I receptor antisense strategy against Ewing's sarcoma cells. *Cancer Gene Ther.* **9**:296-307.
28. Tolcher AW, Sarantopoulos J, Patnaik A, Papadopoulos K, Lin C-C, et al. (2009) Phase I, pharmacokinetic, and pharmacodynamic study of AMG 479, a fully human monoclonal antibody to insulin-like growth factor receptor 1. *J Clin Oncol.* **27**:5800-5807.
29. Juergens H, Daw NC, Geoerger B, Ferrari S, Villarroel M, Aerts I, Whelan J, Dirksen U, Hixon ML, Yin D, Wang T, Green S, Paccagnella L, Gualberto A. (2011) Preliminary efficacy of the anti-insulin-like growth factor type 1 receptor antibody figitumumab in patients with refractory Ewing sarcoma. *J Clin Oncol.* **29**:4534-4540.
30. Pappo AS, Patel SR, Crowley J, Reinke DK, Kuenkele KP, et al. (2011) R1507, a monoclonal antibody to the insulin-like growth factor 1 receptor, in patients with recurrent or refractory Ewing sarcoma family of tumors: results of a phase II Sarcoma Alliance for Research through Collaboration study. *J Clin Oncol.* **29**:4541-4547.
31. Malempati S, Weigel B, Ingle AM, Ahern CH, Carroll JM, Roberts CT, Reid JM, Schmechel S, Voss SD, Cho SY, Chen HX, Krailo MD, Adamson PC, Blaney SM. (2012) Phase I/II trial and pharmacokinetic study of cixutumumab in pediatric patients with refractory solid tumors and Ewing sarcoma: a report from the Children's Oncology Group. *J Clin Oncol.* **30**:256-262.
32. Tap WD, Demetri G, Barnette P, Desai J, Kavan P, et al. (2012) Phase II study of ganitumab, a fully human anti-type-1 insulin-like growth factor receptor antibody, in patients with metastatic Ewing family tumors or desmoplastic small round cell tumors. *J Clin Oncol.* **30**:1849-1856.
33. Garofalo C, Manara MC, Nicoletti G, Marino MT, Lollini PL, Astolfi A, Pandini G, López-Guerrero JA, Schaefer K-L, Belfiore A, Picci P, Scotlandi K. (2011) Efficacy of and resistance to anti-IGF-1R therapies in Ewing's sarcoma is dependent on insulin receptor signaling. *Oncogene.* **30**:2730-2740.
34. Maris JM, Morton CL, Gorlick R, Kolb EA, Lock R, Carol H, Keir ST, Reynolds CP, Kang MH, Wu J, Smith MA, Houghton PJ. (2010) Initial testing of the aurora kinase A inhibitor MLN8237 by the Pediatric Preclinical Testing Program (PPTP). *Pediatr Blood Cancer.* **55**:26-34.
35. Toretsky JA, Erkizan V, Levenson A, Abaan OD, Parvin JD, Cripe TP, Rice AM, Lee SB, Uren A. (2006) Oncoprotein EWS-FLI1 activity is enhanced by RNA helicase A. *Cancer Res.* **66**:5574-5581.
36. Erkizan HV, Kong Y, Merchant M, Schlottmann S, Barber-Rotenberg JS, Yuan L, Abaan OD, Chou T-H, Dakshanamurthy S, Brown ML, Uren A, Toretsky JA. (2009) A small molecule blocking oncogenic protein EWS-FLI1 interaction with RNA helicase A inhibits growth of Ewing's sarcoma. *Nat Med.* **15**:750-756.

37. Kovar H, Aryee DN, Jug G, Henöckl C, Schemper M, Delattre O, Thomas G, Gadner H. (1996) EWS/FLI-1 antagonists induce growth inhibition of Ewing tumor cells in vitro. *Cell Growth Differ.* **7**:429-437.
38. Perez EA, Kassira N, Cheung MC, Koniaris LG, Neville HL, Sola JE. (2011) Rhabdomyosarcoma in children: a SEER population based study. *J Surg Res.* **170**:e243-251.
39. Pizzo PA, Poplack DG (2002) Principles and practice of pediatric oncology. Philadelphia: Lippincott Williams & Wilkins.
40. Keller C, Arenkiel BR, Coffin CM, El-Bardeesy N, DePinho RA, Capecchi MR. (2004) Alveolar rhabdomyosarcomas in conditional Pax3:Fkhr mice: cooperativity of Ink4a/ARF and Trp53 loss of function. *Genes Dev.* **18**:2614-2626.
41. Keller C, Hansen MS, Coffin CM, Capecchi MR. (2004) Pax3:Fkhr interferes with embryonic Pax3 and Pax7 function: implications for alveolar rhabdomyosarcoma cell of origin. *Genes Dev.* **18**:2608-2613.
42. Lagutina I, Conway SJ, Sublett J, Grosveld GC. (2002) Pax3-FKHR knock-in mice show developmental aberrations but do not develop tumors. *Mol Cell Biol.* **22**:7204-7216.
43. Barr FG, Galili N, Holick J, Biegel JA, Rovera G, Emanuel BS. (1993) Rearrangement of the PAX3 paired box gene in the paediatric solid tumour alveolar rhabdomyosarcoma. *Nat Genet.* **3**:113-117.
44. Davis RJ, D'Cruz CM, Lovell MA, Biegel JA, Barr FG. (1994) Fusion of PAX7 to FKHR by the variant t(1;13)(p36;q14) translocation in alveolar rhabdomyosarcoma. *Cancer Res.* **54**:2869-2872.
45. Sumegi J, Streblov R, Frayer RW, Dal Cin P, Rosenberg A, Meloni-Ehrig A, Bridge JA. (2010) Recurrent t(2;2) and t(2;8) translocations in rhabdomyosarcoma without the canonical PAX-FOXO1 fuse PAX3 to members of the nuclear receptor transcriptional coactivator family. *Genes Chromosomes Cancer.* **49**:224-236.
46. Wang Q, Fang W-H, Krupinski J, Kumar S, Slevin M, Kumar P. (2008) Pax genes in embryogenesis and oncogenesis. *J Cell Mol Med.* **12**:2281-2294.
47. Fu Z, Tindall DJ. (2008) FOXOs, cancer and regulation of apoptosis. *Oncogene.* **27**:2312-2319.
48. Sorensen PHB, Lynch JC, Qualman SJ, Tirabosco R, Lim JF, Maurer HM, Bridge JA, Crist WM, Triche TJ, Barr FG. (2002) PAX3-FKHR and PAX7-FKHR gene fusions are prognostic indicators in alveolar rhabdomyosarcoma: a report from the children's oncology group. *J Clin Oncol.* **20**:2672-2679.
49. Williamson D, Missiaglia E, de Reyniès A, Pierron G, Thuille B, Palenzuela G, Thway K, Orbach D, Laé M, Fréneaux P, Pritchard-Jones K, Oberlin O, Shipley J, Delattre O. (2010) Fusion gene-negative alveolar rhabdomyosarcoma is clinically and molecularly indistinguishable from embryonal rhabdomyosarcoma. *J Clin Oncol.* **28**:2151-2158.

50. Ginsberg JP, Davis RJ, Bennicelli JL, Nauta LE, Barr FG. (1998) Up-regulation of MET but not neural cell adhesion molecule expression by the PAX3-FKHR fusion protein in alveolar rhabdomyosarcoma. *Cancer Res.* **58**:3542-3546.
51. Taulli R, Scuoppo C, Bersani F, Accornero P, Forni PE, Miretti S, Grinza A, Allegra P, Schmitt-Ney M, Crepaldi T, Ponzetto C. (2006) Validation of met as a therapeutic target in alveolar and embryonal rhabdomyosarcoma. *Cancer Res.* **66**:4742-4749.
52. Yan D, Dong XDE, Chen X, Wang L, Lu C, Wang J, Qu J, Tu L. (2009) MicroRNA-1/206 targets c-Met and inhibits rhabdomyosarcoma development. *J Biol Chem.* **284**:29596-29604.
53. Taulli R, Bersani F, Foglizzo V, Linari A, Vigna E, Ladanyi M, Tuschl T, Ponzetto C. (2009) The muscle-specific microRNA miR-206 blocks human rhabdomyosarcoma growth in xenotransplanted mice by promoting myogenic differentiation. *J Clin Invest.* **119**:2366-2378.
54. Hou J, Dong J, Sun L, Geng L, Wang J, Zheng J, Li Y, Bridge J, Hinrichs SH, Ding S-J. (2011) Inhibition of phosphorylated c-Met in rhabdomyosarcoma cell lines by a small molecule inhibitor SU11274. *J Transl Med.* **9**:64.
55. Ayalon D, Glaser T, Werner H. (2001) Transcriptional regulation of IGF-I receptor gene expression by the PAX3-FKHR oncoprotein. *Growth Horm IGF Res.* **11**:289-297.
56. El-Badry OM, Minniti C, Kohn EC, Houghton PJ, Daughaday WH, Helman LJ. (1990) Insulin-like growth factor II acts as an autocrine growth and motility factor in human rhabdomyosarcoma tumors. *Cell Growth Differ.* **1**:325-331.
57. Khan J, Bittner ML, Saal LH, Teichmann U, Azorsa DO, Gooden GC, Pavan WJ, Trent JM, Meltzer PS. (1999) cDNA microarrays detect activation of a myogenic transcription program by the PAX3-FKHR fusion oncogene. *Proc Natl Acad Sci U S A.* **96**:13264-13269.
58. Martins AS, Olmos D, Missiaglia E, Shipley J. (2011) Targeting the insulin-like growth factor pathway in rhabdomyosarcomas: rationale and future perspectives. *Sarcoma.* **2011**:209736.
59. Epstein JA, Song B, Lakkis M, Wang C. (1998) Tumor-specific PAX3-FKHR transcription factor, but not PAX3, activates the platelet-derived growth factor alpha receptor. *Mol Cell Biol.* **18**:4118-4130.
60. Taniguchi E, Nishijo K, McCleish AT, Michalek JE, Grayson MH, Infante AJ, Abboud HE, Legallo RD, Qualman SJ, Rubin BP, Keller C. (2008) PDGFR-A is a therapeutic target in alveolar rhabdomyosarcoma. *Oncogene.* **27**:6550-6560.
61. Abraham J, Prajapati SI, Nishijo K, Schaffer BS, Taniguchi E, et al. (2011) Evasion mechanisms to Igf1r inhibition in rhabdomyosarcoma. *Mol Cancer Ther.* **10**:697-707.
62. Mayeenuddin LH, Yu Y, Kang Z, Helman LJ, Cao L. (2010) Insulin-like growth factor 1 receptor antibody induces rhabdomyosarcoma cell death via a process involving AKT and Bcl-x(L). *Oncogene.* **29**:6367-6377.

63. Smith ME, Fisher C, Wilkinson LS, Edwards JC. (1995) Synovial sarcomas lack synovial differentiation. *Histopathology*. **26**:279-281.
64. Naka N, Takenaka S, Araki N, Miwa T, Hashimoto N, Yoshioka K, Joyama S, Hamada K-I, Tsukamoto Y, Tomita Y, Ueda T, Yoshikawa H, Itoh K. (2010) Synovial sarcoma is a stem cell malignancy. *Stem Cells*. **28**:1119-1131.
65. Haldar M, Hancock JD, Coffin CM, Lessnick SL, Capecchi MR. (2007) A conditional mouse model of synovial sarcoma: insights into a myogenic origin. *Cancer Cell*. **11**:375-388.
66. Clark J, Rocques PJ, Crew AJ, Gill S, Shipley J, Chan AM, Gusterson BA, Cooper CS. (1994) Identification of novel genes, SYT and SSX, involved in the t(X;18)(p11.2;q11.2) translocation found in human synovial sarcoma. *Nat Genet*. **7**:502-508.
67. Crew AJ, Clark J, Fisher C, Gill S, Grimer R, Chand A, Shipley J, Gusterson BA, Cooper CS. (1995) Fusion of SYT to two genes, SSX1 and SSX2, encoding proteins with homology to the Kruppel-associated box in human synovial sarcoma. *EMBO J*. **14**:2333-2340.
68. de Leeuw B, Balemans M, Olde Weghuis D, Geurts van Kessel A. (1995) Identification of two alternative fusion genes, SYT-SSX1 and SYT-SSX2, in t(X;18)(p11.2;q11.2)-positive synovial sarcomas. *Hum Mol Genet*. **4**:1097-1099.
69. Skytting B, Nilsson G, Brodin B, Xie Y, Lundeberg J, Uhlén M, Larsson O. (1999) A novel fusion gene, SYT-SSX4, in synovial sarcoma. *J Natl Cancer Inst*. **91**:974-975.
70. Haldar M, Randall RL, Capecchi MR. (2008) Synovial sarcoma: from genetics to genetic-based animal modeling. *Clin Orthop Relat Res*. **466**:2156-2167.
71. Perani M, Ingram CJE, Cooper CS, Garrett MD, Goodwin GH. (2003) Conserved SNH domain of the proto-oncoprotein SYT interacts with components of the human chromatin remodelling complexes, while the QPGY repeat domain forms homo-oligomers. *Oncogene*. **22**:8156-8167.
72. Soulez M, Saurin AJ, Freemont PS, Knight JC. (1999) SSX and the synovial-sarcoma-specific chimaeric protein SYT-SSX co-localize with the human Polycomb group complex. *Oncogene*. **18**:2739-2746.
73. Nagai M, Tanaka S, Tsuda M, Endo S, Kato H, Sonobe H, Minami A, Hiraga H, Nishihara H, Sawa H, Nagashima K. (2001) Analysis of transforming activity of human synovial sarcoma-associated chimeric protein SYT-SSX1 bound to chromatin remodeling factor hBRM/hSNF2 alpha. *Proc Natl Acad Sci U S A*. **98**:3843-3848.
74. Takenaka S, Naka N, Araki N, Hashimoto N, Ueda T, Yoshioka K, Yoshikawa H, Itoh K. (2010) Downregulation of SS18-SSX1 expression in synovial sarcoma by small interfering RNA enhances the focal adhesion pathway and inhibits anchorage-independent growth in vitro and tumor growth in vivo. *Int J Oncol*. **36**:823-831.

75. Guillou L, Benhattar J, Bonichon F, Gallagher G, Terrier P, et al. (2004) Histologic grade, but not SYT-SSX fusion type, is an important prognostic factor in patients with synovial sarcoma: a multicenter, retrospective analysis. *J Clin Oncol.* **22**:4040-4050.
76. Kawai A, Woodruff J, Healey JH, Brennan MF, Antonescu CR, Ladanyi M. (1998) SYT-SSX gene fusion as a determinant of morphology and prognosis in synovial sarcoma. *N Engl J Med.* **338**:153-160.
77. Allander SV, Illei PB, Chen Y, Antonescu CR, Bittner M, Ladanyi M, Meltzer PS. (2002) Expression profiling of synovial sarcoma by cDNA microarrays: association of ERBB2, IGFBP2, and ELF3 with epithelial differentiation. *Am J Pathol.* **161**:1587-1595.
78. de Bruijn DRH, Allander SV, van Dijk AHA, Willemse MP, Thijssen J, van Groningen JJM, Meltzer PS, van Kessel AG. (2006) The synovial-sarcoma-associated SS18-SSX2 fusion protein induces epigenetic gene (de)regulation. *Cancer Res.* **66**:9474-9482.
79. Sun Y, Gao D, Liu Y, Huang J, Lessnick S, Tanaka S. (2006) IGF2 is critical for tumorigenesis by synovial sarcoma oncoprotein SYT-SSX1. *Oncogene.* **25**:1042-1052.
80. Friedrichs N, K uchler J, Endl E, Koch A, Czerwitzki J, et al. (2008) Insulin-like growth factor-1 receptor acts as a growth regulator in synovial sarcoma. *J Pathol.* **216**:428-439.
81. Krskova L, Kalinova M, Břizova H, Mrhalova M, Sumerauer D, Kodet R. (2009) Molecular and immunohistochemical analyses of BCL2, KI-67, and cyclin D1 expression in synovial sarcoma. *Cancer Genet.* **193**:1-8.
82. Mancuso T, Mezzelani A, Riva C, Fabbri A, Dal Bo L, Sampietro G, Perego P, Casali P, Zunino F, Sozzi G, Pierotti MA, Pilotti S. (2000) Analysis of SYT-SSX fusion transcripts and bcl-2 expression and phosphorylation status in synovial sarcoma. *Lab Invest.* **80**:805-813.
83. Albritton KH, Randall RL. (2005) Prospects for targeted therapy of synovial sarcoma. *J Pediatr Hematol Oncol.* **27**:219-222.
84. Joyner DE, Albritton KH, Bastar JD, Randall RL. (2006) G3139 antisense oligonucleotide directed against antiapoptotic Bcl-2 enhances doxorubicin cytotoxicity in the FU-SY-1 synovial sarcoma cell line. *J Orthop Res.* **24**:474-480.
85. Rheingold SR, Hogarty MD, Blaney SM, Zwiebel JA, Sauk-Schubert C, Chandula R, Krailo MD, Adamson PC, Study CasOG. (2007) Phase I Trial of G3139, a bcl-2 antisense oligonucleotide, combined with doxorubicin and cyclophosphamide in children with relapsed solid tumors: a Children's Oncology Group Study. *J Clin Oncol.* **25**:1512-1518.
86. Nielsen TO, West RB, Linn SC, Alter O, Knowling MA, O'Connell JX, Zhu S, Fero M, Sherlock G, Pollack JR, Brown PO, Botstein D, van de Rijn M. (2002) Molecular characterisation of soft tissue tumours: a gene expression study. *Lancet.* **359**:1301-1307.
87. Bozzi F, Ferrari A, Negri T, Conca E, Luca DR, Losa M, Casieri P, Orsenigo M, Lampis A, Meazza C, Casanova M, Pierotti MA, Tamborini E, Pilotti S. (2008) Molecular

- characterization of synovial sarcoma in children and adolescents: evidence of akt activation. *Transl Oncol.* **1**:95-101.
88. Thomas DG, Giordano TJ, Sanders D, Biermann S, Sondak VK, Trent JC, Yu D, Pollock RE, Baker L. (2005) Expression of receptor tyrosine kinases epidermal growth factor receptor and HER-2/neu in synovial sarcoma. *Cancer.* **103**:830-838.
 89. Ray-Coquard I, Le Cesne A, Whelan JS, Schoffski P, Bui BN, Verweij J, Marreaud S, van Glabbeke M, Hogendoorn P, Blay J-Y. (2008) A phase II study of gefitinib for patients with advanced HER-1 expressing synovial sarcoma refractory to doxorubicin-containing regimens. *Oncologist.* **13**:467-473.
 90. Criscione VD, Weinstock MA. (2007) Descriptive epidemiology of dermatofibrosarcoma protuberans in the United States, 1973 to 2002. *J Am Acad Dermatol.* **56**:968-973.
 91. Iqbal CW, St. Peter S, Ishitani MB. (2011) Pediatric dermatofibrosarcoma protuberans: multi-institutional outcomes. *J Surg Res.* **170**:69-72.
 92. Shmookler BM, Enzinger FM, Weiss SW. (1989) Giant cell fibroblastoma. A juvenile form of dermatofibrosarcoma protuberans. *Cancer.* **64**:2154-2161.
 93. Dominguez-Malagon H, Valdez-Carrillo MdC, Cano-Valdez AM. (2006) Dermatofibroma and dermatofibrosarcoma protuberans: a comparative ultrastructural study. *Ultrastruct Pathol.* **30**:283-291.
 94. Simon MP, Pedeutour F, Sirvent N, Grosgeorge J, Minoletti F, et al. (1997) Deregulation of the platelet-derived growth factor B-chain gene via fusion with collagen gene COL1A1 in dermatofibrosarcoma protuberans and giant-cell fibroblastoma. *Nat Genet.* **15**:95-98.
 95. Simon MP, Navarro M, Roux D, Pouysségur J. (2001) Structural and functional analysis of a chimeric protein COL1A1-PDGFB generated by the translocation t(17;22)(q22;q13.1) in Dermatofibrosarcoma protuberans (DP). *Oncogene.* **20**:2965-2975.
 96. Giacchero D, Maire G, Nuin PAS, Berthier F, Ebran N, et al. (2010) No correlation between the molecular subtype of COL1A1-PDGFB fusion gene and the clinico-histopathological features of dermatofibrosarcoma protuberans. *J Invest Dermatol.* **130**:904-907.
 97. Greco A, Fusetti L, Villa R, Sozzi G, Minoletti F, Mauri P, Pierotti MA. (1998) Transforming activity of the chimeric sequence formed by the fusion of collagen gene COL1A1 and the platelet derived growth factor b-chain gene in dermatofibrosarcoma protuberans. *Oncogene.* **17**:1313-1319.
 98. Greco A, Roccato E, Miranda C, Cleris L, Formelli F, Pierotti MA. (2001) Growth-inhibitory effect of STI571 on cells transformed by the COL1A1/PDGFB rearrangement. *Int J Cancer.* **92**:354-360.
 99. McArthur GA, Demetri GD, van Oosterom A, Heinrich MC, Debiec-Rychter M, Corless CL, Nikolova Z, Dimitrijevic S, Fletcher JA. (2005) Molecular and clinical analysis of

- locally advanced dermatofibrosarcoma protuberans treated with imatinib: Imatinib Target Exploration Consortium Study B2225. *J Clin Oncol*. **23**:866-873.
100. Hicks J, Mierau G. (2004) The spectrum of pediatric fibroblastic and myofibroblastic tumors. *Ultrastruct Pathol*. **28**:265-281.
 101. Knezevich SR, McFadden DE, Tao W, Lim JF, Sorensen PH. (1998) A novel ETV6-NTRK3 gene fusion in congenital fibrosarcoma. *Nat Genet*. **18**:184-187.
 102. Knezevich SR, Garnett MJ, Pysher TJ, Beckwith JB, Grundy PE, Sorensen PH. (1998) ETV6-NTRK3 gene fusions and trisomy 11 establish a histogenetic link between mesoblastic nephroma and congenital fibrosarcoma. *Cancer Res*. **58**:5046-5048.
 103. Tognon C, Knezevich SR, Huntsman D, Roskelley CD, Melnyk N, Mathers JA, Becker L, Carneiro F, MacPherson N, Horsman D, Poremba C, Sorensen PHB. (2002) Expression of the ETV6-NTRK3 gene fusion as a primary event in human secretory breast carcinoma. *Cancer Cell*. **2**:367-376.
 104. Eguchi M, Eguchi-Ishimae M, Tojo A. (1999) Fusion of ETV6 to neurotrophin-3 receptor TRKC in acute myeloid leukemia with t (12; 15)(p13; q25). *Blood*. **93**:1355-1363.
 105. Wai DH, Knezevich SR, Lucas T, Jansen B, Kay RJ, Sorensen PH. (2000) The ETV6-NTRK3 gene fusion encodes a chimeric protein tyrosine kinase that transforms NIH3T3 cells. *Oncogene*. **19**:906-915.
 106. Morrison KB, Tognon CE, Garnett MJ, Deal C, Sorensen PHB. (2002) ETV6-NTRK3 transformation requires insulin-like growth factor 1 receptor signaling and is associated with constitutive IRS-1 tyrosine phosphorylation. *Oncogene*. **21**:5684-5695.
 107. Tognon C, Garnett M, Kenward E, Kay R, Morrison K, Sorensen PH. (2001) The chimeric protein tyrosine kinase ETV6-NTRK3 requires both Ras-Erk1/2 and PI3-kinase-Akt signaling for fibroblast transformation. *Cancer Res*. **61**:8909-8916.
 108. Tognon CE, Somasiri AM, Evdokimova VE, Trigo G, Uy EE, Melnyk N, Carboni JM, Gottardis MM, Roskelley CD, Pollak M, Sorensen PHB. (2011) ETV6-NTRK3-mediated breast epithelial cell transformation is blocked by targeting the IGF1R signaling pathway. *Cancer Res*. **71**:1060-1070.
 109. Lannon CL, Sorensen PHB. (2005) ETV6-NTRK3: a chimeric protein tyrosine kinase with transformation activity in multiple cell lineages. *Semin Cancer Biol*. **15**:215-223.
 110. Lannon CL, Martin MJ, Tognon CE, Jin W, Kim S-J, Sorensen PHB. (2004) A highly conserved NTRK3 C-terminal sequence in the ETV6-NTRK3 oncoprotein binds the phosphotyrosine binding domain of insulin receptor substrate-1: an essential interaction for transformation. *J Biol Chem*. **279**:6225-6234.
 111. Jin W, Yun C, Hobbie A, Martin MJ, Sorensen PHB, Kim S-J. (2007) Cellular transformation and activation of the phosphoinositide-3-kinase-Akt cascade by the ETV6-NTRK3 chimeric tyrosine kinase requires c-Src. *Cancer Res*. **67**:3192-3200.

112. Jin W, Kim B-C, Tognon C, Lee H-J, Patel S, Lannon CL, Maris JM, Triche TJ, Sorensen PHB, Kim S-J. (2005) The ETV6-NTRK3 chimeric tyrosine kinase suppresses TGF-beta signaling by inactivating the TGF-beta type II receptor. *Proc Natl Acad Sci U S A*. **102**:16239-16244.
113. Folpe AL, Deyrup AT. (2006) Alveolar soft-part sarcoma: a review and update. *J Clin Pathol*. **59**:1127-1132.
114. Ladanyi M, Lui MY, Antonescu CR, Krause-Boehm A, Meindl A, et al. (2001) The der(17)t(X;17)(p11;q25) of human alveolar soft part sarcoma fuses the TFE3 transcription factor gene to ASPL, a novel gene at 17q25. *Oncogene*. **20**:48-57.
115. Schuberth C, Buchberger A. (2008) UBX domain proteins: major regulators of the AAA ATPase Cdc48/p97. *Cell Mol Life Sci*. **65**:2360-2371.
116. Bogan JS, Hendon N, McKee AE, Tsao T-S, Lodish HF. (2003) Functional cloning of TUG as a regulator of GLUT4 glucose transporter trafficking. *Nature*. **425**:727-733.
117. Hemesath TJ, Steingrimsson E, McGill G, Hansen MJ, Vaught J, Hodgkinson CA, Arnheiter H, Copeland NG, Jenkins NA, Fisher DE. (1994) Microphthalmia, a critical factor in melanocyte development, defines a discrete transcription factor family. *Genes Dev*. **8**:2770-2780.
118. Hershey CL, Fisher DE. (2004) Mitf and Tfe3: members of a b-HLH-ZIP transcription factor family essential for osteoclast development and function. *Bone*. **34**:689-696.
119. Hua X, Miller ZA, Benchabane H, Wrana JL, Lodish HF. (2000) Synergism between transcription factors TFE3 and Smad3 in transforming growth factor-beta-induced transcription of the Smad7 gene. *J Biol Chem*. **275**:33205-33208.
120. Argani P, Antonescu CR, Illei PB, Lui MY, Timmons CF, Newbury R, Reuter VE, Garvin AJ, Perez-Atayde AR, Fletcher JA, Beckwith JB, Bridge JA, Ladanyi M. (2001) Primary renal neoplasms with the ASPL-TFE3 gene fusion of alveolar soft part sarcoma: a distinctive tumor entity previously included among renal cell carcinomas of children and adolescents. *Am J Pathol*. **159**:179-192.
121. Tsuda M, Davis IJ, Argani P, Shukla N, McGill GG, Nagai M, Saito T, Lae M, Fisher DE, Ladanyi M. (2007) TFE3 fusions activate MET signaling by transcriptional up-regulation, defining another class of tumors as candidates for therapeutic MET inhibition. *Cancer Res*. **67**:919-929.
122. Adjei AA, Schwartz B, Garmey E. (2011) Early clinical development of ARQ 197, a selective, non-ATP-competitive inhibitor targeting MET tyrosine kinase for the treatment of advanced cancers. *Oncologist*. **16**:788-799.
123. Lazar AJF, Das P, Tuvin D, Korchin B, Zhu Q, Jin Z, Warneke CL, Zhang PS, Hernandez V, Lopez-Terrada D, Pisters PW, Pollock RE, Lev D. (2007) Angiogenesis-promoting gene patterns in alveolar soft part sarcoma. *Clin Cancer Res*. **13**:7314-7321.

124. Stockwin LH, Vistica DT, Kenney S, Schrupp DS, Butcher DO, Raffeld M, Shoemaker RH. (2009) Gene expression profiling of alveolar soft-part sarcoma (ASPS). *BMC Cancer*. **9**:22.
125. Azizi AA, Haberler C, Czech T, Gupper A, Prayer D, Breitschopf H, Acker T, Slavc I. (2006) Vascular-endothelial-growth-factor (VEGF) expression and possible response to angiogenesis inhibitor bevacizumab in metastatic alveolar soft part sarcoma. *Lancet Oncol*. **7**:521-523.
126. Stacchiotti S, Tamborini E, Marrari A, Brich S, Rota SA, Orsenigo M, Crippa F, Morosi C, Gronchi A, Pierotti MA, Casali PG, Pilotti S. (2009) Response to sunitinib malate in advanced alveolar soft part sarcoma. *Clin Cancer Res*. **15**:1096-1104.
127. Stacchiotti S, Negri T, Zaffaroni N, Palassini E, Morosi C, Brich S, Conca E, Bozzi F, Cassinelli G, Gronchi A, Casali PG, Pilotti S. (2011) Sunitinib in advanced alveolar soft part sarcoma: evidence of a direct antitumor effect. *Ann Oncol*. **22**:1682-1690.

CHAPTER 3
MATERIALS AND METHODS

Cells. ESFT cell lines (RDES, TC-174, SK-N-MC, TC-248, TTC-475, TC-32, SKES, A4573, A673, and 6647) were cultured in Iscove's modified Dulbecco's medium (IMDM) containing 10% fetal calf serum. 293T cells used for virus production were cultured in Dulbecco's modified Eagle medium (DMEM) containing 10% fetal calf serum and supplemented with L-glutamine (2 mM) and penicillin-streptomycin (50 IU/ml and 50 µg/ml, respectively). NIH 3T3 cells were cultured in DMEM containing 5% calf serum. All cells were cultured at 37°C with 5% CO₂.

Plasmids and Viruses. EWS/FLI1 shRNA constructs were cloned into the CSCG lentiviral vector as previously described [1,2]. The dominant negative Stat3 construct, in which tyrosine 705 is mutated to phenylalanine, was cloned from pRc/CMV Stat3 Y705F Flag (Addgene plasmid 8709) [3] into the SR α -MSV-TK Neo retroviral vector [4]. The retroviral triple FLAG epiptope-tagged EWS/FLI1, EWS mutant (DAF), FLAG-tagged ETS mutant (TPM), and ZFM1 constructs were previously described [4-7]. Lentiviral stocks were generated by transiently transfecting 15 µg of expression vector, 5 µg of VSV-G-expressing plasmid pMD.G, and 15 µg of packaging plasmid pDeltaVPR by calcium phosphate into 293T cells. Retroviral stocks were generated by transfecting 15 µg of expression vector and 15 µg of psi packaging plasmid by calcium phosphate into 293T cells. Viral conditioned media was collected 72 to 96 hours after transfection, filtered (0.45 µm), and frozen at -80°C or applied to cells. ESFT cells were subject to two or three rounds of lentiviral transduction, each either 3-4 hours or overnight, to ensure high transduction efficiency. ESFT cells transduced with retrovirus were subjected to one 2-3 hour transduction and two days later selected for transductants with 450 µg/ml G418 for seven days.

BACs and bacterial strains used for recombineering. SW102 is a modified DH10B strain containing the defective lambda prophage. SW105 is a modified DH10B strain containing the defective lambda prophage and an arabinose-inducible *flpe* gene. SW106 is a modified DH10B

strain containing the defective lambda prophage and an arabinose-inducible *cre* gene. Expression of proteins involved in homologous recombination is controlled by a heat-inducible promoter. Additionally, all these strains contain a fully functional *gal* operon, except for a deletion of *galK*. This feature allows for efficient BAC modification using *galK* positive/negative selection. The Upp reporter constructs were generated from the murine BAC clone RP23-85G13 (ID:626091). The Tsp2 construct was generated from the murine BAC clone RP23-456F9 (ID:745199).

Recombineering. BACs were introduced into recombineering strains by electroporation (1.75kV, 200Ω, 25μF) followed by antibiotic selection. Electrocompetent cells were generated by growing cultures until log phase (OD600 = 0.4-0.5), followed by a 1 hour incubation at 42°C (shaking water bath) to induce proteins for homologous recombination. Bacteria are then spun down for 5 min at 6000 rpm at 0°C and re-suspended in decreasing volumes of ice-cold water. The final pellet is resuspended in 10% glycerol and aliquots are frozen at -80°C.

Site-specific homologous recombination is achieved by amplifying the insert with primers that include 50-75 base pair regions of homology to the BAC at the desired area of integration. PCR products are digested with *DpnI* to remove plasmid DNA, then gel purified. 100 ng of PCR product is electroporated into competent cells containing BAC DNA and growth with the appropriate antibiotic is used to select for recombinants. For recombinants containing LoxP/511 sites, induction of Cre is performed by adding 100 μl of 10% L-(+)-arabinose to 10 ml of bacteria culture in log phase growth for a final concentration of 0.1%. After a 1h incubation at 32°C, dilutions of the culture are grown on LB plates containing the appropriate antibiotic. PCR is used to verify recombination has occurred.

Galk positive selection is initiated in an analogous fashion. The *galK* gene is PCR amplified with primers containing homology to either side of the EWS/ETS target gene transcriptional start site, *DpnI* digested, gel purified, then electroporated into competent cells

containing Upp or Tsp2 BAC. Recombinants are selected by washing cells in minimal media, then plating onto minimal media plates that contain galactose. Resulting colonies are streaked on MacConkey + galactose plates and single red, Gal⁺ colonies are selected. After galk insertion is verified by PCR, electrocompetent cells are generated as described above. EGFP is then amplified with primers containing the same regions of homology as for the galk amplification. After *DpnI* digest and gel purification, the PCR product is electroporated into competent cells contain the BAC construct with the galk insertion. Recombinants in which EGFP has been switched for galk are selected for by growth on minimal media containing 2-deoxy-galactose, which is toxic to cells that are able to metabolize galactose. This selects against cells that retain the galk insertion and provides a growth advance to cells that have replaced galk for EGFP.

Reagents. IGF1 was provided by Pinchas Cohen. AMG-479 (Ganitumab, Amgen) was provided by William Tap. Stattic (Stat3 Inhibitor V, sc-202818) was obtained from Santa Cruz Biotechnology. Human recombinant IL-6 (206-IL-010), GM-CSF (215-GM-010), and CXCL1 (275-GR-010) were obtained from R&D Systems.

Quantitative Real Time PCR. RNA was harvested using the RNeasy Mini Kit (Qiagen) or PureLink RNA Mini Kit (Invitrogen). cDNA was synthesized from approximately 2 µg of RNA using the SuperScript III First-Strand Synthesis System (Invitrogen). Primers used to quantify cellular transcript levels are listed in Table 3-1. For real time PCR, a 1:10 dilution of cDNA was combined with forward and reverse primers and master mix containing SYBR green, *Taq*, and dNTPs (Applied Biosystems). Reactions were run at 95°C for 10 min, followed by 40 cycles at 95°C for 10 s, 60°C for 30 s, and 72°C for 20 s. Results were analyzed with Opticon Monitor software (MJ Research/Bio-Rad).

Table 3-1. Primers used for quantitative real time PCR

Name	Direction	Sequence (5' to 3')
QHSGAPDH-388F	Forward	ATGTTTCGTCATGGGTGTGAA
QHSGAPDH-481R	Reverse	CCAGGGGTGCTAAGCAGTT
qEPHB4-1415F	Forward	ATGAGAAGGGCGCCGAGGGT
qEPHB4-1514R	Reverse	ACCAGGTAGCTGGCTCCCCG
qEphrinB2-788F	Forward	ACACGACCACGCTGTCGCTC
qEphrinB2-935R	Reverse	CCGTAGTCGCCGCTGACCTTC
qEPHA2-1521F	Forward	GCAGGCACTGACGCAGGAGG
qEPHA2-1639R	Reverse	GGACCACACCGACAGCCACG
qEPHA5-1247F	Forward	CCCGGCAAAGCGGCCTGAAA
qEPHA5-1365R	Reverse	CCGGGCTCCTGGGCTCAAGT
qEphrinA1-178F	Forward	GCAGACGCTGCCATGGAGCA
qEphrinA1-227R	Reverse	TGCACTGCCAGCGGACTTGG
QESF-798F	Forward	TACAGCCAAGCTCCAAGTCA
QESF-990R	Reverse	GAATTGCCACAGCTGGATCT
QESF-743F	Forward	GCCAAGCTCCAAGTCAATATAGC
QESF-852R	Reverse	GAGGCCAGAATTCATGTTATTGC
IGFBP3 Ex4/Ex5 F	Forward	GGGGTGTACACATTCCCAAC
IGFBP3 Ex4/Ex5 R	Reverse	GGCGTCTACTTGCTCTGCAT

Immunoblot. Cells were lysed for approximately one hour on ice in lysis buffer (50 mM Tris pH 7.6, 0.5% NP-40, 10% glycerol, 30 mM NaCl, 1 mM EDTA) supplemented with Complete Mini EDTA-free protease inhibitor cocktail (Roche), 1 mM Na₃VO₄, and 1 mM NaF. Lysates were combined with 6X protein sample buffer (0.35 M Tris pH 6.8, 10% SDS, 30% glycerol, 0.6 M DTT, 0.012% bromophenol blue) and boiled for 5-10 minutes prior to loading on an 8% or 4-15% gradient polyacrylamide gel. The primary antibodies used for these studies were goat anti-actin (clone C-11, Santa Cruz Biotechnology, sc-1615), mouse anti-β-actin (Sigma, A5316), rabbit anti-phospho-Akt (Ser473) (clone D9E, Cell Signaling Technology, 4060), mouse anti-Akt (pan) (clone 40D4, Cell Signaling Technology, 2920), rabbit anti-phospho-p44/42 MAPK (Erk1/2) (Thr202/Tyr204) XP (clone D13.14.E, Cell Signaling Technology, 4370), mouse anti-p44/42 MAPK (Erk1/2) (clone L34F12, Cell Signaling Technology, 4696), rabbit anti-phospho-Stat3 Tyr705 (clone D3A7, Cell Signaling Technology, 9145), mouse anti-Stat3 (clone 124H6,

Cell Signaling Technology, 9139), rabbit anti-EphA2 XP (clone D4A2, Cell Signaling Technology, 6997), rabbit anti-phospho-EphA2 (Tyr772) (Cell Signaling Technology, 8244), rabbit anti-phospho-EphA2 (Tyr588), mouse anti-EphB4 (clone H-10, Santa Cruz Biotechnology, sc-365510), mouse anti-phosphotyrosine (clone 4G10, HRP conjugate, Millipore, 16-184), rabbit anti-phospho-PTPRA (Tyr789) (Cell Signaling Technology, 4481), goat anti-PTPRA (clone E-20, Santa Cruz Biotechnology, sc-19116), rabbit anti-phospho-PZR (Tyr263) (Cell Signaling Technology, 5543), rabbit anti-PZR XP (clone D17B10, Cell Signaling Technology, 9893), rabbit anti-phospho-Src (Tyr527) (Cell Signaling Technology, 2105), rabbit anti-phospho-Src Family (Tyr416) (clone D49G4, Cell Signaling Technology, 6943), anti-phospho-Jak2 (Tyr1007/1008) (clone C80C3, Cell Signaling Technology, 3776), and mouse anti-FLAG M2 (Sigma, F3165). Secondary antibodies conjugated to HRP were sheep anti-mouse IgG (GE Healthcare, NXA931), bovine anti-goat IgG (Santa Cruz Biotechnology, sc-2350), and goat anti-rabbit IgG (Santa Cruz Biotechnology, sc-2004). Secondary antibodies conjugated to infrared dyes were IRDye 800CW goat anti-mouse IgG (LI-COR Biosciences, 926-32210), IRDye 680RD goat anti-rabbit IgG (LI-COR Biosciences, 926-68071), and IRDye 680RD donkey anti-goat IgG (LI-COR Biosciences, 926-68074). Fluorescent westerns were imaged using the Odyssey system (LI-COR Biosciences). Signals were quantified by measuring the integrated density values of each band using NIH ImageJ software v1.40g.

Phosphotyrosine enrichment. Cells were lysed for approximately one hour on ice in lysis buffer (50 mM Tris pH 7.6, 0.5% NP-40, 10% glycerol, 30 mM NaCl, 1 mM EDTA) supplemented with Complete Mini EDTA-free protease inhibitor cocktail (Roche) and 1 mM Na₃VO₄. Lysates were centrifuged at 1000 g for 5 min and supernatant was saved. Four volumes of ice-cold (-20°C) acetone were added and mixture was vortexed and incubated at -20°C for 1-2 hours. Precipitated proteins were pelleted by centrifuging at 6,000 g for 15 min at 0°C. The pellet was washed once with 10 ml of ice-cold acetone to remove any residual NP-40,

then resuspended in 8M urea, 50 mM Tris pH 7.5, and 1 mM Na₃VO₄ by incubating overnight at 4°C with rotation.

Reduction was performed for 1 h at 37°C with 100 mM sodium phosphate pH 7.5 and 5 mM DTT, followed by alkylation with 25 mM iodoacetamide for 1 h at 25°C in the dark and quenching with 10 mM DTT for 30 min at 25°C. Lysates were then dialyzed against 50 mM Tris pH 8.0, 2 M urea and digested for 2-4 hours with low-grade trypsin (Worthington Biochemical) then overnight at 37°C at pH 7.5 with sequencing grade trypsin (Promega). Trypsin digestion was performed using a 1:100 ratio of trypsin to total protein mass. The digested lysates were passed through Amicon Ultra-15 10 kDa filters (Millipore) and acidified with 5% trifluoroacetic acid (TFA) to pH 2-3 before loading onto a 500 mg PrepSep C18 reverse phase column (Fisher Scientific) to desalt the sample. The peptides were eluted using 30% acetonitrile (ACN) with 0.1% TFA, lyophilized, resuspended in 100 mM Tris pH 8.0, and the resulting pH was titrated to 7.4. Phosphopeptides were immunoprecipitated with agarose-conjugated 4G10 (Millipore) at 4°C overnight. After washing three times with 50 mM Tris pH 7.4 and two times with 25 mM NH₄HCO₃ pH 7.5, phosphopeptides were eluted with 0.1% TFA for 15 min at 37°C, concentrated by vacuum centrifugation, desalted using ZipTip C18-based solid phase extraction as above (Millipore), and resuspended in 0.1% formic acid [8].

Phosphoserine/threonine enrichment. Cell lysates were collected as for those enriched for phosphotyrosine, except 1 mM NaF was added to the lysis buffer. Acetone precipitation, reduction, alkylation, digestion, and reverse phase extraction were performed as for phosphotyrosine enrichment. After lyophilization, peptides were resuspended in 5 mM KH₂PO₄ (pH 2.65), 5 mM KCl, and 30% acetonitrile. Peptides were fractionated by strong cation exchange (SCX) chromatography using solid-phase extraction cartridges containing PolySULFOETHYL A (Poly LC, Columbia, MD). Collection of phosphopeptides started as soon as the SCX cartridge was loaded with peptides and continued throughout an initial wash with

resuspension buffer (fraction Load and Wash; LW). The following fractions were collected with increasing concentrations of KCl in resuspension buffer. Fraction F1 was collected after elution with 17.5 mM KCl and fraction F2 was collected after elution with 70 mM KCl. Afterward, acetonitrile was evaporated by vacuum centrifugation and salts were removed by solid-phase extraction with C18 cartridges and eluted in 50% acetonitrile, 0.1% TFA. Lactic acid was then added to a final concentration of 150 mg/mL to decrease the binding of acidic unphosphorylated peptides in the next step. Phosphopeptides were enriched using TiO₂ (PolyLC) for 45 min mixing constantly at room temperature. TiO₂ material was then washed with 45% acetonitrile, 0.1% TFA and the peptides were eluted with 3% NH₃ in water. NH₃ and water were removed by vacuum centrifugation and the peptides concentrated and desalted using ZipTip C18-based solid phase extraction (twice), then resuspended in 0.1% formic acid [9].

Mass spectrometry and phosphopeptide quantitation. Phosphorylated peptides were analyzed by LC-MS/MS with an Eksigent autosampler coupled with a Nano2DLC pump (Eksigent) and LTQ-Orbitrap (Thermo Fisher Scientific). The samples were loaded onto an analytical column (10 cm, 75 mm inside diameter) packed with 5 mm Integragrit Proteopep2 300 Å C18 (New Objective). Peptides were eluted into the mass spectrometer with a high-performance liquid chromatography (HPLC) gradient of 5 to 40% buffer B in 45 min followed by a quick gradient of 40 to 90% buffer B in 10 min, where buffer A contained 0.1% formic acid in water and buffer B contained 0.1% formic acid in acetonitrile. All HPLC solvents were Ultima Gold quality (Fisher Scientific). Mass spectra were collected in positive ion mode with the Orbitrap for parent mass determination and with the LTQ for data-dependent MS/MS acquisition of the top five most abundant peptides. Each sample was analyzed twice (replicate runs), and in each run one-half of the sample was injected. MS/MS fragmentation spectra were searched with SEQUEST (Version v.27, rev. 12, Thermo Fisher Scientific) against a database containing the combined human-mouse International Protein Index (IPI) protein database (downloaded

December 2006 from ftp.ebi.ac.uk). Search parameters included carbamidomethyl cysteine (*C) as a static modification. Dynamic modifications included phosphorylated tyrosine, serine, or threonine (pY, pS, pT, respectively) and oxidized methionine (*M). Results derived from database searching were filtered using the following criteria: Xcorr >1.0(+1), 1.5(+2), 2(+3); peptide probability score <0.001; dCn >0.1; and mass accuracy <5 ppm (parts per million) with Bioworks version 3.2 (Thermo Electron Corp.). A score was used to more accurately localize the phosphate on the peptide [10]. [11]

To identify phosphopeptide peaks sequenced in some samples but not others, the chromatogram elution profiles are aligned using a dynamic time warping algorithm [12]. The alignment algorithm creates signal maps based on raw MS data (retention time, mass to charge ratio, and intensity) from each sample and aligns samples based on common features from these signal maps. Peaks identified through alignment are visually inspected and manually corrected if necessary. Combination of alignment data with peptide identification allows for calculation of maximal peak intensity across all samples. To determine global change in phosphorylation upon network perturbation, ratios of phosphopeptide peak intensities were calculated by dividing average peak intensity from perturbed cells by average peak intensity from control cells [9].

Growth assays. The numbers of viable cells were determined either directly through the use of a Vi-CELL cell viability analyzer or indirectly by MTT assay. For the Vi-CELL assay, cells were seeded in 6-well plates and counted approximately every 24 hours for 3 days. Each condition and time point was counted in triplicate. Cells were incubated in trypsin long enough to dissociate from plates, then trypsin was neutralized with media containing 10% fetal calf serum and the number of viable cells was determined using a Vi-CELL cell viability analyzer (Beckman Coulter). Natural log of cell number was plotted against time to determine cell doubling time. For the MTT assay, cells were seeded in 96-well plates, with each cell type or treatment

condition performed in triplicate. Approximately every 24 hours for 3 days, 10 μ l of 5 mg/ml MTT (3-(4,5-dimethylthiazolyl-2)-2, 5-diphenyltetrazolium bromide) in PBS was added to cells and allowed to incubate for 2-4 hours at 37°C. Cells were then lysed with 100 μ l of 15% SDS in 15 mM HCl and incubated overnight at room temperature in the dark. All plates were read at 595 nm at the end of the experiment. Absorbance values were normalized to day 0 values and plotted against time to assess relative growth.

Immunoprecipitation. Cells were serum starved in IMDM for 24 hours, then stimulated with 200 ng/ml IGF1 for 30 min at 37°C. Cells were lysed on ice for 30 min with RIPA buffer (50 mM Tris pH 7.4, 150 mM NaCl, 1% NP-40, 0.5% sodium deoxycholate, 0.1% SDS) supplemented with Complete Mini EDTA-free protease inhibitor cocktail (Roche) and 1 mM Na_3VO_4 . 50 μ l of 50% slurry of anti-phosphotyrosine (4G10)-conjugated agarose beads (Millipore) was washed twice with 500 μ l PBS with 0.05% Tween-20 (PBS-T) and added to 500 μ g of cell lysate. The final volume was brought to 500 μ l with PBS-T supplemented with the Roche protease inhibitor cocktail, then incubated with rotation for two hours at 4°C. Beads were washed three times with 500 μ l PBS-T and protein was eluted by boiling for 5 min in 2X protein sample buffer. Eluates were then analyzed by EphB4 immunoblot.

Immunofluorescence. Cells were grown on 4- or 8-well chamber slides, then fixed in 3.7% formaldehyde in PBS for 15 minutes at room temperature and permeabilized with 100% methanol for 10 min at -20°C. Methanol permeabilization was omitted for extracellular proteins. After blocking for one hour with Protein Block (Dako, X0909) diluted 1:10 in PBS, cells were incubated with primary antibody overnight at 4°C or one hour at room temperature and secondary antibody for one hour at room temperature. The primary antibodies used were rabbit anti-phospho-Stat3 Tyr705 (clone D3A7, Cell Signaling Technology, 9145), mouse anti-Stat3 (clone 124H6, Cell Signaling Technology, 9139), and rabbit anti-EphA2 XP (clone D4A2, Cell

Signaling Technology, 6997). The rabbit and mouse secondary antibodies used were conjugated to Alexa Fluor 594 (Invitrogen, A11005, A11012). After antibody incubation, cover slips were mounted with medium containing DAPI (VECTASHIELD Mounting Medium with DAPI, Vector Laboratories, H-1200). Slides were analyzed by fluorescent microscopy with a Zeiss Axiolmager microscope (Carl Zeiss).

Flow cytometry. For phospho-flow experiments, cells were fixed in 1.5% formaldehyde for 10 min at room temperature, then permeabilized with 100% ice-cold methanol for 20 min at 4°C. Cells were then washed twice with staining media (0.5% BSA in PBS, pH 7.4) to remove remaining methanol and incubated with primary antibodies for one hour at room temperature. If using unconjugated primary antibody, cells were again washed twice with staining media, then incubated with fluorochrome-conjugated secondary antibodies. Cells were resuspended in PBS and analyzed by flow cytometry. The primary antibodies used for this analysis were rabbit anti-phospho-Stat3 (Tyr705) XP Alexa Fluor 647 conjugate (clone D3A7, Cell Signaling Technology, 4324) and mouse anti-Stat3 (clone 124H6, Cell Signaling Technology, 9139). The secondary antibody used was Alexa 647 goat anti-mouse IgG (Invitrogen, A-21235). For BAC reporter experiments, live cells were trypsinized, then resuspended in PBS and analyzed by flow cytometry. Flow cytometry data was analyzed using FlowJo.

Conditioned media. ESFT cells were grown in IMDM 10% fetal calf serum for 72 hours in 10 cm plates, between two and five days post lentiviral transduction. Alternatively, ESFT cells were transferred to serum free IMDM two days post transduction and cells were grown for 48 hours. Conditioned media was centrifuged at 2000 rpm for 5 min in a swinging bucket rotor to pellet any cell debris. Supernatant was stored at either 4°C or -20°C. Conditioned media from ESFT cells transduced with EWS/FLI1 shRNA or empty vector control was added to

untransduced cells or cells transduced with empty vector. Whole cell lysates were collected at one hour and approximately 24 hours and subjected to immunoblot analysis.

Cytokine array. The RayBio Human Cytokine Antibody Array C-Series 2000 kit (RayBiotech, Inc.) was used according to the manufacturer's instructions.

ELISA. The concentration of IL-6 in conditioned media was quantified using a human IL-6 Quantikine ELISA Kit (R&D Systems, D6050).

IL-6 immunodepletion and gp130 neutralization. Conditioned media was treated with 2.5 µg/ml of IL-6 neutralizing antibody (R&D Systems, MAB206) and incubated with rotation for one hour at room temperature. The media was next added to 1.5 mg of Protein G Dynabeads (Invitrogen, 10003D) and incubated with rotation for one hour at room temperature. The tube was then placed on a magnet and the IL-6 depleted supernatant was isolated. To neutralize gp130, adherent cells were incubated with 10 µg/ml of gp130 neutralizing antibody (R&D Systems, MAB 228) with gentle agitation for one hour at room temperature.

References

1. Potikyan G, France KA, Carlson MR, Dong J, Nelson SF, Denny CT. (2008) Genetically defined EWS/FLI1 model system suggests mesenchymal origin of Ewing's family tumors. *Lab Invest.* **88**:1291-1302.
2. Potikyan G, Savene RO, Gaulden JM, France KA, Zhou Z, Kleinerman ES, Lessnick SL, Denny CT. (2007) EWS/FLI1 regulates tumor angiogenesis in Ewing's sarcoma via suppression of thrombospondins. *Cancer Res.* **67**:6675-6684.
3. Bromberg JF, Horvath CM, Besser D, Lathem WW, Darnell JE. (1998) Stat3 activation is required for cellular transformation by v-src. *Mol Cell Biol.* **18**:2553-2558.
4. Thompson AD, Teitell MA, Arvand A, Denny CT. (1999) Divergent Ewing's sarcoma EWS/ETS fusions confer a common tumorigenic phenotype on NIH3T3 cells. *Oncogene.* **18**:5506-5513.
5. Ng KP, Potikyan G, Savene ROV, Denny CT, Uversky VN, Lee KAW. (2007) Multiple aromatic side chains within a disordered structure are critical for transcription and transforming activity of EWS family oncoproteins. *Proc Natl Acad Sci U S A.* **104**:479-484.
6. Zhang D, Paley AJ, Childs G. (1998) The transcriptional repressor ZFM1 interacts with and modulates the ability of EWS to activate transcription. *J Biol Chem.* **273**:18086-18091.
7. Welford SM, Hebert SP, Deneen B, Arvand A, Denny CT. (2001) DNA binding domain-independent pathways are involved in EWS/FLI1-mediated oncogenesis. *J Biol Chem.* **276**:41977-41984.
8. Skaggs BJ, Gorre ME, Ryvkin A, Burgess MR, Xie Y, Han Y, Komisopoulou E, Brown LM, Loo JA, Landaw EM, Sawyers CL, Graeber TG. (2006) Phosphorylation of the ATP-binding loop directs oncogenicity of drug-resistant BCR-ABL mutants. *Proc Natl Acad Sci U S A.* **103**:19466-19471.
9. Zimman A, Chen SS, Komisopoulou E, Titz B, Martínez-Pinna R, Kafi A, Berliner JA, Graeber TG. (2010) Activation of aortic endothelial cells by oxidized phospholipids: a phosphoproteomic analysis. *J Proteome Res.* **9**:2812-2824.
10. Beausoleil SA, Villen J, Gerber SA, Rush J, Gygi SP. (2006) A probability-based approach for high-throughput protein phosphorylation analysis and site localization. *Nat Biotechnol.* **24**:1285-1292.
11. Rubbi L, Titz B, Brown L, Galvan E, Komisopoulou E, Chen SS, Low T, Tahmasian M, Skaggs B, Müschen M, Pellegrini M, Graeber TG. (2011) Global phosphoproteomics reveals crosstalk between bcr-abl and negative feedback mechanisms controlling SRC signaling. *Sci Signal.* **4**:ra18.
12. Prakash A, Mallick P, Whiteaker J, Zhang H, Paulovich A, Flory M, Lee H, Aebersold R, Schwikowski B. (2006) Signal maps for mass spectrometry-based comparative proteomics. *Mol Cell Proteomics.* **5**:423-432.

CHAPTER 4

IGF1 SIGNALING IN EWING SARCOMA FAMILY OF TUMORS

Introduction

The insulin-like growth factor (IGF) 1 pathway plays an important role in tumor development due to its regulation of cell proliferation and survival [1,2]. Components of this pathway are dysregulated in multiple neoplasms, including the Ewing sarcoma family of tumors (ESFT). This group of bone and soft tissue malignancies contain reciprocal translocations, most frequently t(11;22), which produces the fusion protein EWS/FLI1. Sarcomagenesis is propelled through a combination of EWS/FLI1 modulation of gene expression and increased IGF1 signaling.

Links between IGF1 signaling and ESFT pathogenesis were first identified through cell line secretion of IGF1 and the ability of a monoclonal antibody targeted against the IGF1 receptor (IGF1R) to inhibit cell growth *in vitro* [3]. The effectiveness of IGF1R inhibitors was later demonstrated in soft agar [4] and xenograft models [5]. Furthermore, IGF1R expression is required for EWS/FLI1-mediated transformation of fibroblasts, providing a connection between IGF and EWS/FLI1 biology [6]. Additionally, EWS/FLI1 represses expression of IGF binding protein 3 (IGFBP3), which controls circulating IGF1 levels [7]. By down regulating a protein that restricts access of the growth factor to its cognate receptor, EWS/FLI1 is able to promote increased IGF1 signaling. Evidence has also been presented that EWS/FLI1 up regulates IGF1 itself, though this has only been demonstrated in transformed mouse mesenchymal progenitor cells [8].

As survival rates for ESFT, in particular recurrent and metastatic cases, have plateaued, the IGF1 pathway has become an attractive candidate for the development of new therapies. The primary focus has been targeting the IGF1 receptor, either with tyrosine kinase inhibitors (TKIs) or monoclonal antibodies. The application of IGF1R TKIs has been primarily limited to pre-clinical studies [9] while antibody therapies have transitioned into the clinic. Early phase I trials of anti-IGF1R monoclonal antibodies in sarcomas and advanced solid tumors showed promising results in Ewing sarcoma patients [10,11]. This included two complete clinical responses, which is rare for a single agent therapy in a phase I study. The success from phase

I trials lead to expanded phase I and II studies for recurrent and refractory Ewing sarcoma [12-15]. Unfortunately, the anti-IGF1R antibodies only displayed modest activity, with objective response rates of approximately 10%. These disappointing results have slowed the clinical development of anti-IGF1R therapies in ESFT. However, efforts are still being made to increase the efficacy of targeting IGF1R in sarcoma, either through combination therapy with other agents or the discovery of predictive biomarkers that can identify subsets of patients who respond to therapy [16,17].

The IGF1R monoclonal antibody clinical trial results accentuate the necessity for better understanding of IGF signaling in ESFT. Characterization of the activity of downstream components, especially in cell lines that are known to be resistant to therapy, can aid in determining which agents should be used in anti-IGF1R combination therapy. To define this pathway, we used quantitative mass spectrometry to measure global changes in tyrosine phosphorylation in ESFT cell lines upon treatment with IGF1 or AMG-479, a fully human monoclonal antibody directed against the IGF1 receptor [18]. Furthermore, we used ESFT cell lines that vary in sensitivity to AMG-479 in order to uncover signaling events that confer drug resistance. Through this analysis we have more thoroughly defined the IGF1 network and identified novel components of signaling in ESFT.

Results

ESFT cells respond to IGF1 stimulation. Initial experiments were performed to validate the rationale of treating ESFT cells with IGF1 or AMG-479 to study signaling. As IGF1 signaling is known to activate the PI3K and MAPK/ERK pathways [19] (Figure 4-3B), we first assessed phosphorylation status of the individual components Akt and Erk. Phospho-specific quantitative immunoblot analysis was performed to measure the activity of these proteins in ESFT cells after IGF1 stimulation. Collection of lysates at multiple time points after growth factor treatment allowed for a dynamic view of IGF1 signaling. As expected, addition of IGF1 results in an up

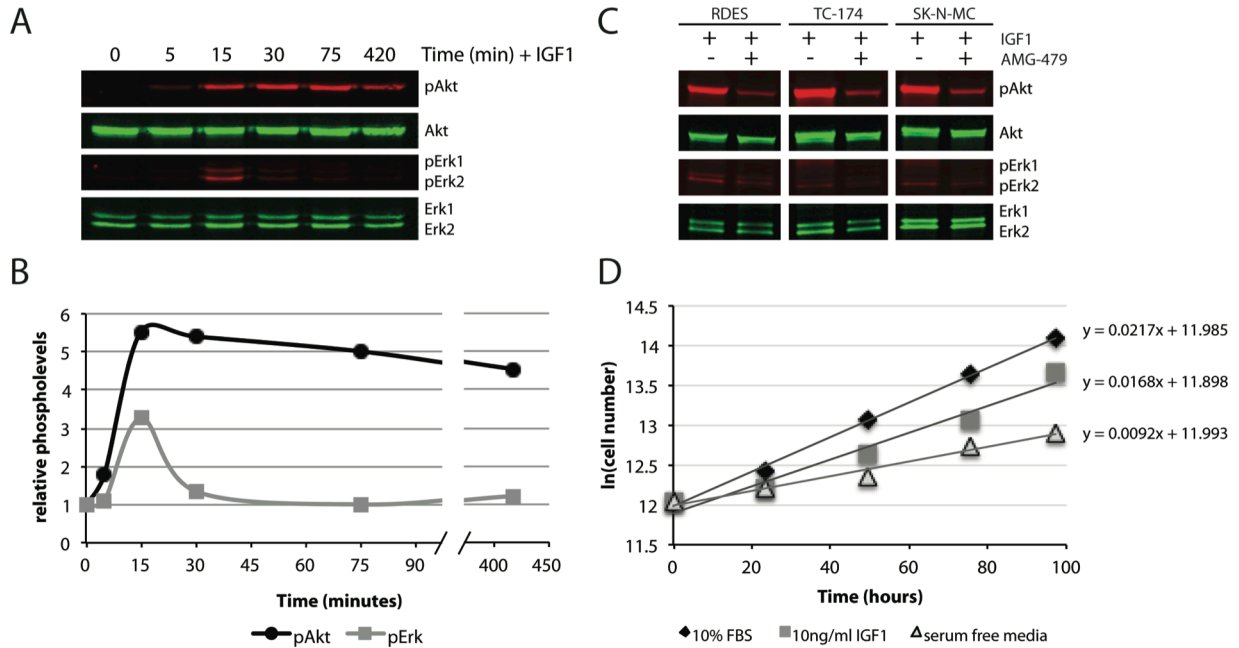


Figure 4-1. IGF1 stimulates activation of downstream components and cell growth in ESFT. (A) After 24 hours of serum starvation, RDES cells were stimulated with 50 ng/ml of IGF1 and whole cell lysates were harvested at time points between 0 and 7 hours. Quantitative immunoblot analysis was performed with antibodies that recognize phospho-Akt (serine 473), phospho-Erk1/2 (threonine 202/204), and corresponding total proteins. (B) Immunoblot signals were quantified by measuring the integrated density of each band with ImageJ. Phospho signals were normalized to total protein for each time point and all time points were normalized to time 0. (C) RDES, TC-174, and SK-N-MC cells growing in complete media were treated with 50 ng/ml IGF1 for 30 min alone or followed by 100 μ g/ml AMG-479 for 20 min. Whole cell lysates were subject to immunoblot analysis as in A. (D) RDES cells were grown in either 10% FBS, 10 ng/ml IGF1, or serum free media. Cells were counted using a Vi-CELL cell viability analyzer and media was changed approximately every 24 hours. Natural log of cell number was plotted against time in order to calculate cell doubling time.

regulation of phospho-Akt and phospho-Erk. Akt displays prolonged phosphorylation that persists up to seven hours while Erk shows a peak of activity at 15 minutes after IGF1 treatment (Figure 4-1A,B). Abrogation of this effect due to treatment with AMG-479 demonstrates that activation of Akt and Erk occurs primarily via signaling through IGF1R (Figure 4-1C). This pathway promotes a mitogenic response in ESFT, as IGF1 is able to sustain cell growth at a doubling time faster than serum-free media alone (Figure 4-1D). RDES cell doubling time in 10% FBS, 10 ng/ml IGF1, and serum-free media was calculated to be 31.9, 41.3, and 75.3 hours, respectively.

After validating the response to IGF1 treatment, we wished to obtain a broader view of downstream signaling components in ESFT cells. Cell lines used for this analysis were selected based on their sensitivity to anti-IGF1R treatment and growth upon IGF1 stimulation. Growth of RDES, TC-174, and SK-N-MC cells is inhibited by anti-IGF1R treatment while A673 cells are highly resistant to this therapy (Figure 4-2B). Sensitive cell lines were treated with 50 ng/ml IGF1 or 100 µg/ml AMG-479 and whole cell lysates were harvested at various time points after treatment. Global changes in tyrosine phosphorylation downstream of IGF1 were assessed by immunoblot using a pan-specific anti-tyrosine (4G10) antibody. An overall increase was observed upon IGF1 treatment and decrease upon IGF1R inhibition (Figure 4-2A, 2C), suggesting further investigation of tyrosine signaling would be an effective strategy to define the IGF1 network in ESFT.

Phosphotyrosine profiling identifies known IGF system components as well as novel regulators of ESFT signaling. To define tyrosine signaling downstream of IGF1, we applied a quantitative, mass spectrometry-based approach [20,21]. ESFT cells were treated with IGF1, AMG-479, or a combination of the two and whole cell lysates were harvested after 20-30 minutes. Following trypsin digestion, tyrosine phosphopeptides were enriched by

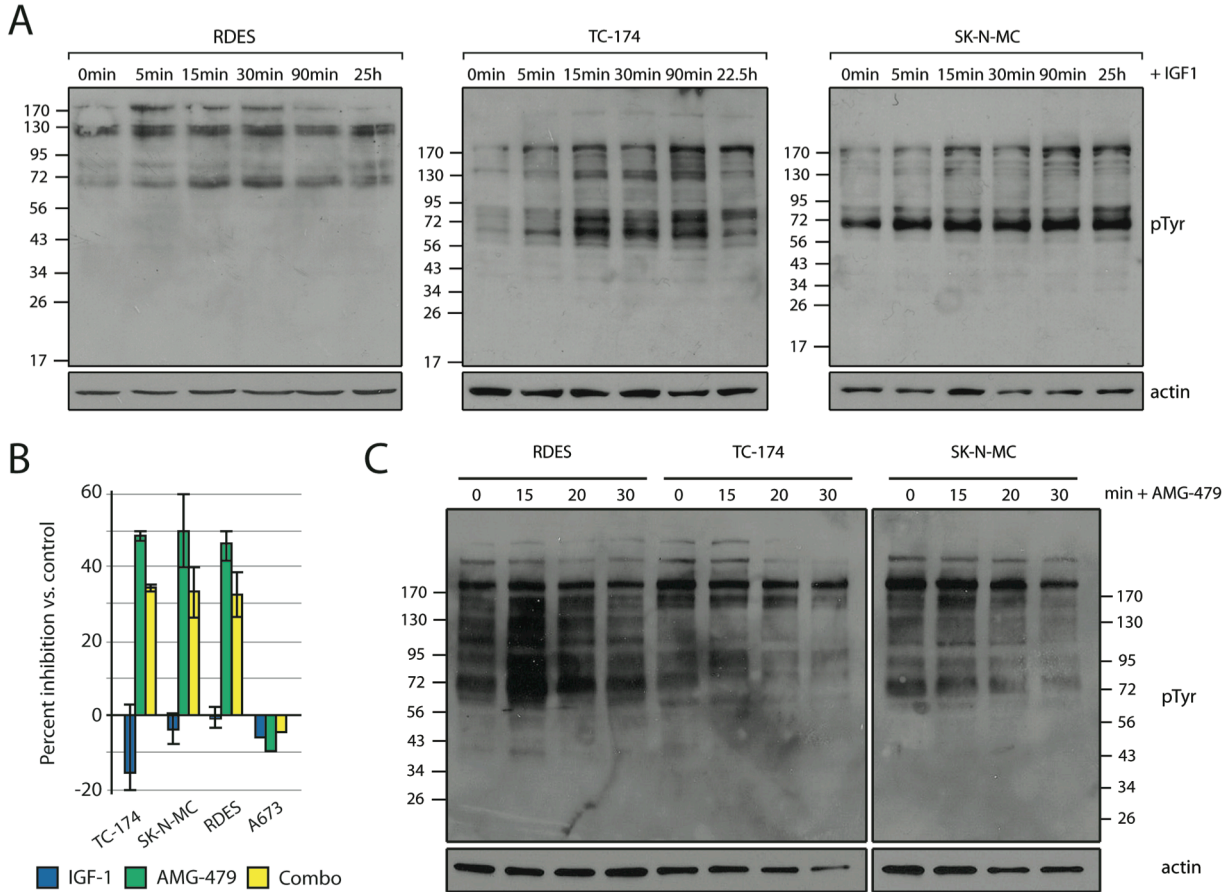


Figure 4-2. ESFT cells display an increase in tyrosine phosphorylation upon IGF1 treatment and decrease with IGF1R inhibitor. (A) After 24 hours of serum starvation, RDES, TC-174, and SK-N-MC cells were treated with 50 ng/ml of IGF1 and whole cell lysates were collected at various time points up to approximately 24 hours. Immunoblot analysis with the 4G10 phospho-tyrosine (pTyr) antibody was used to measure tyrosine phosphorylation. **(B)** Selected data from a panel of ESFT cells treated with 100 μ g/ml AMG-479, 2 nm IGF1, or both, courtesy of William Tap. Data is plotted as percent inhibition of cell growth as compared to controls. **(C)** The same cell lines as used in A were grown in complete media and treated with 100 μ g/ml AMG-479. Whole cell lysates were collected at 0, 15, 20, and 30 minutes and subjected to anti-4G10 immunoblot analysis as in A.

immunoprecipitation with the 4G10 anti-tyrosine antibody. Peptides were then subjected to liquid chromatography coupled to tandem mass spectrometry for identification and quantitation. Global changes in phosphorylation levels upon network perturbation were calculated by determining the phosphopeptide ratio between treated and control cells.

In our initial phosphotyrosine profiling experiment, ESFT cells were treated with 50 ng/ml IGF1 for 30 min and phosphopeptide levels were compared to untreated controls. 15 sets of paired samples (IGF1 treated and control) were run through the mass spectrometer. Between 30 and 80 phosphopeptides were detected per sample, resulting in the identification of a total of 113 unique phosphopeptides corresponding to 76 proteins. Phosphopeptides were ranked based on the sum of the fold change in levels between IGF1 stimulated and control cells across all samples. Figure 4-3 displays a heatmap of the log ratios of phosphopeptides that were identified in more than one set of samples, with enlarged regions corresponding to the top 20 and selected Eph receptors. As indicated in red, the peptides that show the greatest increase in phosphorylation upon IGF1 treatment are enriched for known members of the IGF1 pathway (Figure 4-3C), indicating our approach is effective in defining the IGF1 network in ESFT.

To build upon this preliminary data set, we also treated ESFT cells with the IGF1R inhibitor AMG-479 (100 μ g/ml for 20 min) alone or in combination with 2.5 ng/ml IGF1. The goal of this experiment was to construct an IGF1-driven network with greater confidence through identification of phosphopeptides whose levels both increase in response to IGF1 and decrease upon blockage of its receptor. We also wished to pinpoint proteins that display differences in phosphorylation modulation in anti-IGF1R sensitive and resistant cell lines in hopes of uncovering mechanisms that lead to drug resistance. This was difficult to accomplish in our previous data set because the variability in which peptides were sequenced prevented direct comparison of samples. However, in this experiment, all samples used for the analysis were run consecutively through the mass spectrometer, allowing peptides sequenced in one sample to be quantified in each of the others based on a chromatogram alignment algorithm [22].

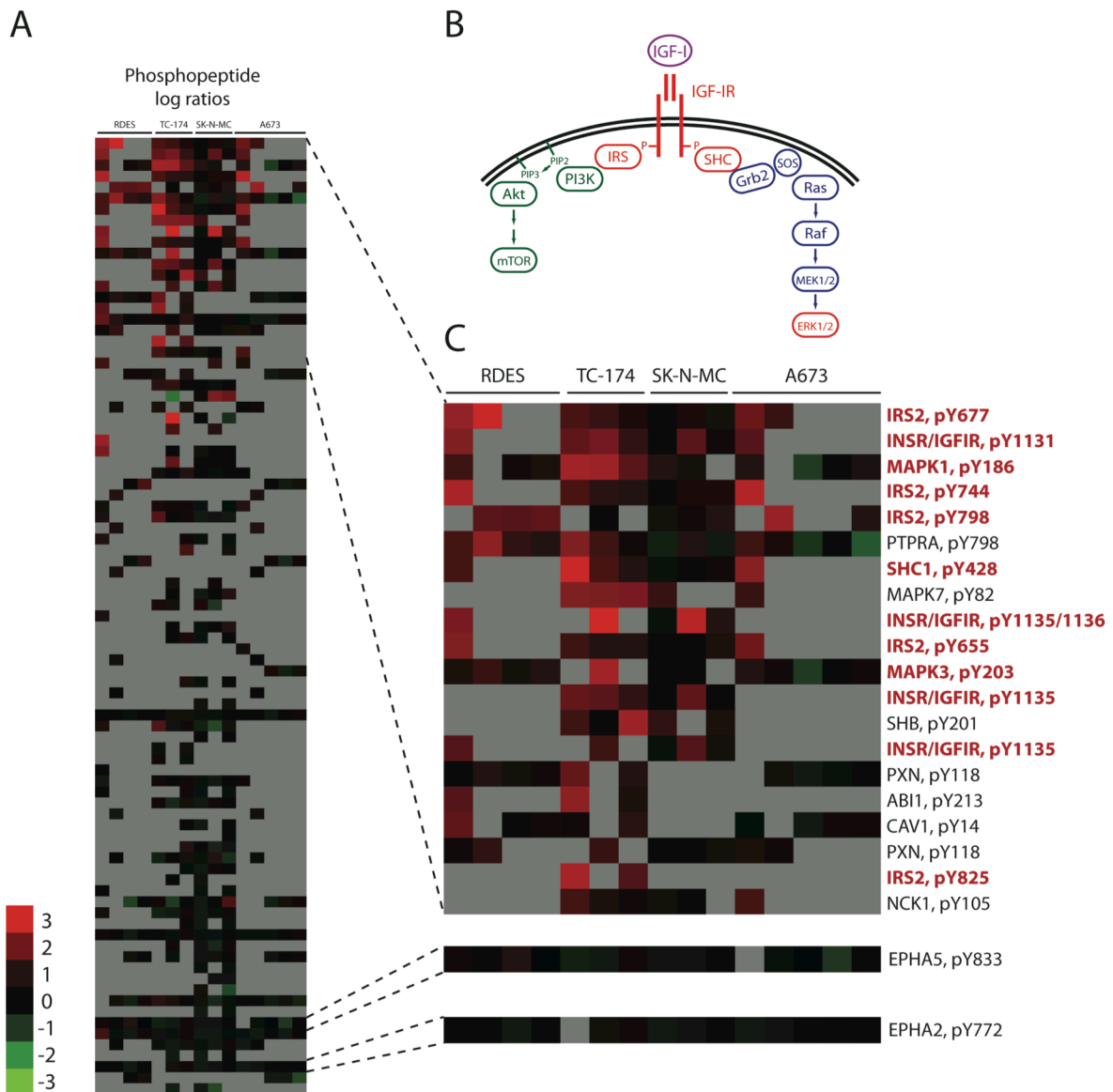


Figure 4-3. Initial IGF1 phosphotyrosine profiling results. (A) Ranking analysis of phosphopeptides. The heatmap displays the log₂ of the fold change in phosphopeptide levels between IGF1 stimulated and control cells. Red indicates positive and green indicates negative log ratios. Gray indicates missing data. Peptides were ranked based on the sum of the fold change across all samples. (B) Schematic of IGF1 signaling pathway highlighting components identified in phosphotyrosine profiling analysis. (C) Enlarged view of the top 20 and selected Eph receptor phosphopeptides. Known components of the IGF1 pathway are indicated in red.

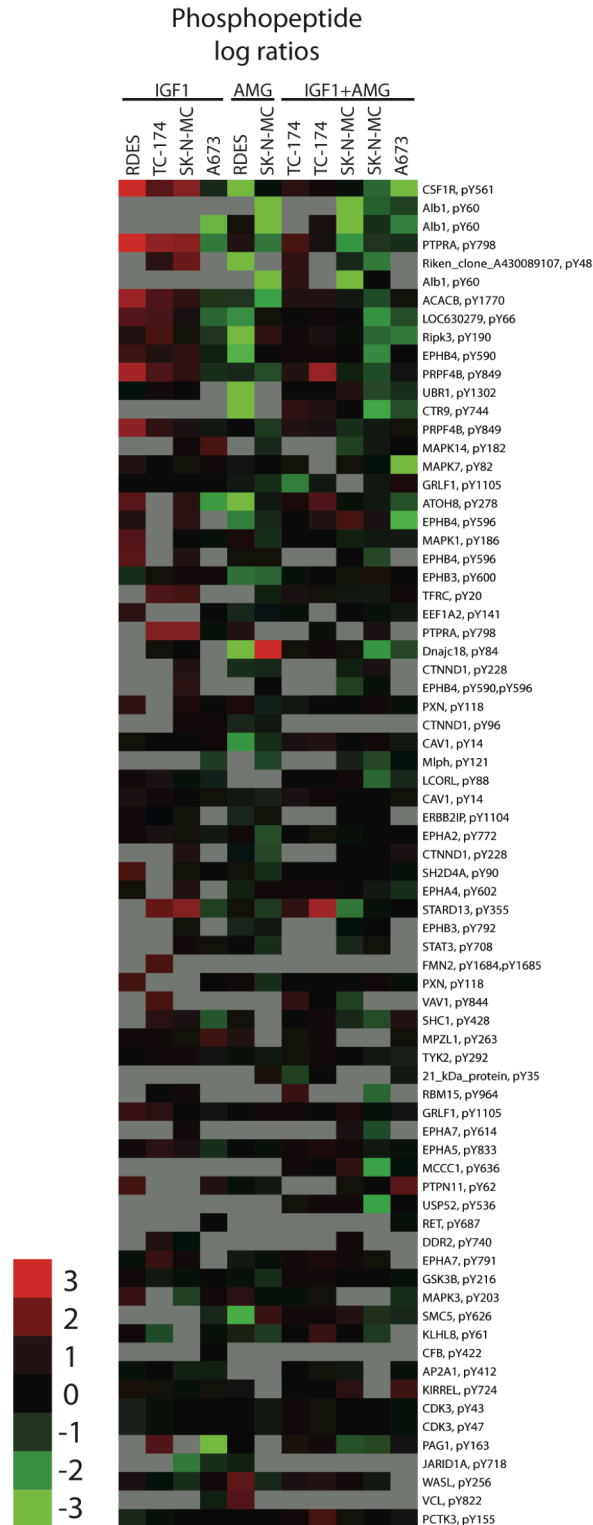


Figure 4-4. IGF1/AMG-479 phosphotyrosine profiling results. The heatmap displays the log₂ of the fold change in phosphopeptide levels between ESFT cells treated with IGF1, AMG-479, or both and control cells. Peptides were ranked based on the sum of the positive fold change of IGF1 treated samples and negative fold change of AMG-479 treated samples.

Phosphotyrosine profiling of ESFT cells treated with IGF1, AMG-479, or both identified 73 phosphopeptides corresponding to 58 proteins. Phosphopeptide ranking was performed in an analogous fashion to the previous experiment, except that positive and negative log fold change were summed from IGF1 and AMG-479 treated samples, respectively (Figure 4-4).

Expression of Eph receptors in ESFT suggests Eph-ephrin signaling may play a role in

tumorigenesis. In addition to known components of the IGF1 pathway, phosphotyrosine profiling also identified phosphorylated Eph receptors (Table 4-1, Figure 4-3C). The most frequently sequenced phosphopeptides were associated with EphA2, EphA5, and EphB4. To further define Eph-ephrin signaling in ESFT, quantitative real time PCR was performed using primers specific to the receptors these receptors and their ligands ephrinA1 and ephrinB2. Analysis of mRNA levels in seven ESFT cell lines revealed EphB4 to be the most highly expressed, followed by EphA2. EphA5 and both ligands displayed low expression (Figure 4-5). Subsequent immunoblot analysis confirmed EphA2 and EphB4 expression in a panel of ESFT cell lines (Figure 4-6A,B). Immunofluorescence experiments displayed the expression of EphA2 on the surface of EFT cell lines (Figure 4-7). Further analysis using EphA2 phosphospecific antibodies confirmed the mass spectrometry results identifying EphA2 Y772 phosphorylation. Comparison of samples with and without IGF1 treatment also confirmed phospho-EphA2 levels do not change upon IGF1 stimulation (Figure 4-6A,C). Additionally, immunoblot analysis using an antibody against phospho-EphA2 Y588, a residue indicated in enzymatic activation, revealed active EphA2 signaling in certain ESFT cell lines (Figure 4-6C). Although EphA2 phosphorylation levels do not change in response to IGF1, our second phosphotyrosine profiling experiment indicated that EphB4 phosphorylation increases in response to IGF1 and decreases upon treatment with AMG-479. Unfortunately, the lack of phospho-EphB4 antibodies has made it difficult to validate these results. Phosphotyrosine immunoprecipitation followed by EphB4 immunoblotting has been performed, confirming the presence of phosphorylated EphB4 in one

ESFT cell line. However, repetition of this experiment with samples with and without IGF1 treatment showed no difference in phospho-EphB4 levels (Figure 4-6D). This may be due to absence of modulation of EphB4 downstream of IGF1R or lack of ability of the immunoprecipitation assay to detect minor phosphorylation changes, as mass spectrometry is more sensitive than immunoblot analysis.

Table 4-1. List of Eph receptor phosphopeptides identified by phosphotyrosine profiling.

Receptor	Phosphopeptide sequence	Phosphosite
EPHA2	TYVDPHTpYEDPNQAVLK	pY594
EPHA2	VLEDDPEATpYTTSGGK	pY772
EPHA3	TpYVDPHTYEDPTQAVHEFAK	pY596
EPHA3	TYVDPHTpYEDPTQAVHEFAK	pY602
EPHA3	TpYVDPHTpYEDPTQAVHEFAK	pY596,pY602
EPHA4	TpYVDPFTYEDPNQAVR	pY596
EPHA4	TYVDPFTpYEDPNQAVR	pY602
EPHA5	VLEDDPEAApYTTR	pY833
EPHA7	TYIDPETpYEDPNR	pY614
EPHA7	VIEDDPEAVpYTTTGGK	pY791
EPHB1	IYIDPFTpYEDPNEAVR	pY600
EPHB2	FLEDDTSDPTpYTSALGGK	pY780
EPHB3	LQQpYIAPGMK	pY600
EPHB3	FLEDDPSDPTpYTSSLGGK	pY792
EPHB4	VpYIDPFTYEDPNEAVR	pY590
EPHB4	VYIDPFTpYEDPNEAVR	pY596
EPHB4	VpYIDPFTpYEDPNEAVR	pY590,pY596
EPHB4	FLEENSSDPTpYTSSLGGK	pY774

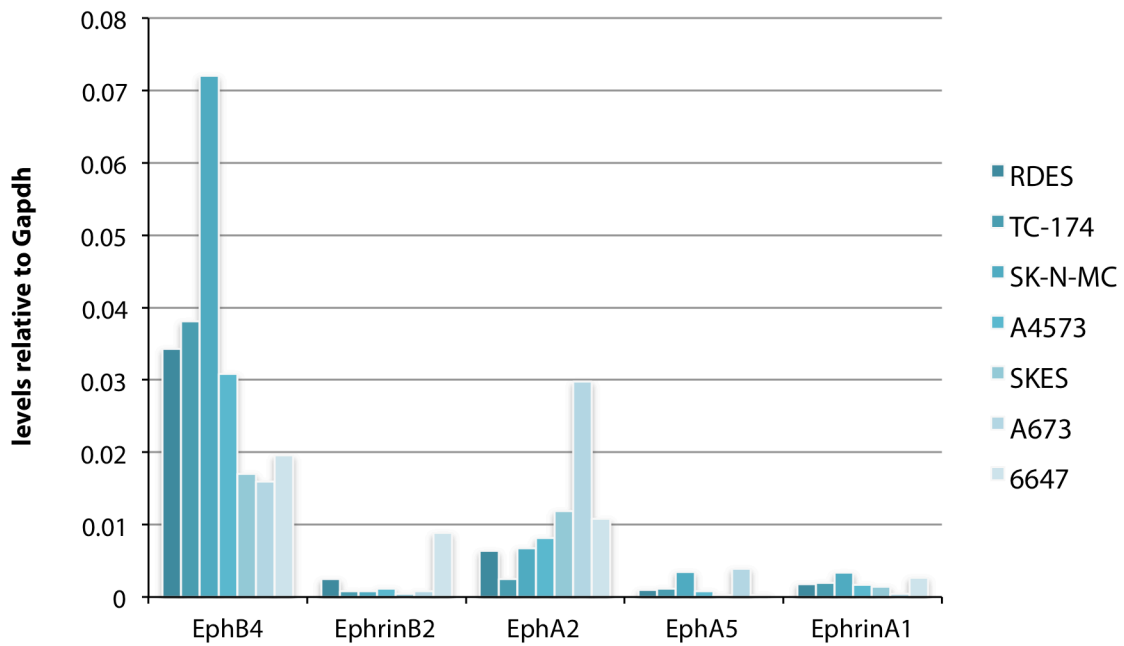


Figure 4-5. Eph receptor and ephrin ligand transcript levels in ESFT cells. Quantitative real time PCR was performed to measure mRNA levels of the Eph receptors EphB4, EphA2, and EphA5 and the ligands ephrinB2 and ephrinA1 in seven ESFT cell lines. C(t) values were compared to those of loading control GAPDH to assess relative levels of expression. Data is plotted as $1/2^{\Delta C(t)}$, where $\Delta C(t)$ is the difference between Eph/ephrin and GAPDH C(t) values.

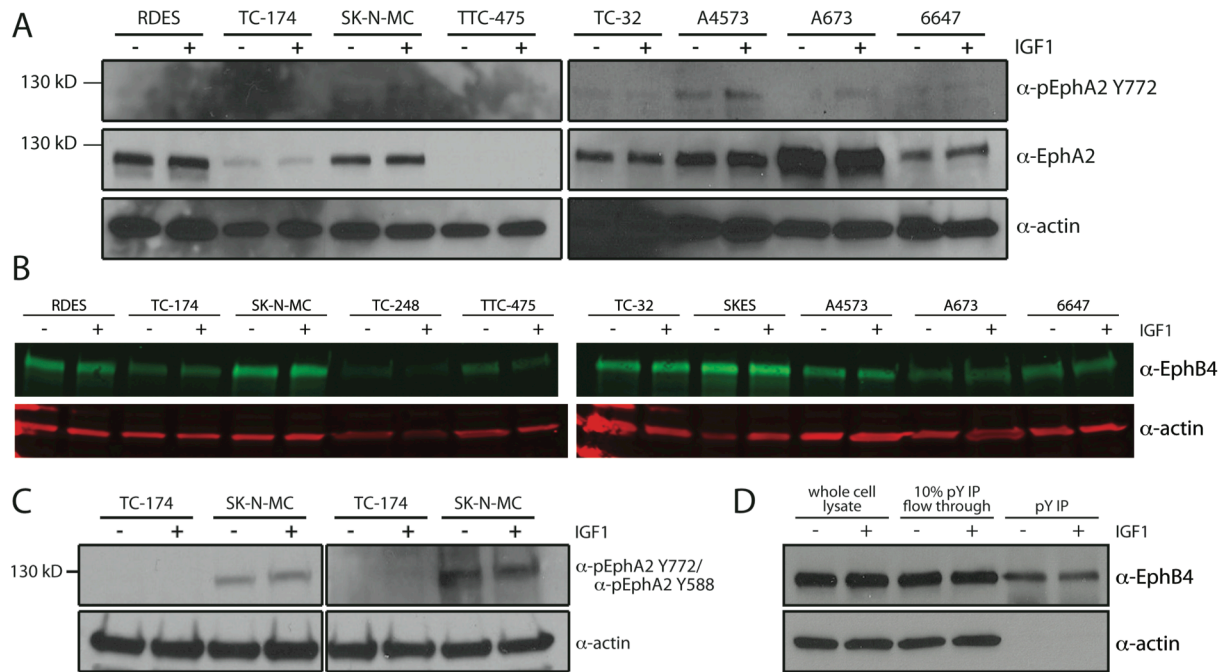


Figure 4-6. EphA2 and EphB4 are expressed and phosphorylated in ESFT cell lines. (A) ESFT cells were serum starved for 24 hours in IMDM, then treated with 50 ng/ml IGF1 and whole cell lysates were collected after 30 minutes. Immunoblot analysis was used to measure total and phospho-EphA2 (Y772) levels. **(B)** Quantitative immunoblot analysis was used to measure EphB4 expression in cell lysates isolated as in A. **(C)** Immunoblot analysis was used to measure phospho-EphA2 levels in TC-174 and SK-N-MC cells in the presence and absence of IGF1. Cells were treated as in A. **(D)** EphB4 immunoblot of SK-N-MC whole cell lysate and phospho-tyrosine immunoprecipitate. SK-N-MC cells were serum starved in IMDM for 24 hours, then stimulated with 200 ng/ml IGF1 for 30 min.

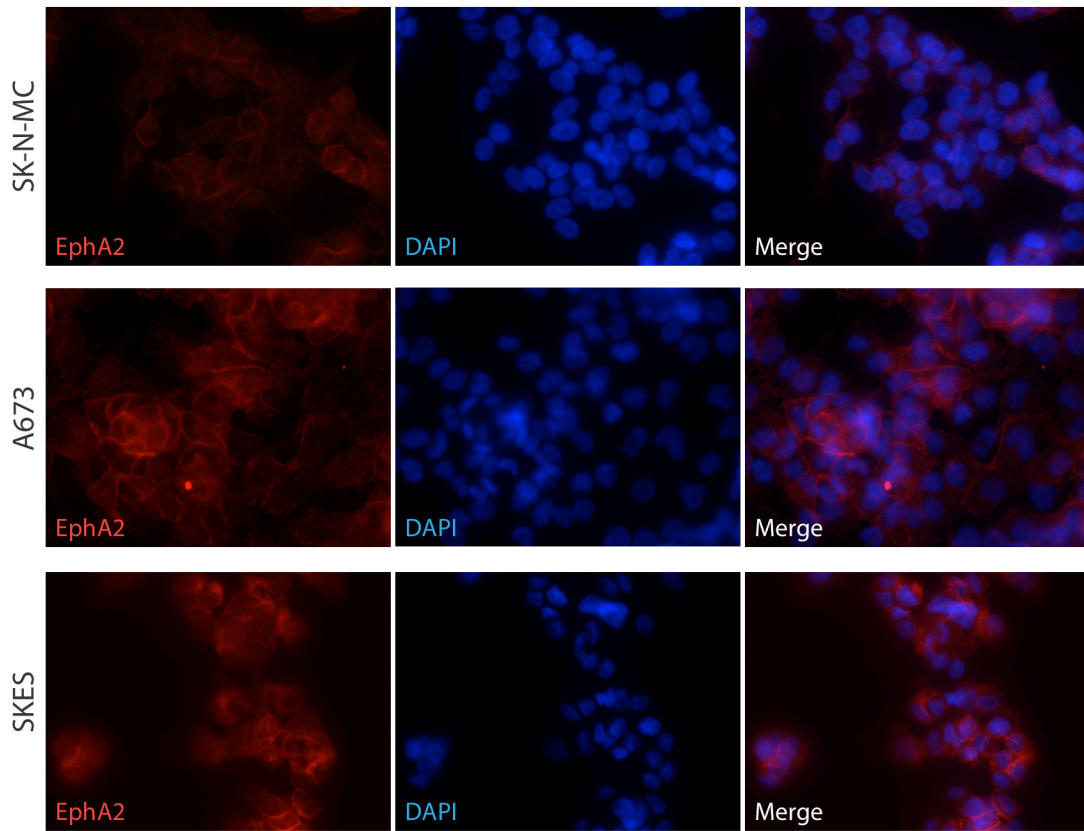


Figure 4-7. EphA2 is expressed on the surface of ESFT cells at sites of cell-to-cell contact. Immunofluorescence using an EphA2-specific antibody followed by a fluorochrome-conjugated secondary antibody was used to visualize expression in SK-N-MC, A673, and SKES cells.

Phosphotyrosine profiling of ESFT cells that vary in sensitivity to AMG-479 treatment

identifies potential candidates involved in drug resistance. To assess differences in anti-

IGF1R sensitive and resistant cell lines, a t-test was used to compare mean fold change in

phosphopeptide levels in samples corresponding to each cell type. Phosphopeptides were

sorted based on p-value and a subset of those with the lowest p-values were selected for further

analysis based on the availability of phospho-specific antibodies. Because only one anti-IGF1R

resistant cell line was used for phosphotyrosine profiling, immunoblot analysis was used to

examine phosphorylation levels in a larger panel of cell lines. For these experiments, ten ESFT

cell lines that vary in their sensitivity to anti-IGF1R treatment were treated with IGF1 and probed

for phospho-PTPRA (Y789), phospho-PZR (MPZL1) (Y263), and phospho-Src (Y527). The

phospho-MPZL1 and phospho-PTPRA immunoblots reflected the phosphotyrosine profiling

results, displaying higher levels after IGF1 stimulation in anti-IGF1R sensitive cell lines. A673

cells displayed low levels of phospho-PTPRA in both the absence and presence of IGF1, most

likely the reason this phosphopeptide was identified as being differentially regulated in anti-

IGF1R resistant cells. However, the other resistant line used in this analysis showed the same

pattern as the sensitive lines, suggesting PTPRA is not involved in anti-IGF1R resistance. Src

phosphorylation at tyrosine 527 renders the kinase less active [23] and PTPRA functions to

enhance its activity by removing the phosphate group at this residue [24]. Yet our immunoblot

analysis did not reflect this regulation as phospho-Src levels did not change upon IGF1

treatment and were low even in the absence of phospho-PTPRA. In the case of phospho-PZR,

weak signals allowed for comparison between only a few cell lines so we were unable to

conclude whether there was differential regulation between sensitive and resistant cell lines.

Discussion

Despite the initial aim of identifying components downstream of IGF1, phosphotyrosine profiling

also uncovered phosphopeptides whose levels did not change in response to IGF1 or AMG-479

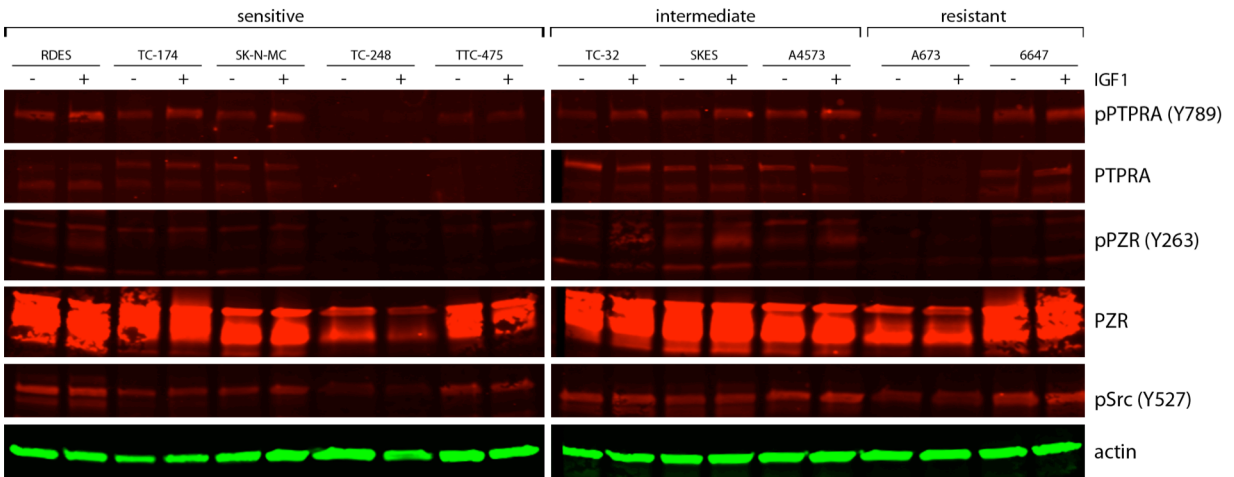


Figure 4-8. Comparison of IGF1 modulation between anti-IGF1R sensitive and resistant ESFT cell lines. Cells were treated as in Figure 4-6A,B. Quantitative immunoblot analysis was performed to measure phospho-PTPRA (Y789), PTPRA, phospho-PZR (Y263), PZR, and phospho-Src (Y527) levels.

treatment, such as those corresponding to Eph receptors. Immunoblot analysis confirmed broad expression of EphA2 and EphB4 in ESFT cell lines, yet only detected low levels of phosphorylation. This may be due to low ligand expression as indicated by real time PCR analysis of transcript levels.

High receptor but low ligand expression has been observed in other types of cancer, such as breast and colorectal. In a study of colorectal cancer tumor specimens, EphB4 was expressed in all of the samples analyzed and absent in normal colon tissue. Cell lines also displayed high levels of EphB4 while ephrinB2 was only expressed in a small population of cells. EphB4 was shown to be phosphorylated in cells cultured with serum and still retained this state even when siRNA was used to abolish ephrinB2 expression, suggesting receptor phosphorylation occurs through a ligand-independent mechanism [25]. In breast cancer, EphB4 is expressed in a broad panel of cell lines, but is not tyrosine phosphorylated. As with the colorectal cancer cell lines, ephrinB2 expression is very low, accounting for the absence of phosphorylation on its receptor. In this system, activation of EphB4 by ephrinB2 stimulation inhibits tumorigenesis, suggesting breast cancer cells evade the tumor suppressing effects of Eph forward signaling through ligand down regulation [26]. The association between reduced EphB activity and accelerated tumorigenesis has also been demonstrated in colorectal cancer [27]. Additionally, inverse correlation between receptor and ligand expression has also been observed with EphA2 and its ligand ephrinA1 in breast cancer cell lines [28].

The patterns of receptor and ligand expression, low receptor phosphorylation, and evidence from other neoplasms argue against active transmission of Eph forward signals in EFST. Crosstalk with other pathways such as PI3K and MAPK has been reported [28,29], so it is possible that Eph signaling may be occurring through one of these mechanisms. Additionally, a recent sarcoma phosphotyrosine profiling study identified multiple members of the Eph family, particularly in ESFT cell lines [30]. Analysis in sarcoma tumor samples revealed EphB4 to be one of the most abundant phosphopeptides. This data combined with the characterization of

Eph receptor expression and signaling in osteosarcoma [31,32] and rhabdomyosarcoma [33] warrant further study of this pathway in ESFT.

Our phosphotyrosine profiling analysis identified approximately 100 phosphopeptides in anti-IGF1R sensitive and resistant ESFT cell lines treated with IGF1 and/or AMG-479. Although our second experiment generated a more complete data set, quantitation values were unavailable for phosphopeptides in some samples, resulting in missing data. This limited the number of peptides that could be statistically analyzed for differences in phosphorylation fold change between sensitive and resistant cell lines. Our analysis was also limited by the utilization of only three sensitive lines and one resistant. The limitation was established by the large amount of protein (~30 mg) and thus cells required for phosphotyrosine profiling. To overcome these constraints, we selected two phosphopeptides for phospho-specific immunoblot analysis that varied in their response to IGF1 and AMG-479 in sensitive and resistant cell lines, based on phosphopeptide ranking and t-test p-value. As immunoblot analysis requires much less protein, we were able to extend the analysis to ten ESFT cell lines treated with IGF1.

Although results correlated with those from the phosphotyrosine profiling, inconsistencies in phosphoprotein levels between anti-IGF1R resistant cell lines and weak immunoblot signals made it difficult to make any definite conclusions. Additionally, the availability of phospho-specific antibodies restricted our ability to validate additional proteins that might be implicated in AMG-479 resistance based on our mass spectrometry results. In this case, a more targeted approach may be more effective than an unbiased method. Recent studies have identified up regulation of mTOR, ERK, and insulin receptor signaling in drug resistant tumors and cell lines by measuring phosphorylation of specific downstream components [34,35]. Use of more global methods, such as antibody arrays, may aid in further defining these drug resistance mechanisms.

Although our drug resistance study was inconclusive, immunoblot analysis of PTPRA confirmed phosphorylation increases upon IGF1 treatment. This implicates involvement of Src

family kinases (SFks) in IGF1 signaling in ESFT, as PTPRA is known to regulate Src. Although there did not appear to be modulation at tyrosine 527, some ESFT cell lines displayed increased phosphorylation at tyrosine 416 (Figure 4-9B), which is required for enzymatic activation. However, there was not a consistent trend between anti-IGF1R sensitive and resistant cell lines so it is unclear exactly what role SFks play in IGF1 signaling. Additionally, motif analysis of phosphopeptides identified by phosphotyrosine profiling after IGF1 treatment indicated enrichment of a Src motif when examining only the top 50 peptides based on the ranking in Figure 4-3 (Figure 4-9A). The involvement of SFks in ESFT is further demonstrated by the ability to decrease tumor growth by targeting the SFk member Lyn [36]. The previously mentioned sarcoma phosphotyrosine profiling study [30] also detected phosphorylated SFks in ESFT cells, adding to the evidence that SFks are important factors in ESFT signaling.

Phosphotyrosine profiling in ESFT cells provided a global, unbiased view of IGF1 signaling that uncovered known IGF mediators as well as novel signaling components. Identification of Eph receptors and SFks has provided new insight into ESFT biology. Although further work is needed to define these networks, they offer avenues of research for discovery of novel drug targets.

References

1. Pollak M. (2008) Insulin and insulin-like growth factor signalling in neoplasia. *Nat Rev Cancer*. **8**:915-928.
2. Pollak MN, Schernhammer ES, Hankinson SE. (2004) Insulin-like growth factors and neoplasia. *Nat Rev Cancer*. **4**:505-518.
3. Yee D, Favoni RE, Lebovic GS, Lombana F, Powell DR, Reynolds CP, Rosen N. (1990) Insulin-like growth factor I expression by tumors of neuroectodermal origin with the t(11;22) chromosomal translocation. A potential autocrine growth factor. *J Clin Invest*. **86**:1806-1814.
4. Scotlandi K, Benini S, Sarti M, Serra M, Lollini PL, Maurici D, Picci P, Manara MC, Baldini N. (1996) Insulin-like growth factor I receptor-mediated circuit in Ewing's sarcoma/peripheral neuroectodermal tumor: a possible therapeutic target. *Cancer Res*. **56**:4570-4574.
5. Scotlandi K, Benini S, Nanni P, Lollini PL, Nicoletti G, Landuzzi L, Serra M, Manara MC, Picci P, Baldini N. (1998) Blockage of insulin-like growth factor-I receptor inhibits the growth of Ewing's sarcoma in athymic mice. *Cancer Res*. **58**:4127-4131.
6. Toretsky JA, Kalebic T, Blakesley V, LeRoith D, Helman LJ. (1997) The insulin-like growth factor-I receptor is required for EWS/FLI-1 transformation of fibroblasts. *J Biol Chem*. **272**:30822-30827.
7. Prieur A, Tirode F, Cohen P, Delattre O. (2004) EWS/FLI-1 silencing and gene profiling of Ewing cells reveal downstream oncogenic pathways and a crucial role for repression of insulin-like growth factor binding protein 3. *Mol Cell Biol*. **24**:7275-7283.
8. Riggi N, Cironi L, Provero P, Suva ML, Kaloulis K, Garcia-Echeverria C, Hoffmann F, Trumpp A, Stamenkovic I. (2005) Development of Ewing's sarcoma from primary bone marrow-derived mesenchymal progenitor cells. *Cancer Res*. **65**:11459-11468.
9. Manara MC, Landuzzi L, Nanni P, Nicoletti G, Zambelli D, Lollini PL, Nanni C, Hofmann F, Garcia-Echeverria C, Picci P, Scotlandi K. (2007) Preclinical in vivo study of new insulin-like growth factor-I receptor--specific inhibitor in Ewing's sarcoma. *Clin Cancer Res*. **13**:1322-1330.
10. Olmos D, Postel-Vinay S, Molife LR, Okuno SH, Schuetze SM, et al. (2010) Safety, pharmacokinetics, and preliminary activity of the anti-IGF-1R antibody figitumumab (CP-751,871) in patients with sarcoma and Ewing's sarcoma: a phase 1 expansion cohort study. *Lancet Oncol*. **11**:129-135.
11. Tolcher AW, Sarantopoulos J, Patnaik A, Papadopoulos K, Lin C-C, et al. (2009) Phase I, pharmacokinetic, and pharmacodynamic study of AMG 479, a fully human monoclonal antibody to insulin-like growth factor receptor 1. *J Clin Oncol*. **27**:5800-5807.
12. Juergens H, Daw NC, Geoerger B, Ferrari S, Villarroel M, Aerts I, Whelan J, Dirksen U, Hixon ML, Yin D, Wang T, Green S, Paccagnella L, Gualberto A. (2011) Preliminary

Efficacy of the Anti-Insulin-Like Growth Factor Type 1 Receptor Antibody Figitumumab in Patients With Refractory Ewing Sarcoma. *J Clin Oncol*.

13. Pappo AS, Patel SR, Crowley J, Reinke DK, Kuenkele K-P, et al. (2011) R1507, a Monoclonal Antibody to the Insulin-Like Growth Factor 1 Receptor in Patients With Recurrent or Refractory Ewing Sarcoma Family of Tumors: Results of a Phase II Sarcoma Alliance for Research through Collaboration Study. *J Clin Oncol*.
14. Malempati S, Weigel B, Ingle AM, Ahern CH, Carroll JM, Roberts CT, Reid JM, Schmechel S, Voss SD, Cho SY, Chen HX, Krailo MD, Adamson PC, Blaney SM. (2012) Phase I/II trial and pharmacokinetic study of cixutumumab in pediatric patients with refractory solid tumors and Ewing sarcoma: a report from the Children's Oncology Group. *J Clin Oncol*. **30**:256-262.
15. Tap WD, Demetri G, Barnette P, Desai J, Kavan P, et al. (2012) Phase II Study of Ganitumab, a Fully Human Anti-Type-1 Insulin-Like Growth Factor Receptor Antibody, in Patients With Metastatic Ewing Family Tumors or Desmoplastic Small Round Cell Tumors. *J Clin Oncol*.
16. Ho AL, Schwartz GK. (2011) Targeting of insulin-like growth factor type 1 receptor in Ewing sarcoma: unfulfilled promise or a promising beginning? *J Clin Oncol*. **29**:4581-4583.
17. Beltran PJ, Chung YA, Moody G, Mitchell P, Cajulis E, Vonderfecht S, Kendall R, Radinsky R, Calzone FJ. (2011) Efficacy of ganitumab (AMG 479), alone and in combination with rapamycin, in Ewing's and osteogenic sarcoma models. *J Pharmacol Exp Ther*. **337**:644-654.
18. Beltran PJ, Mitchell P, Chung Y-A, Cajulis E, Lu J, Belmontes B, Ho J, Tsai MM, Zhu M, Vonderfecht S, Baserga R, Kendall R, Radinsky R, Calzone FJ. (2009) AMG 479, a fully human anti-insulin-like growth factor receptor type I monoclonal antibody, inhibits the growth and survival of pancreatic carcinoma cells. *Mol Cancer Ther*. **8**:1095-1105.
19. Chitnis MM, Yuen JSP, Protheroe AS, Pollak M, Macaulay VM. (2008) The type 1 insulin-like growth factor receptor pathway. *Clin Cancer Res*. **14**:6364-6370.
20. Rubbi L, Titz B, Brown L, Galvan E, Komisopoulou E, Chen SS, Low T, Tahmasian M, Skaggs B, Mutschen M, Pellegrini M, Graeber TG. (2011) Global phosphoproteomics reveals crosstalk between bcr-abl and negative feedback mechanisms controlling SRC signaling. *Sci Signal*. **4**:ra18.
21. Skaggs BJ, Gorre ME, Ryvkin A, Burgess MR, Xie Y, Han Y, Komisopoulou E, Brown LM, Loo JA, Landaw EM, Sawyers CL, Graeber TG. (2006) Phosphorylation of the ATP-binding loop directs oncogenicity of drug-resistant BCR-ABL mutants. *Proc Natl Acad Sci U S A*. **103**:19466-19471.
22. Prakash A, Mallick P, Whiteaker J, Zhang H, Paulovich A, Flory M, Lee H, Aebersold R, Schwikowski B. (2006) Signal maps for mass spectrometry-based comparative proteomics. *Molecular & cellular proteomics : MCP*. **5**:423-432.
23. Hunter T. (1987) A tail of two src's: mutatis mutandis. *Cell*. **49**:1-4.

24. den Hertog J, Pals CE, Peppelenbosch MP, Tertoolen LG, de Laat SW, Kruijjer W. (1993) Receptor protein tyrosine phosphatase alpha activates pp60c-src and is involved in neuronal differentiation. *EMBO J.* **12**:3789-3798.
25. Kumar SR, Scehnet JS, Ley EJ, Singh J, Krasnoperov V, et al. (2009) Preferential induction of EphB4 over EphB2 and its implication in colorectal cancer progression. *Cancer Res.* **69**:3736-3745.
26. Noren NK, Foos G, Hauser CA, Pasquale EB. (2006) The EphB4 receptor suppresses breast cancer cell tumorigenicity through an Abl-Crk pathway. *Nat Cell Biol.* **8**:815-825.
27. Battle E, Bacani J, Begthel H, Jonkheer S, Jonkeer S, Gregorieff A, van de Born M, Malats N, Sancho E, Boon E, Pawson T, Gallinger S, Pals S, Clevers H. (2005) EphB receptor activity suppresses colorectal cancer progression. *Nature.* **435**:1126-1130.
28. Macrae M, Neve RM, Rodriguez-Viciano P, Haqq C, Yeh J, Chen C, Gray JW, McCormick F. (2005) A conditional feedback loop regulates Ras activity through EphA2. *Cancer Cell.* **8**:111-118.
29. Miao H, Li D-Q, Mukherjee A, Guo H, Petty A, Cutter J, Basilion JP, Sedor J, Wu J, Danielpour D, Sloan AE, Cohen ML, Wang B. (2009) EphA2 mediates ligand-dependent inhibition and ligand-independent promotion of cell migration and invasion via a reciprocal regulatory loop with Akt. *Cancer Cell.* **16**:9-20.
30. Bai Y, Li J, Fang B, Edwards A, Zhang G, Bui M, Eschrich S, Altioek S, Koomen J, Haura EB. (2012) Phosphoproteomics identifies driver tyrosine kinases in sarcoma cell lines and tumors. *Cancer Res.* **72**:2501-2511.
31. Abdou AG, Abd El-Wahed MM, Asaad NY, Samaka RM, Abdallaha R. (2009) Immunohistochemical profile of ephrin A4 expression in human osteosarcoma. *APMIS.* **117**:277-285.
32. Fritsche-Guenther R, Noske A, Ungethüm U, Kuban R-J, Schlag PM, Tunn P-U, Karle J, Krenn V, Dietel M, Sers C. (2010) De novo expression of EphA2 in osteosarcoma modulates activation of the mitogenic signalling pathway. *Histopathology.* **57**:836-850.
33. Berardi AC, Marsilio S, Rofani C, Salvucci O, Altavista P, Perla FM, Diomedi-Camassei F, Uccini S, Kokai G, Landuzzi L, McDowell HP, Dominici C. (2008) Up-regulation of EphB and ephrin-B expression in rhabdomyosarcoma. *Anticancer Res.* **28**:763-769.
34. Garofalo C, Manara MC, Nicoletti G, Marino MT, Lollini PL, Astolfi A, Pandini G, Lopez-Guerrero JA, Schaefer KL, Belfiore A, Picci P, Scotlandi K. (2011) Efficacy of and resistance to anti-IGF-1R therapies in Ewing's sarcoma is dependent on insulin receptor signaling. *Oncogene.* **30**:2730-2740.
35. Subbiah V, Naing A, Brown RE, Chen H, Doyle L, LoRusso P, Benjamin R, Anderson P, Kurzrock R. (2011) Targeted morphoproteomic profiling of Ewing's sarcoma treated with insulin-like growth factor 1 receptor (IGF1R) inhibitors: response/resistance signatures. *PLoS ONE.* **6**:e18424.

36. Guan H, Zhou Z, Gallick GE, Jia SF, Morales J, Sood AK, Corey SJ, Kleinerman ES. (2008) Targeting Lyn inhibits tumor growth and metastasis in Ewing's sarcoma. *Mol Cancer Ther.* 7:1807-1816.

CHAPTER 5

EWS/FLI1-MEDIATED SIGNALING IN EWING SARCOMA FAMILY OF TUMORS

Introduction

The Ewing sarcoma family of tumors (ESFT) is a group of bone and soft tissue malignancies that includes Ewing sarcoma, primitive peripheral neuroectodermal tumors, extraosseous Ewing sarcoma, and Ewing sarcoma of the chest wall. They are associated by the presence of reciprocal chromosomal translocations that unite the EWS gene with an ETS transcription factor, most commonly FLI1 [1,2]. The resulting fusion protein joins the potent activation domain of EWS to the DNA-binding domain of FLI1, generating an aberrant transcription factor [3,4]. Subsequent modulation of target genes plays a primary role in driving tumorigenesis.

Microarray analysis of ESFT cell lines after siRNA-mediated down regulation of EWS/FLI1 or heterologous cell types with ectopic expression have revealed a large number of dysregulated genes [5]. Potential direct targets have been confirmed through demonstration of EWS/FLI1 upstream binding. This set includes genes involved in a wide variety of cellular processes including transcriptional regulation [6,7], cell cycle progression [8], angiogenesis [9,10], and survival [11,12]. Although much work has been done to characterize these genes and their individual roles in oncogenesis, less focus has been placed on the role of EWS/FLI1 in signal transduction.

Although EWS/FLI1 primarily functions as a transcriptional regulator, dysregulation of target genes ultimately triggers biochemical pathways that promote tumorigenesis. In particular, EWS/FLI1 modulation of insulin-like growth factor binding protein 3 (IGFBP3) leads to activation of the insulin-like growth factor 1 (IGF1) pathway [11]. IGF1 binding to its cognate receptor stimulates downstream PI3K and MAPK pathways, which promote cellular proliferation and survival [13]. IGFBP3 binds IGF1, restricting its access to the IGF1 receptor (IGF1R). EWS/FLI1 down regulation of IGFBP3 releases this inhibition, resulting in increased IGF1 signaling and tumor growth.

To improve ESFT survival rates, an increased emphasis has been placed on targeted therapies, especially agents directed against signaling molecules. IGF1R monoclonal

antibodies have been the main focus based on the involvement of the IGF1 pathway in ESFT biology [14] and initial clinical success [15,16]. More recently, mTOR (mammalian target of rapamycin) inhibitors have also been used either alone or in combination with IGF1R inhibitors [17,18]. However, clinical studies have shown minimal response rates to these therapies, indicating that additional pathways may be engaged in ESFT pathogenesis [19]. In order to identify these pathways, we sought to characterize cellular signaling downstream of EWS/FLI1. An unbiased mass spectrometry-based approach was applied to quantify global changes in phosphorylation in an ESFT cell line after siRNA-mediated EWS/FLI1 knock down. This analysis uncovered a paracrine signaling mechanism that activates Stat3, highlighting the heterogeneity that can exist within the tumor and the importance of the microenvironment. Further understanding of this pathway may lead to new therapeutic strategies when treating ESFT.

Results

Phosphoproteomic profiling identifies up regulation of Stat3 phosphorylation at residue 705 upon EWS/FLI1 knock down. Advancements in mass spectrometry have enabled the analysis of entire phosphoproteomes, detecting hundreds to thousands of peptides in a single experiment [20,21]. The specificity of this approach allows for identification and quantitation of phosphorylation at specific amino acid residues. A further advantage is the unbiased nature of this technique, thus studies are not limited to a few proteins of interest. We applied this global, unbiased method to delineate cellular signaling networks modulated by EWS/FLI1.

In order to determine which signaling components are regulated by EWS/FLI1, we utilized quantitative, label-free mass spectrometry to measure changes in protein phosphorylation levels upon siRNA-mediated EWS/FLI1 knock down (Figure 5-1A) [22,23]. The ESFT cell line A673 was transduced with lentivirus containing an shRNA targeting the coding region of FLI1 (U6 818) or an empty vector control (U6). This cell line was selected due to its

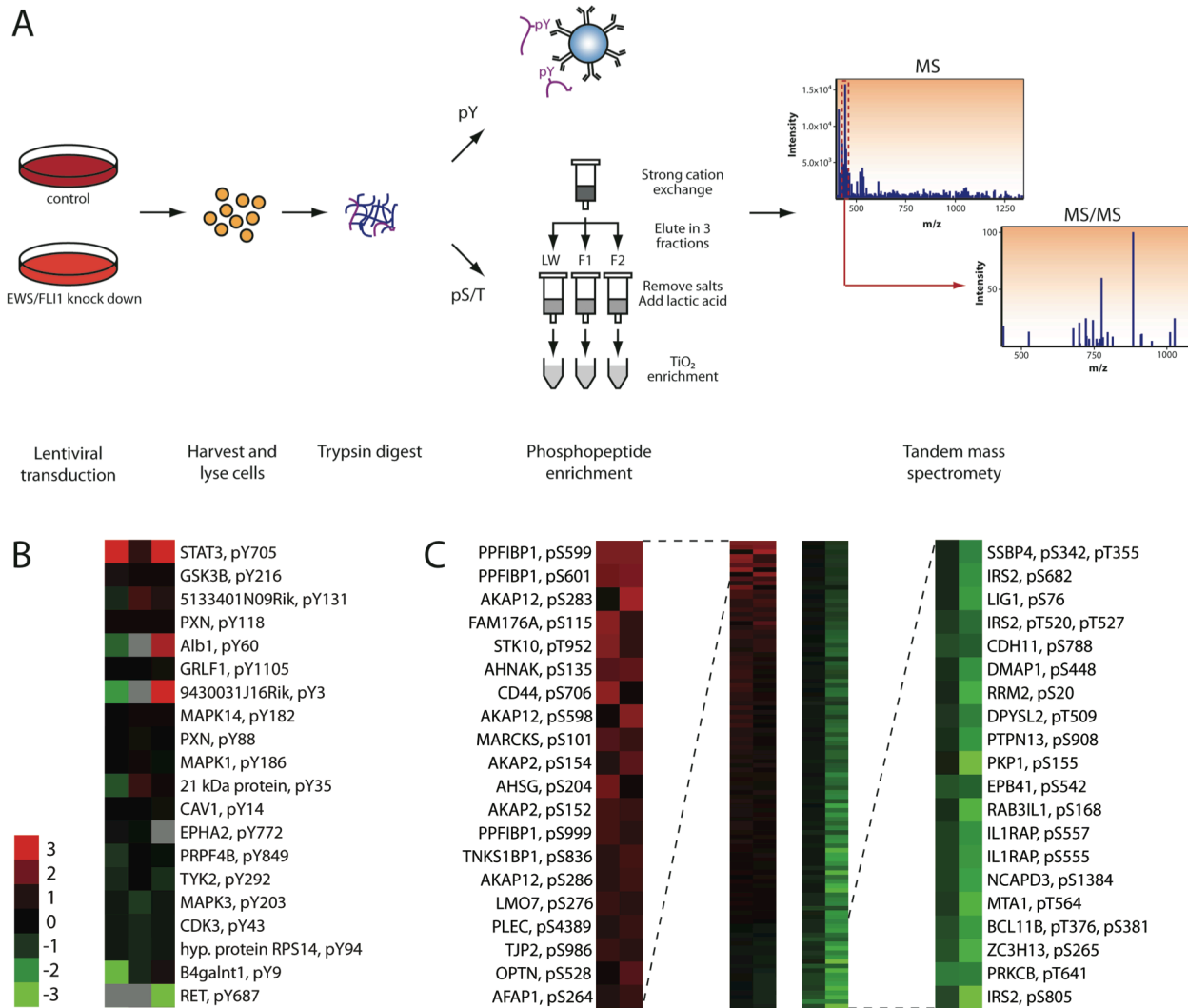


Figure 5-1. Phosphoproteomic profiling identifies proteins whose phosphorylation status is modulated downstream of EWS/FLI1. (A) Experimental workflow. After lentiviral transduction, cells are harvested and lysates are subjected to trypsin digestion. Phosphotyrosine (pY) peptides are enriched by immunoprecipitation with an anti-phosphotyrosine (4G10) antibody. Phosphoserine/threonine (pS/T) peptides are first enriched by strong cation exchange, in which three elution fractions are collected. Each fraction is run through a reverse phase (C18) column to remove salts. TiO_2 metal affinity in the presence of lactic acid is used as an additional enrichment step. Phosphopeptides are identified and quantified by tandem mass spectrometry subsequent to liquid chromatography. **(B,C)** The heatmaps display the log₂ of the fold change in phosphopeptide levels between knock down and control A673 cells. Red indicates positive and green indicates negative log ratios. Gray indicates missing data. Peptides were ranked based on the sum of the fold change across all samples. **(B)** Phosphotyrosine profiling results of three biological replicates. **(C)** Phosphoserine/threonine profiling results of phosphopeptides modulated by EWS/FLI1. The top and bottom 20 phosphopeptides based on the ranking analysis are enlarged. Only two biological replicates were used in this experiment since each sample was separated into three fractions after strong cation exchange chromatography.

ability to maintain proliferation with decreased EWS/FLI1 expression. Whole cell lysates were collected after transduced cells were expanded for three to eight days to generate enough protein for mass spectrometry analysis. Proteins were digested into peptides by trypsin, which next underwent phosphopeptide enrichment. Tyrosine phosphorylated peptides were isolated by immunoaffinity purification while serine/threonine phosphopeptides were purified by a combination of strong cation exchange chromatography and titanium dioxide (TiO₂) enrichment. Enriched samples were analyzed by liquid chromatography coupled to tandem mass spectrometry.

Phosphotyrosine profiling identified only 20 phosphopeptides (Figure 5-1B), while analysis of serine/threonine phosphopeptides detected 547 unique phosphopeptides corresponding to 331 proteins. The phosphoserine/threonine data set was filtered for peptides that were modulated greater than 1.2-fold upon EWS/FLI1 knock down. This generated a list of 210 phosphopeptides, 86 of which that showed an increase in phosphorylation and 124 of which that displayed a decrease (Figure 5-1C). DAVID (**D**atabase for **A**nnotation, **V**isualization and **I**ntegrated **D**iscovery) was used to determine pathways and biological process that were enriched in response to EWS/FLI1 in each of these subsets (Table 5-1, 5-2) [24,25]. Phosphopeptides whose levels were increased after EWS/FLI1 knock down were associated with adhesion and cytoskeletal organization while those that displayed a decrease were mainly associated with cell cycle regulation. Proteins associated with tight junctions were found to be enriched in both sets of phosphopeptides that were modulated by EWS/FLI1. This could either be due to the presence of positive and negative regulators of this process or the enrichment is not significant since the corrected p-values (Benjamini) are greater than 0.05.

Phosphotyrosine and phosphoserine/threonine peptides were rank ordered based on the sum of the fold change in phosphopeptide levels between EWS/FLI1 knock down and control samples. Because inhibiting the expression of EWS/FLI1 results in an up regulation of IGFBP3, a negative regulator of IGF signaling, we expected to see mainly a decrease in phosphopeptide

Table 5-1. Over represented Gene Ontology biological processes

Phosphorylation increase				
Term	Count	Pop Hits	P-value	Benjamini
GO:0006907~pinocytosis	2	4	0.0118	0.9995
GO:0016192~vesicle-mediated transport	6	576	0.0272	0.9999
GO:0007010~cytoskeleton organization	5	436	0.0399	0.9998
GO:0051128~regulation of cellular component organization	5	458	0.0464	0.9995
GO:0007155~cell adhesion	6	700	0.0554	0.9994
GO:0022610~biological adhesion	6	701	0.0557	0.9979
GO:0010033~response to organic substance	6	721	0.0614	0.9971
GO:0051493~regulation of cytoskeleton organization	3	136	0.0618	0.9941
GO:0031032~actomyosin structure organization	2	28	0.0801	0.9975
Phosphorylation decrease				
Term	Count	Pop Hits	P-value	Benjamini
GO:0007049~cell cycle	20	776	1.08E-07	7.18E-05
GO:0000279~M phase	13	329	5.51E-07	1.83E-04
GO:0022403~cell cycle phase	14	414	9.70E-07	2.15E-04
GO:0022402~cell cycle process	16	565	1.08E-06	1.79E-04
GO:0000278~mitotic cell cycle	12	370	1.20E-05	0.0016
GO:0000280~nuclear division	9	220	5.00E-05	0.0055
GO:0007067~mitosis	9	220	5.00E-05	0.0055
GO:0000087~M phase of mitotic cell cycle	9	224	5.68E-05	0.0054
GO:0048285~organelle fission	9	229	6.63E-05	0.0055

Count: number of genes from list submitted to DAVID that are associated with a GO process, Pop Hits: number of genes in the human genome that are associated with that GO process, P-value: p-value from a modified Fisher's exact test to determine if the percentage of submitted genes (count/total number) is statistically enriched compared to the percentage of genes in the human genome (pop hits/number of genes in genome), Benjamini: multiple testing correction technique to globally correct enrichment p-value to control family-wide false discovery rate.

Table 5-2. Over represented pathways

Phosphorylation increase					
Database	Term	Count	Pop Hits	P-value	Benjamini
KEGG	hsa04530:Tight junction	4	134	0.0065	0.1384
	hsa04670:Leukocyte transendothelial migration	3	118	0.0460	0.4184
Biocarta	h_neutrophilPathway:Neutrophil and Its Surface Molecules	2	8	0.0491	0.7434
	h_lymphocytePathway:Adhesion Molecules on Lymphocyte	2	9	0.0551	0.5349
	h_monocytePathway:Monocyte and its Surface Molecules	2	11	0.0670	0.4643
Reactome	REACT_578:Apoptosis	3	129	0.0629	0.7895
Phosphorylation decrease					
Database	Term	Count	Pop Hits	P-value	Benjamini
KEGG	hsa04530:Tight junction	6	134	0.0012	0.0745
	hsa05223:Non-small cell lung cancer	4	54	0.0041	0.1293
	hsa05214:Glioma	4	63	0.0064	0.1329
	hsa04012:ErbB signaling pathway	4	87	0.0154	0.2288
	hsa04666:Fc gamma R-mediated phagocytosis	4	95	0.0195	0.2314
	hsa04960:Aldosterone-regulated sodium reabsorption	3	41	0.0254	0.2501
	hsa04510:Focal adhesion	5	201	0.0323	0.2699
	hsa04670:Leukocyte transendothelial migration	4	118	0.0342	0.2525
	hsa05416:Viral myocarditis	3	71	0.0689	0.4124
	hsa04370:VEGF signaling pathway	3	75	0.0758	0.4105
	hsa04010:MAPK signaling pathway	5	267	0.0768	0.3853
Biocarta	h_tnfr1Pathway:TNFR1 Signaling Pathway	4	30	0.0064	0.2397
	h_fasPathway:FAS signaling pathway (CD95)	4	31	0.0070	0.1397
	h_vdrPathway:Control of Gene Expression by Vitamin D Receptor	3	27	0.0478	0.5042
Reactome	REACT_152:Cell Cycle, Mitotic	8	304	0.0039	0.0894
	REACT_383:DNA Replication	5	97	0.0043	0.0501
	REACT_498:Signaling by Insulin receptor	3	39	0.0302	0.2177
	REACT_7970:Telomere Maintenance	3	56	0.0584	0.3031

Count: number of genes from list submitted to DAVID that are associated with a pathway, Pop Hits: number of genes in the human genome that are associated with that pathway, P-value: p-value from a modified Fisher's exact test to determine if the percentage of submitted genes (count/total number) is statistically enriched compared to the percentage of genes in the human genome (pop hits/number of genes in genome), Benjamini: multiple testing correction technique to globally correct enrichment p-value to control family-wide false discovery rate.

levels, which was reflected in the phosphoserine/threonine analysis. However, our phosphotyrosine rank ordering revealed the most differentially regulated phosphopeptide corresponded to an increase in phosphorylation of Stat3 at tyrosine 705 (Figure 5-1B, 5-2A). This result was confirmed with a phospho-specific antibody (Figure 5-2B). Quantitative immunoblot analysis showed a 2.5-fold increase in phospho-Stat3 levels between A673 U6 818 and control cells (Figure 5-2C). Phospho-Stat3 up regulation upon EWS/FLI1 knock down was also observed with the use of a second shRNA construct (EF4), verifying this response is not a result of off-target effects (Figure 5-2B). This effect is specific to phosphorylation at tyrosine 705, as serine 727 is not modulated upon knock down (Figure 5-2D).

Since only one ESFT cell line was used for the phosphoproteomic analysis, we next examined phospho-Stat3 levels after EWS/FLI1 knock down in six additional lines. Only the A673 cell line showed an increase at two days post transduction. However, when this analysis was extended to five days, five additional cell lines also displayed an increase in Stat3 phosphorylation (Figure 5-2E). The response was not as robust as that of the A673 line and appeared to correlate with the level of EWS/FLI1 knock down (data not shown).

Phospho-Stat3 up regulation primarily occurs in a subset of cells untransduced by lentiviral shRNA. As activation of Stat3 promotes tumorigenesis through up regulation of cell survival and proliferation factors [26], we sought to further characterize this pathway in ESFT. After validating that Stat3 phosphorylation is increased upon EWS/FLI1 knock down, we asked whether Stat3 activity is also increased. To answer this question, Stat3 immunofluorescence was performed to visualize localization before and after EWS/FLI1 knock down in A673 cells. Phosphorylation at tyrosine 705 allows Stat3 to dimerize, then translocate to the nucleus where it acts as a transcription factor [27,28]. Because ESFT cells display only low levels of phospho-Stat3, we expected to observe primarily cytoplasmic localization, followed by increased nuclear localization after EWS/FLI1 knock down. However, Stat3 immunostaining showed largely

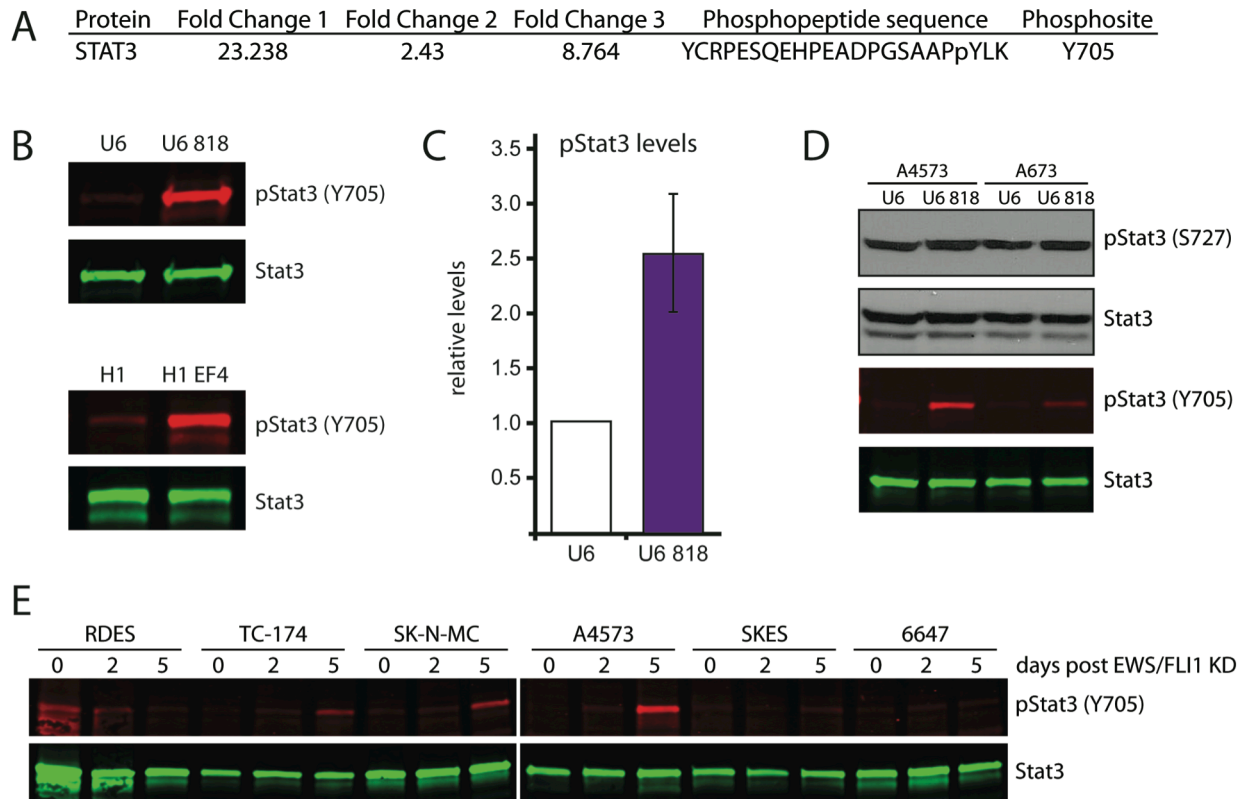
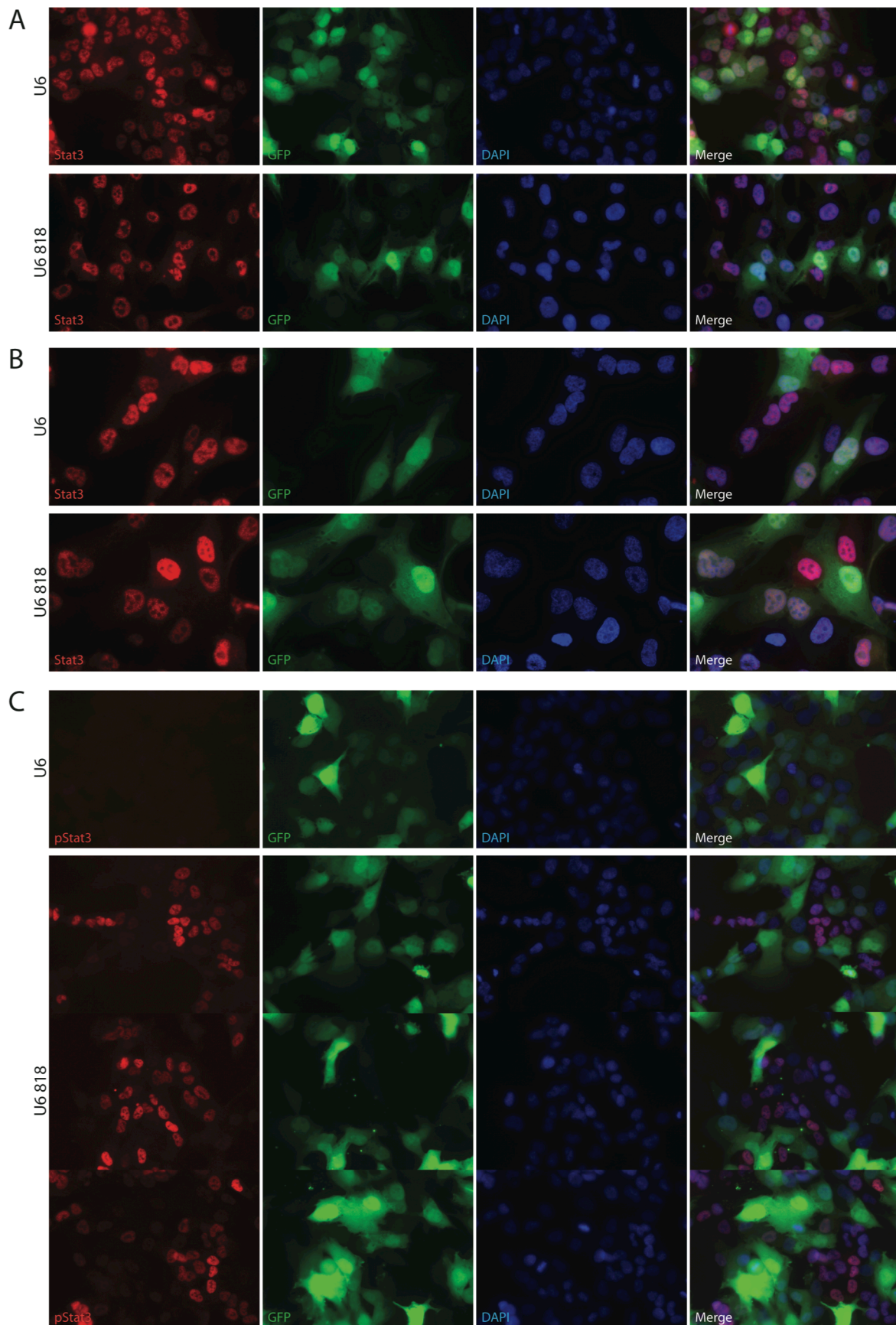


Figure 5-2. Phosphotyrosine profiling identifies up regulation of Stat3 phosphorylation at residue 705 upon EWS/FLI1 knock down. (A) Summary of fold change in phospho-Stat3 levels upon EWS/FLI1 knock down based on mass spectrometry quantitation values. (B) Immunoblot analysis of phospho-Stat3 (Y705) and total Stat3 levels in A673 cells transduced with EWS/FLI1 shRNA (818 or EF4) and corresponding vector controls (U6 or H1). (C) Quantitation of phospho-Stat3 immunoblot signals from EWS/FLI1 knock down and control samples based on ImageJ integrated density values. Phospho-Stat3 levels were normalized to total Stat3 levels. The data plotted is an average of three biological replicates. Error bars represent standard deviation. (D) Immunoblot analysis of phospho-Stat3 (S727 and Y705) and total Stat3 in A4573 and A673 cells transduced with vector control (U6) or EWS/FLI1 shRNA (U6 818). Cell lysates were harvested five days post lentiviral transduction. (E) Immunoblot analysis of phospho-Stat3 (Y705) and total Stat3 levels in ESFT cell lines transduced with vector control or EWS/FLI1 shRNA. EWS/FLI1 knock down cell lysates were collected two and five days post lentiviral transduction.

Figure 5-3. Immunofluorescence displays nearly mutually exclusive phospho-Stat3 and GFP expression. (A) Stat3 immunostaining of A673 cells transduced with vector control (U6) or EWS/FLI1 shRNA (U6 818). Transduced cells are GFP positive as the lentiviral vector contains a GFP marker. Cell nuclei were visualized using DAPI. Pictures were taken at 40X magnification. (B) Same as in A, except for pictures were taken at 63X magnification. (C) Phospho-Stat3 (Y705) immunostaining of A673 cells transduced with vector control (U6) and EWS/FLI1 shRNA (U6 818). Pictures were taken at 40X magnification.



nuclear signals in both knock down and control cells (Figure 5-3A). Examination at higher magnification suggested there might be more intense nuclear staining in the knock down cells (Figure 5-3B).

The similarity in Stat3 staining between U6 and U6 818 cells led us to also perform phospho-specific staining (Figure 5-3C). A673 U6 cells displayed a low level of phospho-Stat3 while a subset of 818 cells showed prominent staining, as expected based our immunoblot results. Interestingly, the subset of 818 cells that displayed high levels of phospho-Stat3 showed almost no overlap with the GFP positive population marking cells transduced with the lentiviral shRNA. We had initially suspected a direct regulation of Stat3 by EWS/FLI1, but this data suggests a paracrine mechanism.

To quantitate phospho-Stat3 levels in ESFT U6 and U6 818 GFP positive and negative populations, we performed phospho-specific flow cytometry (Figure 5-4) [29]. Because the CSCG lentiviral vector contains a GFP marker, we were able to determine which U6 818 cells have decreased EWS/FLI1 expression based on GFP expression. Both A673 U6 and U6 818 cells were divided into two populations based on GFP fluorescence intensity and phospho-Stat3 levels were measured through the use of a fluorochrome-conjugated phospho-specific antibody. When comparing all A673 U6 and U6 818 cells, U6 818 displayed an increase in median fluorescence intensity (MFI) of 3.17, a number similar to the one obtained through our quantitative western blot analysis. However, when this comparison was performed on GFP negative and GFP positive populations, the GFP negative cells showed a nearly 4-fold increase in MFI in U6 818 cells while GFP positive cells showed only a 1.9-fold increase (Figure 5-4A). The U6 818 GFP negative population also showed an increase in total Stat3 levels compared to U6, whereas the amount of Stat3 remained constant in the GFP positive populations (5-4B). Similar effects were observed using A4573 cells, though of a lesser magnitude (Figure 5-4C,D). These results support our postulation that the up regulation of phospho-Stat3 after EWS/FLI1

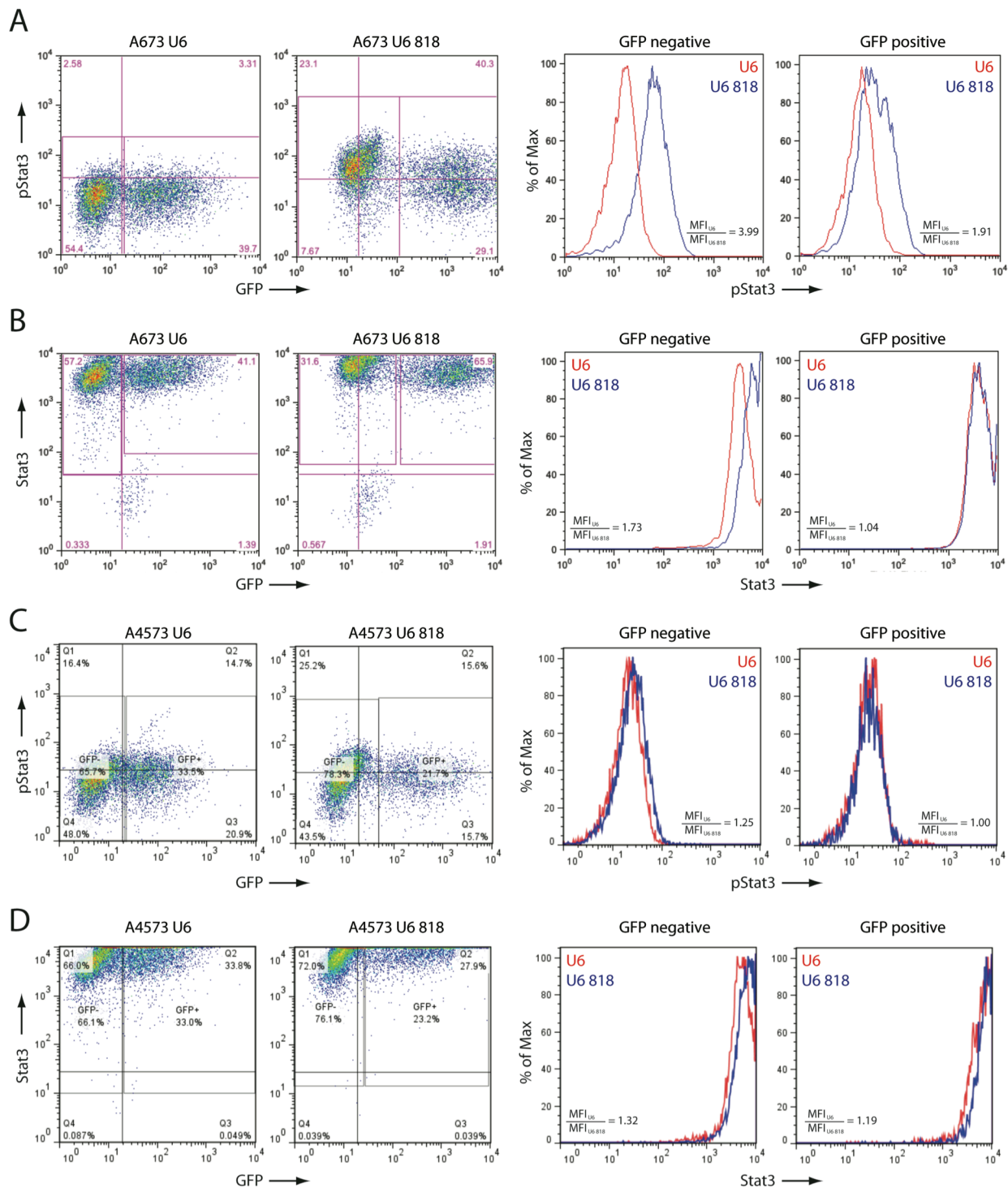


Figure 5-4. Phospho-specific flow cytometry confirms difference in phospho-Stat3 levels between transduced and untransduced populations of ESFT cells after EWS/FLI1 knock down. (A,B) Flow cytometric analysis of phospho-Stat3 (Y705) (A) or total Stat3 (B) and GFP levels in A673 cells transduced with vector control (U6) or EWS/FLI1 shRNA (U6 818). Phospho-Stat3/Stat3 fluorescence intensity levels are plotted for GFP negative and positive populations. The ratio of median fluorescence intensity (MFI) between U6 and U6 818 cells is indicated on the graphs. **(C,D)** Same as in A and B, except for A4573 cells were used.

knock down occurs primarily in a population untransduced by the lentiviral shRNA and is thus uninfluenced by EWS/FLI1 knock down.

Soluble factors secreted upon EWS/FLI1 knock down are sufficient to induce Stat3

phosphorylation. The evidence that phospho-Stat3 up regulation and EWS/FLI1 knock down occur in separate subsets of cells suggested these populations are communicating with each other either through direct cell-to-cell contact or secretion of soluble factors. To test for the presence of soluble factors, conditioned media from ESFT cells transduced with either vector control (U6) or EWS/FLI1 shRNA (U6 818) was added to U6 cells and Stat3 phosphorylation was assayed by immunoblot. Conditioned media from U6 818 cells but not U6 was able to stimulate phospho-Stat3. Consistent with previous immunoblots, treatment with conditioned media from A673 U6 818 cells resulted in the highest increase in phospho-Stat3. Additionally, conditioned media from A673 cells transduced with the EF4 EWS/FLI1 shRNA and serum free EF4 conditioned media were able to stimulate Stat3 phosphorylation (Figure 5-5A).

Two of the four ESFT cell lines assayed for the ability of conditioned media to stimulate phospho-Stat3 displayed only a weak response. To determine if this is due to a lack of secreted factor in the conditioned media or expression of the appropriate receptor on the cell surface, we added A673 U6 818 conditioned media to TC-174 and SK-N-MC cells (Figure 5-5B). Both cell lines showed a large increase in phospho-Stat3, indicating they express the appropriate receptors, but do not secrete as much of the soluble factor upon EWS/FLI1 knock down as the A673 cells. This is most likely due to a combination of lower viral transduction rates when compared to the A673 cells and that TC-174 and SK-N-MC U6 818 cells are beginning to undergo cell death at five days after EWS/FLI1 knock down. This results in a smaller population of cells affected by EWS/FLI1 knock down and thus fewer cells that secrete a factor able to stimulate phospho-Stat3.

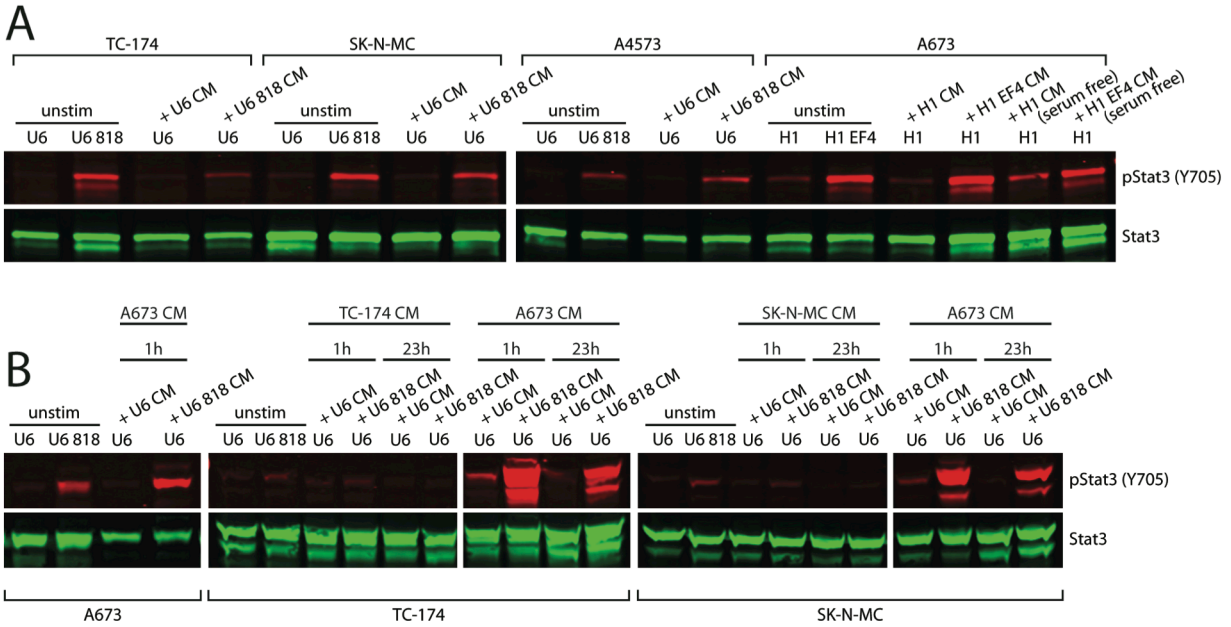


Figure 5-5. ESFT cells secrete a factor capable of stimulating Stat3 phosphorylation. (A,B) Immunoblot analysis of phospho-Stat3 (Y705) and total Stat3 in ESFT cells transduced with EWS/FLI1 shRNA (818 or EF4) or corresponding vector controls (U6 or H1) five days post lentiviral transduction, or ESFT cells transduced with vector controls that were stimulated with conditioned media from knock down or control cells for one hour (A) or one and 23 hours (B).

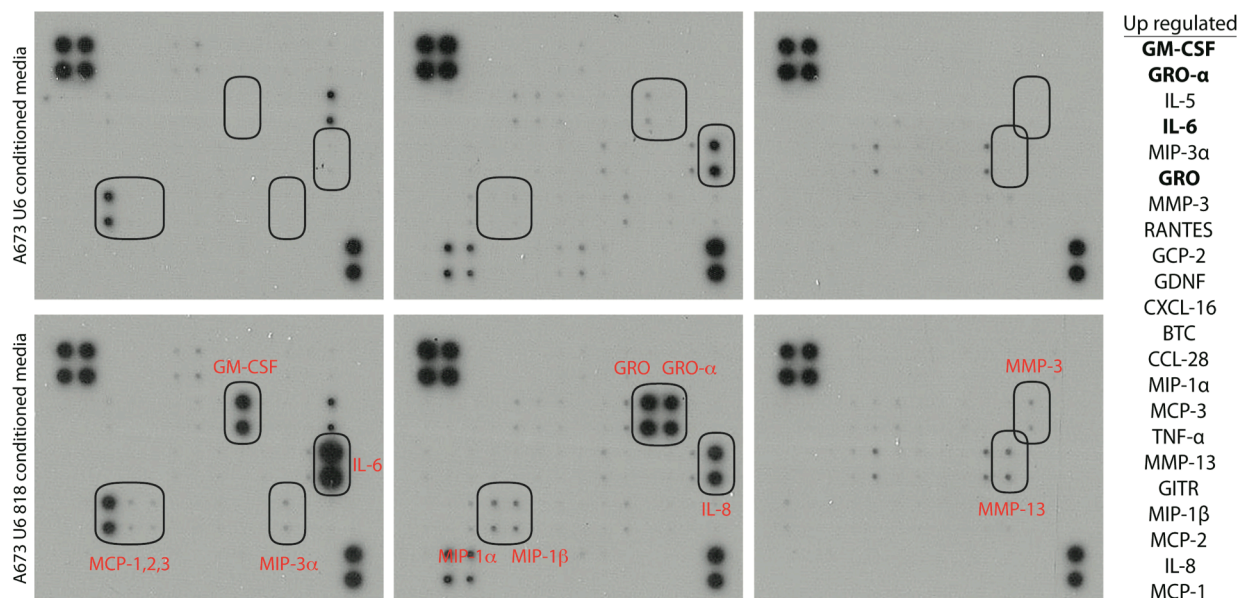


Figure 5-6. EWS/FLI1 knock down modulates levels of secreted factors. Cytokine array analysis of 174 growth factor and cytokines in conditioned media from A673 cells transduced with vector control (U6) and EWS/FLI1 shRNA (U6 818). Cells were transferred to serum-free media two days post lentiviral transduction and conditioned media was collected two days later. Selected growth factors that are up regulated upon EWS/FLI1 knock down are circled and labeled in red. A complete list of up regulated factors is displayed on the right, ordered by decreasing magnitude of fold change. Fold change was estimated for factors that did not display a signal above background for control conditioned media. Those that show the most dramatic increase are indicated in bold.

IL-6, GM-CSF, and CXCL1 are secreted by ESFT cells after EWS/FLI1 knock down. In order to determine which soluble factor(s) were responsible for the increase in phospho-Stat3, we used an antibody array to simultaneously measure 174 cytokines and growth factors in serum free conditioned media from A673 U6 and U6 818 cells. The majority of the factors showed little or no change upon EWS/FLI1 knock down, but a few displayed a dramatic increase in signal intensity. In particular, IL-6, GM-CSF, and CXCL1 (GRO- α) were present in much higher levels in the U6 818 conditioned media compared to that of U6 (Figure 5-6). To test which of these factors is able to activate Stat3, each protein was added to ESFT cells and phospho-Stat3 levels were compared to cells treated with U6 818 conditioned media. Only IL-6 was able to stimulate Stat3 phosphorylation, though not to the level of the conditioned media (Figure 5-7A). As IL-6 is known activator of Stat3, we chose to further investigate its role in ESFT signaling.

ELISA analysis was performed to validate the results of the cytokine array and quantitate the levels of IL-6 secreted by ESFT cells. Conditioned media from A4573 and A673 U6 818 cells contained elevated levels of IL-6 (Figure 5-7D). Furthermore, the concentration of IL-6 in the A673 conditioned media was in the nanogram range, which explains why cells treated with this media show such a strong up regulation of phospho-Stat3. There were also low levels IL-6 present in A673 U6 conditioned media harvested from cells that were serum starved.

Blocking IL-6 or gp130 inhibits up regulation of phospho-Stat3. To determine if IL-6 is necessary for Stat3 activation, we inhibited either the ligand or its receptor gp130. First, an IL-6 neutralization antibody was added to U6 818 conditioned media and subsequently immunoprecipitated. Immunodepletion of IL-6 was confirmed by ELISA (Figure 5-7E) and the media was added to untransduced cells. Resulting phospho-Stat3 levels were compared to cells treated with unmanipulated U6 or U6 818 conditioned media (Figure 5-7B). Especially in A673 cells, removing IL-6 prevents phosphorylation of Stat3. An analogous experiment was

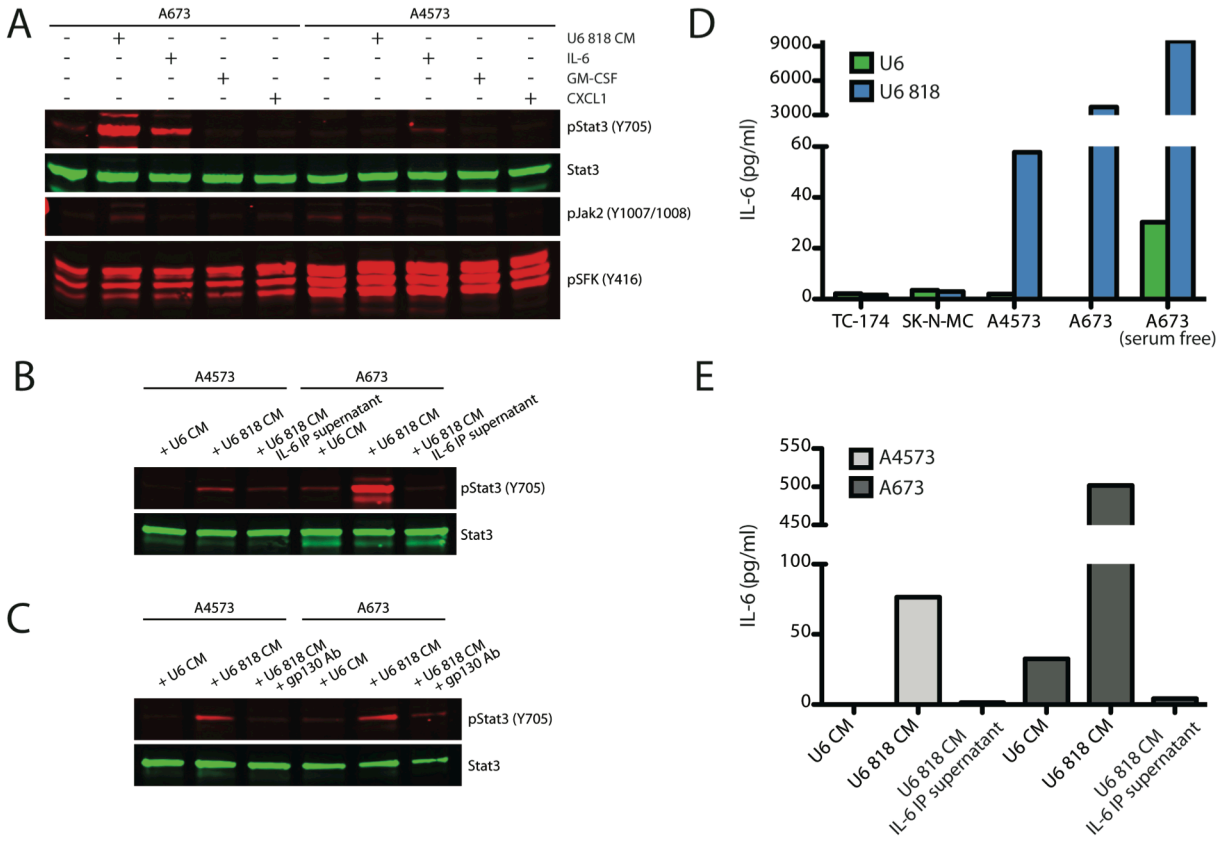


Figure 5-7. Stat3 phosphorylation after EWS/FLI1 down appears to be mediated primarily by IL-6 secretion. (A) Immunoblot analysis of phospho-Stat3 (Y705), total Stat3, phospho-Jak2 (Y1007/1008), and phospho-Src (Y416) in A673 and A4573 cells treated with conditioned media from cells transduced with EWS/FLI1 shRNA (U6 818 CM) or 50 ng/ml of human recombinant IL-6, GM-CSF, or CXCL1. The phospho-Src antibody recognizes multiple members of the Src family kinases (SFKs). (B) Immunoblot analysis of phospho-Stat3 (Y705) and total Stat3 in A4573 and A673 cells treated with conditioned media from cells transduced with vector control (U6 CM) or EWS/FLI1 shRNA (U6 818 CM), or U6 818 CM in which IL-6 has been removed by immunoprecipitation. A673 U6 818 CM was diluted 1:4 for this experiment. (C) Immunoblot analysis of phospho-Stat3 (Y705) and total Stat3 in A4573 and A673 cells treated with conditioned media from cells transduced with vector control (U6 CM) or EWS/FLI1 shRNA (U6 818 CM), or treated with U6 818 CM after a one hour incubation with gp130 blocking antibody. A673 U6 818 CM was diluted 1:10 for this experiment. (D) ELISA analysis of IL-6 levels in conditioned media from ESFT cells transduced with vector control (U6) or EWS/FLI1 knock down (U6 818). (E) ELISA analysis of IL-6 levels in conditioned media samples used to treat cells in B.

performed in which ESFT cells were pre-incubated with a gp130 neutralization antibody. U6 818 conditioned media was added to these cells as well as those that were not treated with the antibody. Evaluation of Stat3 phosphorylation revealed that blocking gp130 also inhibited up-regulation of phospho-Stat3 (Figure 5-7C). These results provide evidence that Stat3 is being activated in part through an IL-6 dependent mechanism.

Discussion

We utilized a global, unbiased approach to identify modulated signal transducers downstream of EWS/FLI1. Our results provided information on a network of proteins involved in ESFT pathogenesis, including Stat3. Tyrosine phosphoproteomics revealed Stat3 phosphorylation to be up regulated upon EWS/FLI1 knock down. We initially thought this occurred through direct regulation, but single cell studies uncovered a paracrine mechanism of Stat3 activation.

Stat3 is persistently activated in multiple malignancies and promotes tumorigenesis by up regulating cellular proliferation and survival factors as well as those that promote immunosuppression [30]. In ESFT, Stat3 is phosphorylated in approximately 50% of tumor samples in addition to multiple cell lines [31,32]. Specific inhibition of Stat3 by blocking phosphorylation was demonstrated to reduce tumor proliferation [31]. Our own experiments with a distinct Stat3 inhibitor corroborate these results (Figure 5-8B). Additional growth assays using a dominant negative construct also diminished ESFT cell growth. Furthermore, combined inhibition of Stat3 and EWS/FLI1 appeared to have an increased effect compared to targeting EWS/FLI1 alone (Figure 5-8D). However, this result was not statistically significant.

Initial studies concluded there was no connection between Stat3 and EWS/FLI1, as heterologous expression of the fusion failed to induce Stat3 phosphorylation [32]. Our own experiments may have also missed the link if we had obtained a homogeneous population after EWS/FLI1 knock down. However, due to the inefficiency of lentiviral transduction, we acquired a mixed population of ESFT cells with reduced and unchanged EWS/FLI1 expression. Initial

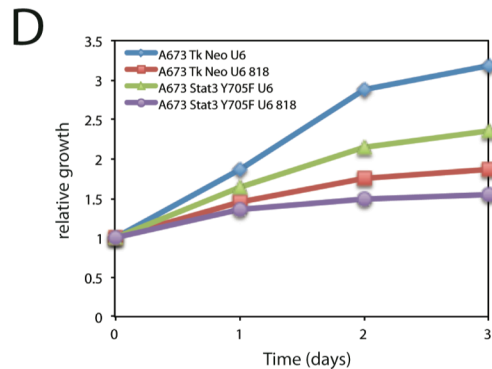
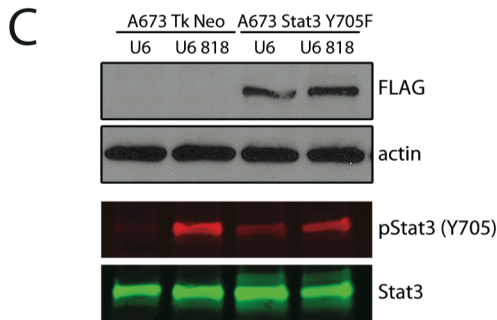
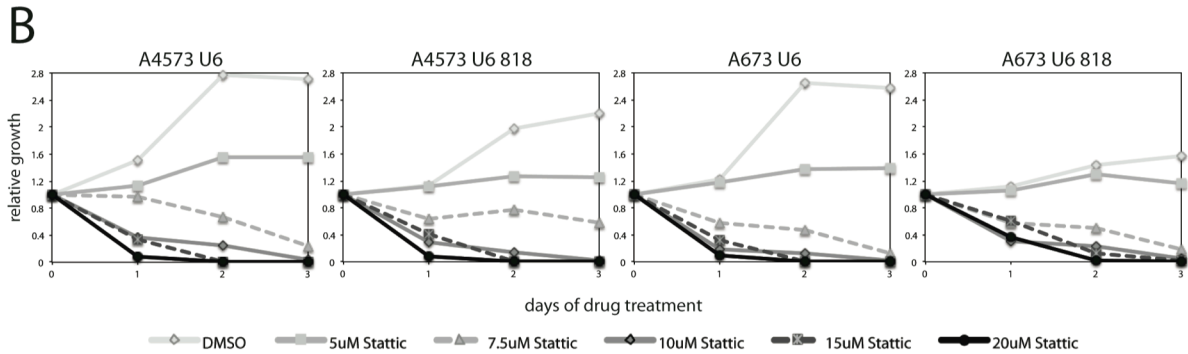
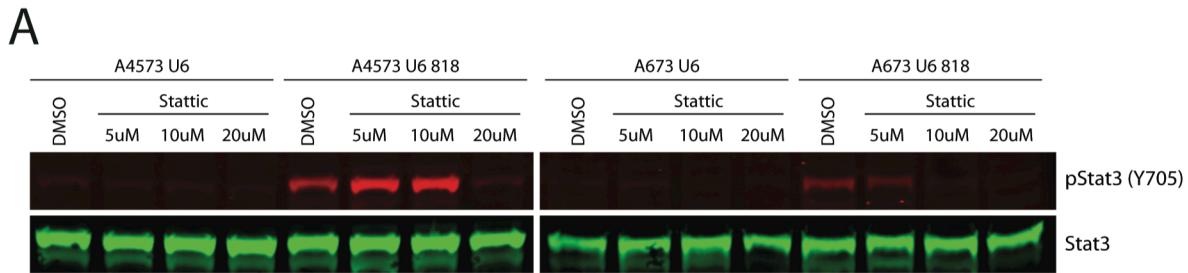


Figure 5-8. Stat3 small molecular inhibitor and dominant negative Stat3 decrease ESFT growth. (A) Immunoblot analysis of phospho-Stat3 and total Stat3 levels after treatment with DMSO or 5 μ M, 10 μ M, or 20 μ M Stattic for 3 hours. Cells were treated five days post lentiviral transduction. **(B)** Growth curves for ESFT EWS/FLI1 knock down (U6 818) and control (U6) cells treated with increasing concentrations of Stattic for 0 to 3 days. Cell growth was measured using an MTT assay. Absorbance values for each treatment condition were normalized to day 0 to assess relative growth. Data plotted is from one representative experiment. **(C)** Immunoblot analysis of FLAG, phospho-Stat3 (Y705), and total Stat3 levels to verify expression of exogenous, FLAG-tagged dominant negative Stat3 (Stat3 Y705F) construct used in part D. Stat3 Y705F was introduced into ESFT cells with a retroviral vector. Tk Neo is the corresponding empty vector control. **(D)** Growth curves for A673 cells transduced with EWS/FLI1 shRNA (U6 818), dominant negative Stat3 (Stat3 Y705F), or empty vector controls (U6, Tk Neo). Cell growth was measured using an MTT assay. Absorbance values for each treatment condition were normalized to day 0 to assess relative growth. Data plotted is from the average of five experiments.

immunoblot experiments were performed under the assumption of a uniform population, which led to the early conclusion of direct regulation of Stat3 by EWS/FLI1. It was not until immunofluorescence experiments were performed to observe Stat3 phosphorylation in individual cells that we realized discrete subsets displayed different levels of phospho-Stat3. This emphasizes the necessity for single cell studies when investigating tumor biology. Although the tumor heterogeneity observed in our experiments was created by targeting only a portion of ESFT cells, phospho-Stat3 immunohistochemical staining of tumors exhibited cell to cell variation [31,32], suggesting this heterogeneity may also exist *in vivo*.

Our results indicate that Stat3 is primarily activated by IL-6 secretion. However, although blocking IL-6 or gp130 caused decreased Stat3 phosphorylation when cells were treated with conditioned media, the signal was not completely abrogated. This argues that other secreted factors may play a role in Stat3 activation. The cytokine array results revealed multiple growth factors and cytokines that were up regulated upon EWS/FLI1 knock down. Some of these factors, such as IL-8, are known to be induced by IL-6 so may only be a secondary response. Although GM-CSF and CXCL1 do not appear to be able to stimulate Stat3 phosphorylation in ESFT cells, it is possible that the combination of other factors that display a less dramatic induction cooperate with IL-6 to mediate its effect.

Paracrine activation of Stat3 has been observed in breast cancer and glioblastoma. In breast cancer, cell lines that display higher levels of Stat3 phosphorylation are able to induce activation of Stat3 in those with previously undetectable phospho-Stat3 levels through the secretion of IL-6 [33]. Glioblastoma multiforme tumors contain subpopulations of cells that express either amplified or mutated epidermal growth factor receptors (EGFR). The heterogeneity of the tumor is maintained through IL-6 secretion by cells with mutated EGFR, which in turn activates Stat3 in amplified wild type EGFR-expressing cells and stimulates their proliferation [34]. This evidence that one population within a tumor is transmitting a mitogenic signal to another has implications for therapeutics.

Although most ESFT therapies do not target EWS/FLI1, there have been a few pre-clinical studies that aim to decrease its activity either through siRNA-mediated down regulation or inhibiting its interaction with a protein that enhances transcription [35,36]. The efficacy of this strategy would be decreased as cells that receive the therapy secrete factors that activate Stat3 in the remainder of the tumor. What remains to be addressed is if IL-6 secretion is specific to EWS/FLI1 targeting or is a general response to cell stress. Our ELISA results that demonstrate elevated IL-6 levels in serum starved A673 cells transduced with empty vector suggest it may be a general response. If other therapies also result in the secretion of IL-6, this could account for one mechanism of drug resistance. Further investigation is warranted to understand paracrine activation of Stat3 in ESFT to determine if combination therapy with Stat3 inhibitors would benefit the treatment of these tumors.

References

1. Arvand A, Denny CT. (2001) Biology of EWS/ETS fusions in Ewing's family tumors. *Oncogene*. **20**:5747-5754.
2. Ludwig JA. (2008) Ewing sarcoma: historical perspectives, current state-of-the-art, and opportunities for targeted therapy in the future. *Curr Opin Oncol*. **20**:412-418.
3. Lessnick SL, Braun BS, Denny CT, May WA. (1995) Multiple domains mediate transformation by the Ewing's sarcoma EWS/FLI-1 fusion gene. *Oncogene*. **10**:423-431.
4. Bailly RA, Bosselut R, Zucman J, Cormier F, Delattre O, Roussel M, Thomas G, Ghysdael J. (1994) DNA-binding and transcriptional activation properties of the EWS-FLI-1 fusion protein resulting from the t(11;22) translocation in Ewing sarcoma. *Mol Cell Biol*. **14**:3230-3241.
5. Hancock JD, Lessnick SL. (2008) A transcriptional profiling meta-analysis reveals a core EWS-FLI gene expression signature. *Cell Cycle*. **7**:250-256.
6. Kinsey M, Smith R, Iyer AK, McCabe ER, Lessnick SL. (2009) EWS/FLI and its downstream target NR0B1 interact directly to modulate transcription and oncogenesis in Ewing's sarcoma. *Cancer Res*. **69**:9047-9055.
7. Smith R, Owen LA, Trem DJ, Wong JS, Whangbo JS, Golub TR, Lessnick SL. (2006) Expression profiling of EWS/FLI identifies NKX2.2 as a critical target gene in Ewing's sarcoma. *Cancer Cell*. **9**:405-416.
8. Sanchez G, Bittencourt D, Laud K, Barbier J, Delattre O, Auboeuf D, Dutertre M. (2008) Alteration of cyclin D1 transcript elongation by a mutated transcription factor up-regulates the oncogenic D1b splice isoform in cancer. *Proc Natl Acad Sci U S A*. **105**:6004-6009.
9. Fuchs B, Inwards CY, Janknecht R. (2004) Vascular endothelial growth factor expression is up-regulated by EWS-ETS oncoproteins and Sp1 and may represent an independent predictor of survival in Ewing's sarcoma. *Clin Cancer Res*. **10**:1344-1353.
10. Potikyan G, Savene RO, Gauden JM, France KA, Zhou Z, Kleinerman ES, Lessnick SL, Denny CT. (2007) EWS/FLI1 regulates tumor angiogenesis in Ewing's sarcoma via suppression of thrombospondins. *Cancer Res*. **67**:6675-6684.
11. Prieur A, Tirode F, Cohen P, Delattre O. (2004) EWS/FLI-1 silencing and gene profiling of Ewing cells reveal downstream oncogenic pathways and a crucial role for repression of insulin-like growth factor binding protein 3. *Mol Cell Biol*. **24**:7275-7283.
12. Tirado OM, Mateo-Lozano S, Villar J, Dettin LE, Llorca A, Gallego S, Ban J, Kovar H, Notario V. (2006) Caveolin-1 (CAV1) is a target of EWS/FLI-1 and a key determinant of the oncogenic phenotype and tumorigenicity of Ewing's sarcoma cells. *Cancer Res*. **66**:9937-9947.
13. Chitnis MM, Yuen JSP, Protheroe AS, Pollak M, Macaulay VM. (2008) The type 1 insulin-like growth factor receptor pathway. *Clin Cancer Res*. **14**:6364-6370.

14. Scotlandi K, Picci P. (2008) Targeting insulin-like growth factor 1 receptor in sarcomas. *Curr Opin Oncol.* **20**:419-427.
15. Olmos D, Postel-Vinay S, Molife LR, Okuno SH, Schuetze SM, et al. (2010) Safety, pharmacokinetics, and preliminary activity of the anti-IGF-1R antibody figitumumab (CP-751,871) in patients with sarcoma and Ewing's sarcoma: a phase 1 expansion cohort study. *Lancet Oncol.* **11**:129-135.
16. Tolcher AW, Sarantopoulos J, Patnaik A, Papadopoulos K, Lin C-C, et al. (2009) Phase I, pharmacokinetic, and pharmacodynamic study of AMG 479, a fully human monoclonal antibody to insulin-like growth factor receptor 1. *J Clin Oncol.* **27**:5800-5807.
17. Beltran PJ, Chung Y-A, Moody G, Mitchell P, Cajulis E, Vonderfecht S, Kendall R, Radinsky R, Calzone FJ. (2011) Efficacy of ganitumab (AMG 479), alone and in combination with rapamycin, in Ewing's and osteogenic sarcoma models. *J Pharmacol Exp Ther.* **337**:644-654.
18. Subbiah V, Anderson P. (2011) Targeted Therapy of Ewing's Sarcoma. *Sarcoma.* **2011**:686985.
19. Ho AL, Schwartz GK. (2011) Targeting of insulin-like growth factor type 1 receptor in Ewing sarcoma: unfulfilled promise or a promising beginning? *J Clin Oncol.* **29**:4581-4583.
20. Choudhary C, Mann M. (2010) Decoding signalling networks by mass spectrometry-based proteomics. *Nat Rev Mol Cell Biol.* **11**:427-439.
21. Kolch W, Pitt A. (2010) Functional proteomics to dissect tyrosine kinase signalling pathways in cancer. *Nat Rev Cancer.* **10**:618-629.
22. Skaggs BJ, Gorre ME, Ryvkin A, Burgess MR, Xie Y, Han Y, Komisopoulou E, Brown LM, Loo JA, Landaw EM, Sawyers CL, Graeber TG. (2006) Phosphorylation of the ATP-binding loop directs oncogenicity of drug-resistant BCR-ABL mutants. *Proc Natl Acad Sci U S A.* **103**:19466-19471.
23. Zimman A, Chen SS, Komisopoulou E, Titz B, Martínez-Pinna R, Kafi A, Berliner JA, Graeber TG. (2010) Activation of aortic endothelial cells by oxidized phospholipids: a phosphoproteomic analysis. *J Proteome Res.* **9**:2812-2824.
24. Huang da W, Sherman BT, Lempicki RA. (2009) Bioinformatics enrichment tools: paths toward the comprehensive functional analysis of large gene lists. *Nucleic Acids Res.* **37**:1-13.
25. Huang da W, Sherman BT, Lempicki RA. (2009) Systematic and integrative analysis of large gene lists using DAVID bioinformatics resources. *Nat Protoc.* **4**:44-57.
26. Yu H, Jove R. (2004) The STATs of cancer — new molecular targets come of age. *Nat Rev Cancer.* **4**:97-105.

27. Levy DE, Darnell JE. (2002) Stats: transcriptional control and biological impact. *Nat Rev Mol Cell Biol.* **3**:651-662.
28. Li WX. (2008) Canonical and non-canonical JAK-STAT signaling. *Trends Cell Biol.* **18**:545-551.
29. Schulz KR, Danna EA, Krutzik PO, Nolan GP. (2012) Single-cell phospho-protein analysis by flow cytometry. *Curr Protoc Immunol.* **Chapter 8**:Unit 8 17 11-20.
30. Yu H, Pardoll D, Jove R. (2009) STATs in cancer inflammation and immunity: a leading role for STAT3. *Nat Rev Cancer.* **9**:798-809.
31. Behjati S, Basu BP, Wallace R, Bier N, Sebire N, Hasan F, Anderson J. (2012) STAT3 Regulates Proliferation and Immunogenicity of the Ewing Family of Tumors In Vitro. *Sarcoma.* **2012**:987239.
32. Lai R, Navid F, Rodriguez-Galindo C, Liu T, Fuller CE, Ganti R, Dien J, Dalton J, Billups C, Khoury JD. (2006) STAT3 is activated in a subset of the Ewing sarcoma family of tumours. *J Pathol.* **208**:624-632.
33. Lieblein JC, Ball S, Hutzen B, Sasser AK, Lin H-J, Huang TH, Hall BM, Lin J. (2008) STAT3 can be activated through paracrine signaling in breast epithelial cells. *BMC Cancer.* **8**:302.
34. Inda M-d-M, Bonavia R, Mukasa A, Narita Y, Sah DWY, Vandenberg S, Brennan C, Johns TG, Bachoo R, Hadwiger P, Tan P, DePinho RA, Cavenee W, Furnari F. (2010) Tumor heterogeneity is an active process maintained by a mutant EGFR-induced cytokine circuit in glioblastoma. *Genes Dev.* **24**:1731-1745.
35. Erkizan HV, Kong Y, Merchant M, Schlottmann S, Barber-Rotenberg JS, Yuan L, Abaan OD, Chou T-H, Dakshanamurthy S, Brown ML, Uren A, Toretsky JA. (2009) A small molecule blocking oncogenic protein EWS-FLI1 interaction with RNA helicase A inhibits growth of Ewing's sarcoma. *Nat Med.* **15**:750-756.
36. Hu-Lieskovan S, Heidel JD, Bartlett DW, Davis ME, Triche TJ. (2005) Sequence-specific knockdown of EWS-FLI1 by targeted, nonviral delivery of small interfering RNA inhibits tumor growth in a murine model of metastatic Ewing's sarcoma. *Cancer Res.* **65**:8984-8992.

CHAPTER 6
EWS/FLI1 MECHANISMS OF GENE REGULATION

Introduction

Transcriptional deregulation is a major mechanism underlying human oncogenesis. In some tumors, crucial transcription factors are inappropriately expressed. In other malignancies, chromosomal translocations juxtapose two normally distinct genomic loci and result in the expression of chimeric mRNAs and proteins. One example is the Ewing sarcoma family of tumors (ESFT), a pediatric cancer that invariably contains a fusion gene consisting of the N-terminus of EWS linked to the C-terminus of one of five ETS genes, FLI1 being the most common [1]. There is now a considerable body of data to suggest that EWS/ETS fusions play crucial roles in the genesis and maintenance of ESFT by acting as aberrant transcription factors. However, the mechanism of transcriptional regulation has not been elucidated.

The functional characterization of EWS/ETS fusions requires robust model systems in which to study gene regulation. Several EWS/ETS direct targets have been identified, including uridine phosphorylase (Upp) [2], thrombospondin 2 (Tsp2) [3], and insulin-like growth factor binding protein 3 (IGFBP3) [4]. Upp is up regulated by EWS/FLI1, while Tsp2 and IGFBP3 are down regulated. Quantitative real time PCR analysis displayed 10-300 fold modulation of these genes upon introduction of EWS/FLI1 into NIH-3T3 cells or siRNA-mediated knock down in ESFT cells. However, a model reporter consisting of the Upp promoter linked to the luciferase gene was up regulated only 2-3 fold [2]. Moreover, this poor response is not limited to just Upp. This same disparity between endogenous loci and model reporters has been seen with all the other EWS/FLI1 target genes that have been tested in this manner [3,5].

The lack of a robust functional assay to measure EWS/ETS transcriptional regulatory activity has been a major impediment to understanding how these fusions modulate target gene expression. In a perfect world, this would be accomplished using knock-in strategies at the genomic loci of endogenous target genes. However, the very low rates of homologous recombination in mammalian cells makes this unfeasible. On the other hand due to their limited size, standard reporter assays are readily modified and easily transduced into cells. But in

many instances, these reporters fail to accurately model their corresponding endogenous gene loci. We addressed this issue by developing a novel reporter model system using bacterial artificial chromosomes (BACs) as substrates. The BACs contain the entire genomic locus of EWS/ETS target genes as well as additional flanking sequence. Fluorescent reporter genes inserted within the BAC allow transcriptional activity to be assayed by flow cytometry.

In addition to measuring EWS/ETS target gene expression, functional information can be gained through mutational analysis of individual components of the fusion. Previous studies have shown both the EWS and FLI1 components of the fusion are required for oncogenic transformation of NIH-3T3 cells [6]. Further characterization of the FLI1 DNA binding domain revealed that mutation of specific residues that are necessary for DNA interaction results in reduced transforming activity in culture and loss of the ability to regulate known target genes [7]. EWS functional studies demonstrated that the tyrosine residues present within its repetitive activation domain are required for transcriptional activation and cellular transformation [8]. Although these experiments provided early mechanistic information, they were performed in heterologous cell types and focused on the role of EWS/ETS in transcription activation. We were able to add to this knowledge by studying the effects of EWS and FLI1 loss of function mutants on expression of a down-regulated target gene in their native context.

Results

BAC EWS/ETS target gene reporters only reflect two-fold modulation. BAC reporter constructs were generated in a previously engineered *E. coli* host that (i) has the λ phage RedET homologous recombination system under heat shock regulation and (ii) Cre recombinase under the control of an arabinose-inducible promoter [9]. Three BAC modifications were performed. First, a galK positive and negative selection system was utilized to seamlessly insert high turnover enhanced green fluorescent protein (EGFP) at the translational start site of EWS/ETS target genes [10]. This site was initially marked by knocking in the galK gene, which

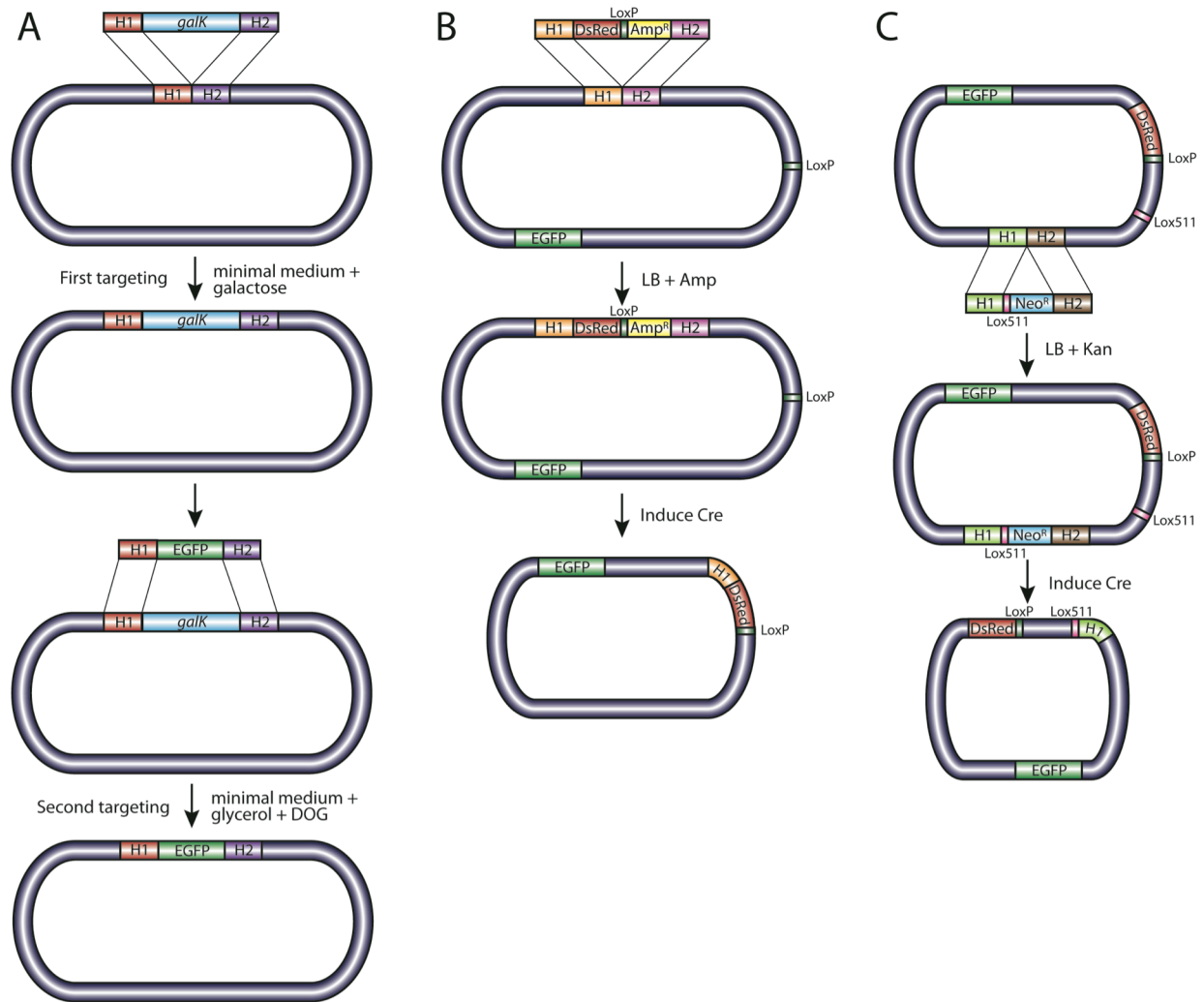


Figure 6-1. Schematic of recombination-mediated genetic engineering methods used to generate BAC reporter constructs. (A) EGFP insertion. *GalK* is inserted into the BAC at the EWS/ETS target gene transcription start site by homologous recombination. Recombinants are selected via growth on minimal media containing galactose. A second recombination is performed using the same regions of homology (H1 and H2) flanking EGFP, followed by growth on medium containing 2-deoxy-galactose (DOG). DOG is toxic to *galK* containing cells, which provides a selective advantage for cells that lack this gene and contain EGFP in its place. (B) DsRed insertion and 5' BAC shortening. Homologous recombination is used to insert DsRed followed by a LoxP site and ampicillin resistance gene. Recombinants are selected via growth on media containing ampicillin. After insertion, Cre is induced to generate recombination between the inserted LoxP site and the corresponding site in BAC vector backbone. This results in the removal of approximately 20kb from the 3' end of the target gene locus. (C) 3' BAC shortening. Similarly to B, a Lox511 site followed by a neomycin/kanamycin resistance gene is inserted by homologous recombination, but 3' of the target gene locus. Cre is induced to mediate recombination between the inserted and vector backbone Lox511 sites. This second size reduction shrinks the size of the BAC constructs to approximately 60kb.

allowed recombinants to grow on minimal media containing galactose. GalK was subsequently switched for GFP in a second recombination and recombinants were selected by resistance to 2-deoxy-galactose, a substrate that is toxic to galK expressing cells (Figure 6-1A). Next, a combination of DsRed insertion and 5' deletion was performed by knocking in a fragment containing the fluorescent reporter in addition to a LoxP site by RedET mediated site-specific recombination. Brief induction of Cre removed genomic segments lying between the inserted LoxP site and corresponding site present in the BAC vector backbone, resulting in deletion of the 5' genomic locus (Figure 6-1B). Insertion of a Lox511 site and deletion of sequence upstream of the 3' end of EWS/ETS target genes was performed in an analogous manner (Figure 6-1C).

These recombination strategies were applied to create five BAC reporter constructs for two EWS/ETS targets, Upp and Tsp2 (Figure 6-2). Initially, EGFP was inserted at the Upp transcriptional start site, followed by a PEST (proline, glutamic acid, serine, threonine) sequence to shorten its half-life via increased proteasomal degradation. Insertions were made with and without the addition of the SV40 polyA sequence following the EGFP stop codon to generate constructs that were either transcribed through only the GFP locus or through the entire Upp locus. Unfortunately, the construct lacking the polyA sequence was degraded by nonsense-mediated decay due to the presence of a premature stop codon, so only the construct containing the polyA sequence could be tested. To address this issue, we also generated Upp reporter constructs in which EGFP was fused to Upp in order to possess a reporter system that transcribes the entire Upp locus. Fusions were created with and without the PEST sequence in order to select a reporter with appropriate GFP intensity. Finally, a Tsp2 reporter was generated by inserting EGFP at the transcriptional start site, followed by a porcine teschovirus-1 2A (P2A) sequence [11]. This reporter allows for transcription through the Tsp2 locus, but separate translation of EGFP and Tsp2.

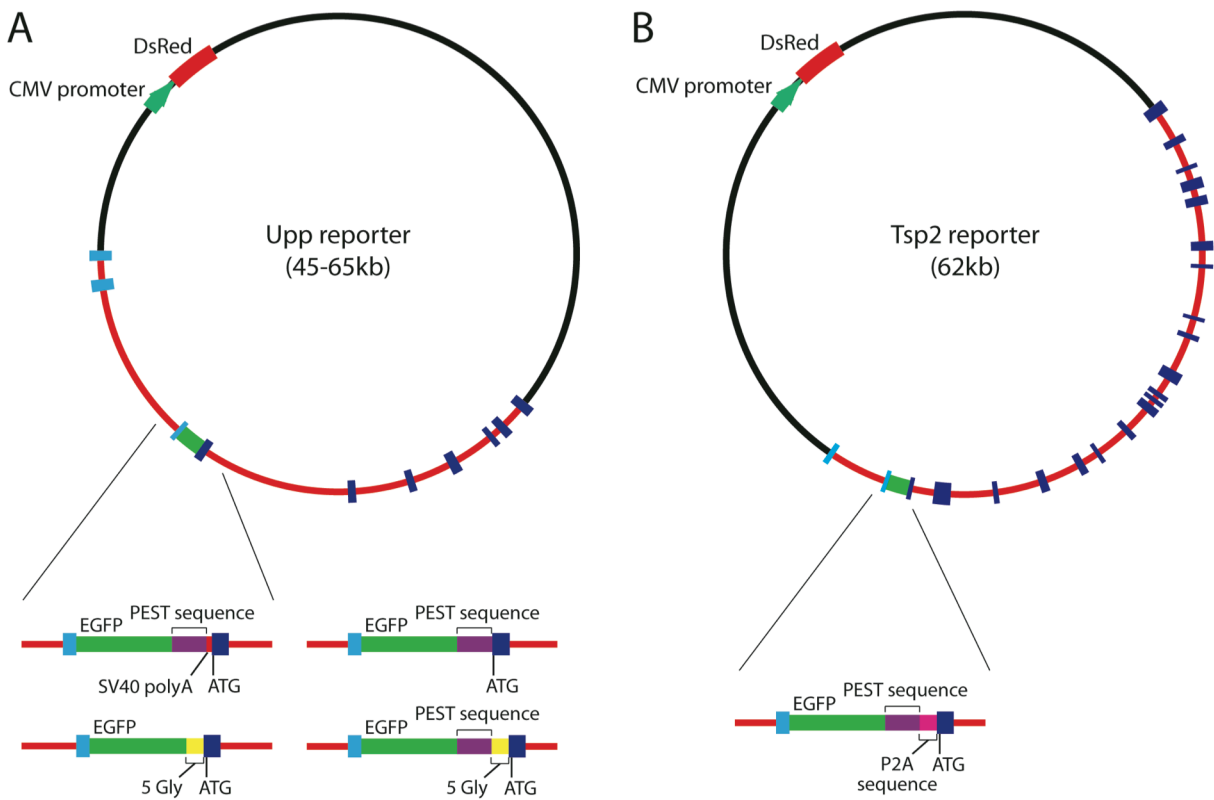


Figure 6-2. Schematic of BAC reporter constructs. (A) Upp reporter constructs. Four Upp constructs were generated. The first two integrated high turnover EGFP (EGFP followed by a PEST sequence) with and without the SV40 polyA sequence following the EGFP stop codon. The next two fused EGFP to Upp using a 5 glycine linker with or without a PEST sequence following EGFP. (B) Tsp2 reporter construct. EGFP was inserted at the Tsp2 transcription start site followed by a PEST sequence and P2A sequence. Upp and Tsp2 non-coding exons are indicated in light blue and coding exons are colored dark blue.

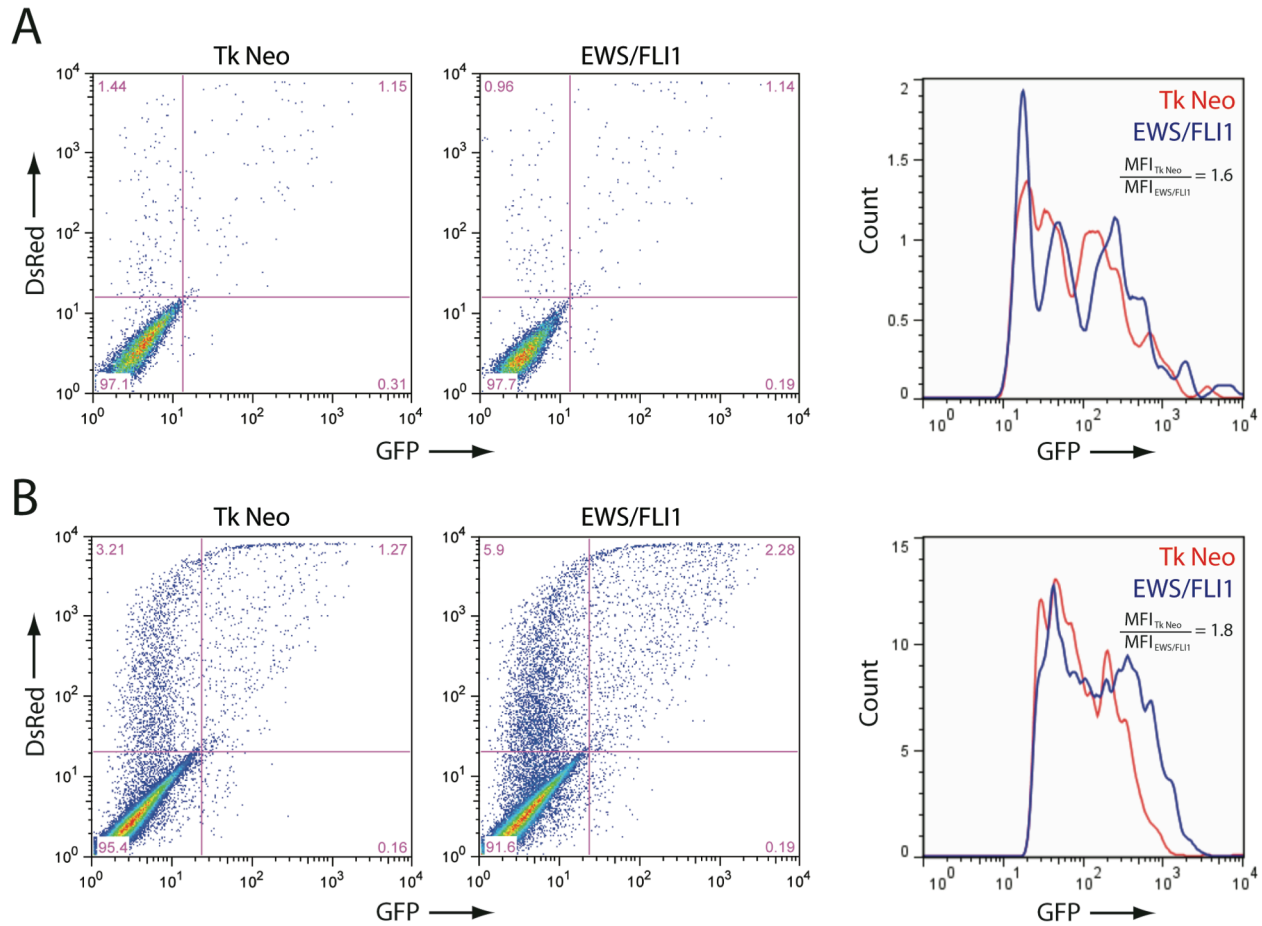


Figure 6-3. Upp reporters show approximately two-fold induction by EWS/FLI1. (A) Flow cytometry results of NIH-3T3 cells transduced with empty vector (Tk Neo) or EWS/FLI1 that were transiently transfected with the Upp reporter containing the SV40 polyA sequence following EGFP. 10,000 cells were analyzed for each cell type. A histogram was generated of the GFP fluorescent intensity of the DsRed, GFP double positive population. The mean fluorescence intensity ratio between Tk Neo and EWS/FLI1 cells is displayed on the graph. (B) Same as in A, except for the Upp reporter containing high turnover EGFP linked to Upp by five glycines was used for the analysis. Also, 50,000 cells were analyzed for each cell type.

After construction, BAC reporters were transiently transfected into NIH 3T3 cells with and without EWS/FLI1. The DsRed insertion made in the vector backbone served to monitor transfection efficiency since expression was driven by the constitutive CMV promoter and thus not dependent on EWS/FLI1 target gene expression. GFP fluorescence intensity provided readout for EWS/FLI1 modulation. Both DsRed and GFP intensity levels were measured by flow cytometry. Since the Upp reporters in which EGFP was inserted followed by a polyA site or fused to Upp displayed the highest GFP expression, these two reporters were analyzed by flow cytometry (Figure 6-3A,B). Unfortunately, EWS/FLI1 expression only increased GFP intensity by approximately 2-fold, which was the same response observed by standard reporter assays. We failed to achieve sufficient transfection of the Tsp2 reporter into NIH-3T3 cells so this construct was not assessed by flow cytometry.

Intact EWS and ETS domains are required for EWS/FLI1 repression of IGFBP3. Our BAC reporter experiments investigated EWS/FLI1 transcriptional regulation in a murine model of ESFT. We performed additional experiments in a native environment by utilizing siRNA knock down of EWS/FLI1. In order to investigate specific domains involved in EWS/FLI1-mediated transcriptional repression, we re-expressed wild type and mutant EWS/FLI1 in ESFT cells lacking endogenous fusion expression. Two mutant fusions were used, representing the loss of function of EWS or FLI1 domains, respectively. In EWS(DAF)/FLI1, critical tyrosine residues contained in the degenerate hexapeptide repeats of the EWS transcriptional activation domain are changed to alanine, resulting in a mutant that is defective in both transcriptional activation and cellular transformation [8]. The EWS/FLI1(TPM) mutant contains alterations of three amino acids within the FLI1 ETS domain: R337N, R340N, and Y341V. As a result, this mutant has lost the capacity to directly bind to DNA and to transform cells [7].

A673 cells were first transduced with lentiviruses containing a GFP expression construct and an shRNA (H1 EF4) that specifically targeted the 3' untranslated region found on

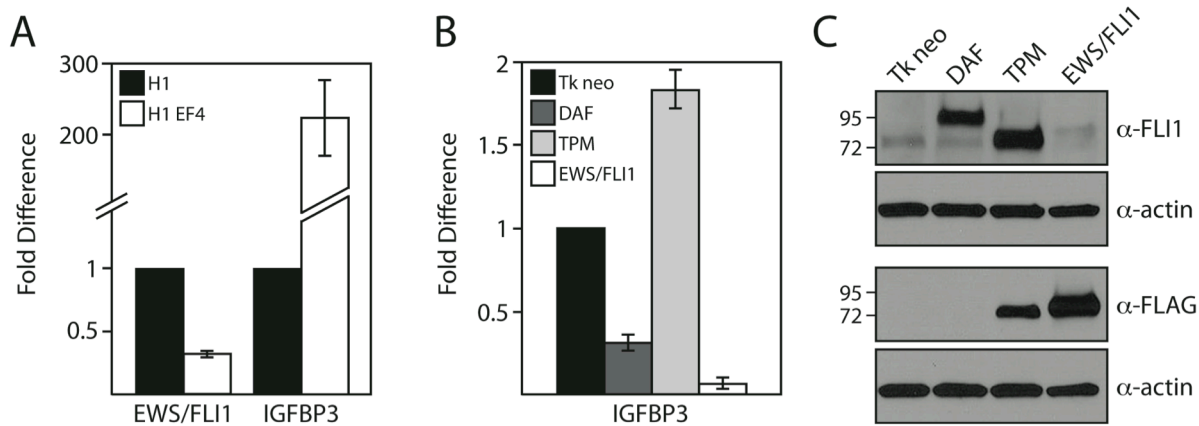


Figure 6-4. Re-expression of wild-type EWS/FLI1 and EWS mutant suppresses IGFBP3 expression, whereas introduction of the ETS domain mutant increases mRNA levels. (A) Mean difference in EWS/FLI1 and IGFBP3 levels by qRT-PCR analysis in A673 cells transduced with lentiviral shRNA against EWS/FLI1 (H1 EF4) or empty vector control (H1). Total RNA was harvested 14 days post-transduction. EWS/FLI1 and IGFBP3 qRT-PCR values were normalized to GAPDH. Error bars represent range of experimental values. **(B)** Mean difference in IGFBP3 mRNA levels by qRT-PCR analysis in A673 cells transduced with lentiviral shRNA against EWS/FLI1 (H1 EF4) and then transduced with retroviral empty vector (Tk neo), EWS mutant (DAF), FLAG-tagged ETS mutant (TPM), or triple FLAG-tagged wild-type EWS/FLI1. Levels are relative to A673 H1 EF4 cells transduced with retroviral empty vector. IGFBP3 qRT-PCR values were normalized to GAPDH. **(C)** FLI1 and FLAG immunoblot analysis of EWS/FLI1 levels in A673 cells transduced as described in B. Lysates were harvested 14 days post-lentiviral transduction. FLI1 immunoblot analysis reveals that exogenous EWS/FLI1 constructs display higher levels of expression than the endogenous protein. The higher wild-type EWS/FLI1 signal in the FLAG immunoblot analysis compared with the TPM mutant is due to the presence of a triple FLAG tag. The DAF mutant is not FLAG-tagged, therefore no signal is observed.

endogenous EWS/FLI1 transcripts but not on those from exogenous constructs [12]. Flow-sorted (>95% GFP-positive) polyclonal populations were expanded and transduced with amphotropic retroviruses containing intact or mutant EWS/FLI1. Cells transduced with either empty lentiviral (H1) or retroviral (Tk neo) vectors served as negative controls. After antibiotic selection, polyclonal populations were harvested for protein and total RNA. The expression of the EWS/FLI1 and IGFBP3 transcripts was determined using qRT-PCR. These experiments were repeated in duplicate starting from shRNA knockdown through IGFBP3 quantitation.

Transduction of the H1 EF4 shRNA construct resulted in an average 220-fold increase in IGFBP3 mRNA, which is similar to that found with the U6 818 shRNA (Figure 6-4A). Re-expression of wild-type EWS/FLI1 resulted in a 15-fold decrease in IGFBP3 mRNA levels compared with the Tk neo empty vector control, further validating that EWS/FLI1 transcriptionally represses this target gene (Fig. 6-4B). When the EWS(DAF)/FLI1 mutant was expressed, a 3-fold decrease in IGFBP3 mRNA levels was observed. In contrast, expression of the EWS/FLI1(TPM) mutant resulted in a 2-fold increase in IGFBP3 mRNA levels. Immunoblot analyses of transduced cells showed that mutant constructs were expressed at levels greater than wild-type EWS/FLI1, indicating that the loss of function seen with the mutant fusions was not simply due to protein instability (Fig. 6-4C). Together these data demonstrate that both the EWS and ETS domains are necessary for full down-regulation of IGFBP3 mRNA.

EWS/FLI1(TPM) mutant acts in a dominant negative fashion. In addition to revealing roles for both the EWS and FLI1 domains in IGFBP3 repression, our knock down re-expression studies suggested the EWS/FLI1(TPM) acts as a dominant negative. Upon introduction of this mutant, we detected not only a lack of repression, but also an increase in IGFBP3 mRNA levels (Figure 6-4B). Since these experiments were performed in the absence of endogenous EWS/FLI1, we also introduced the EWS/FLI1(TPM) into ESFT cells without prior EWS/FLI1

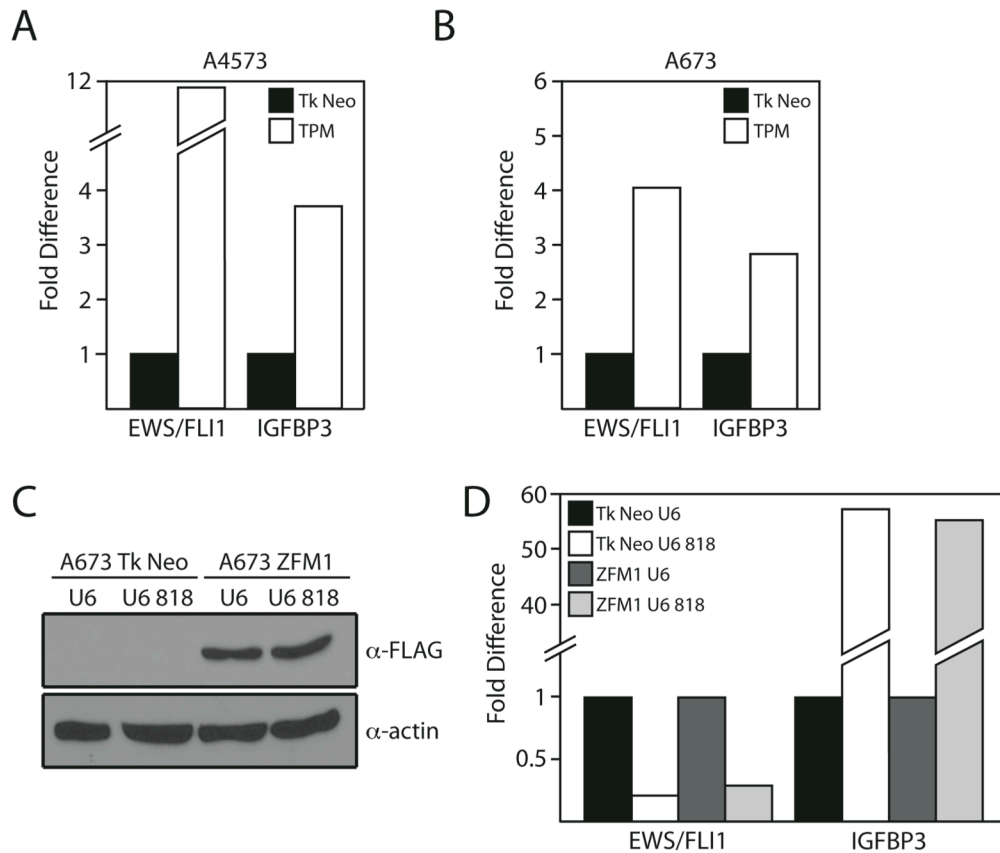


Figure 6-5. EWS/FLI1(TPM) elevates IGFBP3 transcript levels in the presence of the endogenous fusion. (A) Mean difference in EWS/FLI1 and IGFBP3 transcript levels by qRT-PCR analysis in A4573 cells transduced with EWS/FLI1 ETS mutant (TPM) or empty vector (Tk Neo). Total RNA was harvested 9 days post-transduction, including 7 days of selection with 450 μ g/ml G418. EWS/FLI1 and IGFBP3 qRT-PCR values were normalized to GAPDH. Data represents the average of two independent experiments. (B) Same as in A, except A673 cells were used. (C) Immunoblot analysis of A673 cells transduced with ZFM1 retrovirus or empty vector (Tk Neo), selected for 7 days with 450 μ g/ml G418, then transduced with lentiviral EWS/FLI1 shRNA (U6 818) or empty vector (U6). Cell lysates were collected 3 days post lentiviral transduction. (D) Mean difference in EWS/FLI1 and IGFBP3 transcript levels by qRT-PCR analysis in A673 cells transduced with ZFM1 or empty vector (Tk Neo), followed by transduction with EWS/FLI1 shRNA (U6 818) or empty vector (U6). Total RNA was harvested 3-7 days post lentiviral transduction. EWS/FLI1 and IGFBP3 qRT-PCR values were normalized to GAPDH. Data represents the average of three independent experiments.

knock down. The mutant elevated IGFBP3 levels even in the presence of the endogenous fusion, further validating its ability to act as a dominant negative (Figure 6-5A,B).

We hypothesize that the EWS/FLI1(TPM) raises IGFBP3 levels by sequestering factors that native EWS/FLI1 associates with to facilitate transcriptional repression. To further characterize this mechanism, we took a candidate approach to identify one of these factors. One possible mediator of EWS/FLI1 transcriptional repression is SF1 (splicing factor 1)/ZFM1 (zinc finger gene in MEN1 locus). ZFM1 interacts with EWS and ZFM1 overexpression represses EWS transactivation activity [13]. If ZFM1 contributes to EWS/FLI1 down regulation of IGFBP3, over expression in theory should aggravate this effect or counteract decreased EWS/FLI1 levels. As a result, we assayed for the ability of ZFM1 to compensate for lack of EWS/FLI1. A673 cells were transduced with retrovirus containing ZFM1 or empty vector (Tk Neo). After antibiotic selection, these cells were transduced with lentivirus containing EWS/FLI1 shRNA (U6 818) or empty vector control (U6). The ability of siRNA-mediated knock down to affect EWS/FLI1 transcriptional repression of IGFBP3 was compared in cells with and without ZFM1. Initial experiments demonstrated higher levels of repression of IGFBP3 in the presence of ZFM1, indicating this protein might facilitate EWS/FLI1 transcriptional repression. However, additional replicates did not display this response (Figure 6-5B).

Discussion

Despite the hopes that our BAC reporter system could more accurately reflect endogenous gene regulation, we observed a response similar to traditional reporter assays. In the case of the Upp reporter with the polyA sequence inserted after GFP, this model only measured EWS/FLI1 modulation of Upp at the level of transcriptional initiation. Other studies performed in our lab demonstrated there was no difference in RNA polymerase II (Pol II) occupancy at the Upp promoter in the absence and presence of EWS/FLI1 [14]. This suggests EWS/FLI1 regulation of Upp occurs at a later stage of transcription, which indicated our GFP-Upp fusion

might serve as a better reporter. Regrettably, it displayed the same results as the previous reporter construct. At the time these assays were performed, qRT-PCR measured only a 4-fold induction of Upp by EWS/FLI1 as opposed to the previous 8-10 fold increase. This smaller dynamic range might contribute to the limited response we observed with our BAC reporter. Additionally, the stability of the GFP-Upp fusion may also affect GFP intensity levels, decreasing the sensitivity of our assay. To address these issues, we shifted focus to a different target gene, Tsp2, which is down regulated approximately 30 fold by EWS/FLI1. Additionally, we inserted a viral P2A sequence in between GFP and Tsp2, so although one transcript is generated, the proteins are translated independently. Having a larger dynamic range without the technical obstacles of a fusion protein, we hoped to have created a more efficient reporter. However, technical difficulties with transient transfection methods prevented us from testing this construct.

The obstacles encountered with our BAC reporters were due in part to construct design and technical difficulties with our model system, but may also be due to their failure to accurately portray endogenous conditions. This system was chosen because BACs are large enough to harbor entire genomic loci plus flanking sequence. Furthermore, unlike plasmids, BACs are associated with chromatin, which makes this method of gene expression more similar to that of the native locus. However, in our shortening of the BAC constructs to increase transfection efficiency, we might have deleted sequence required for the action of distant regulatory elements. Despite the advantages of a BAC system, it appears target genes are best studied at the endogenous locus due to the multitude of mechanisms involved in EWS/FLI1 regulation [14]. The reason this approach was not previously taken is the difficulty of genomic manipulation. However, recent advances in protocols utilizing zinc-finger nucleases (ZFNs) provide a method to generate an endogenous reporter system [15]. ZFNs increase the efficiency of homologous recombination to achieve site-specific genomic modifications. Recently, this approach has been used to integrate an EGFP reporter at the endogenous PIG-A

locus in both human embryonic and human induced pluripotent stem cells [16]. These results suggest this is a feasible method to generate endogenous EWS/FLI1 target gene reporters.

Our mechanistic studies demonstrated the loss of repression of IGFBP3 in A673 cells expressing an shRNA construct targeting endogenous EWS/FLI1 can be re-established by transducing EWS/ FLI1, which drives down IGFBP3 mRNA levels. However, neither transduction of EWS nor ETS EWS/FLI1 mutants was able to fully repress IGFBP3 to the extent seen with the wild-type fusion. This suggests that both these domains play functional roles in this process, perhaps by promoting protein-protein and DNA binding interactions through the EWS and ETS domains, respectively. The fact that IGFBP3 levels consistently increased in cells transduced with the EWS/FLI1(TPM) construct also suggests that this mutant might be acting in a dominant negative fashion by sequestering factors involved with EWS/FLI1 target gene repression. Introduction of the EWS/FLI1(TPM) into ESFT cells with native EWS/FLI1 levels corroborated our dominant negative theory. However, the mechanism through which this occurs is still unknown as the one candidate we tested did not appear to mediate EWS/FLI1 regulation of IGFBP3. An unbiased approach should be taken to uncover proteins that associate with EWS/FLI1 to confer transcriptional repression. Although co-immunoprecipitation studies of wild-type EWS/FLI1 have been unsuccessful, it is possible potential proteins may have a stronger interaction with the EWS/FLI1(TPM) based on its ability to act as a dominant negative. Candidates identified as a result of this analysis would provide further insight into mechanisms of EWS/FLI1 regulation of down regulated target genes.

References

1. Arvand A, Denny CT. (2001) Biology of EWS/ETS fusions in Ewing's family tumors. *Oncogene*. **20**:5747-5754.
2. Deneen B, Hamidi H, Denny CT. (2003) Functional analysis of the EWS/ETS target gene uridine phosphorylase. *Cancer Res*. **63**:4268-4274.
3. Potikyan G, Savene RO, Gaulden JM, France KA, Zhou Z, Kleinerman ES, Lessnick SL, Denny CT. (2007) EWS/FLI1 regulates tumor angiogenesis in Ewing's sarcoma via suppression of thrombospondins. *Cancer Res*. **67**:6675-6684.
4. Prieur A, Tirode F, Cohen P, Delattre O. (2004) EWS/FLI-1 silencing and gene profiling of Ewing cells reveal downstream oncogenic pathways and a crucial role for repression of insulin-like growth factor binding protein 3. *Mol Cell Biol*. **24**:7275-7283.
5. Tirado OM, Mateo-Lozano S, Villar J, Dettin LE, Llorca A, Gallego S, Ban J, Kovar H, Notario V. (2006) Caveolin-1 (CAV1) is a target of EWS/FLI-1 and a key determinant of the oncogenic phenotype and tumorigenicity of Ewing's sarcoma cells. *Cancer Res*. **66**:9937-9947.
6. May WA, Gishizky ML, Lessnick SL, Lunsford LB, Lewis BC, Delattre O, Zucman J, Thomas G, Denny CT. (1993) Ewing sarcoma 11;22 translocation produces a chimeric transcription factor that requires the DNA-binding domain encoded by FLI1 for transformation. *Proc Natl Acad Sci U S A*. **90**:5752-5756.
7. Welford SM, Hebert SP, Deneen B, Arvand A, Denny CT. (2001) DNA binding domain-independent pathways are involved in EWS/FLI1-mediated oncogenesis. *J Biol Chem*. **276**:41977-41984.
8. Ng KP, Potikyan G, Savene RO, Denny CT, Uversky VN, Lee KAW. (2007) Multiple aromatic side chains within a disordered structure are critical for transcription and transforming activity of EWS family oncoproteins. *Proc Natl Acad Sci U S A*. **104**:479-484.
9. Copeland NG, Jenkins NA, Court DL. (2001) Recombineering: a powerful new tool for mouse functional genomics. *Nat Rev Genet*. **2**:769-779.
10. Warming S, Costantino N, Court DL, Jenkins NA, Copeland NG. (2005) Simple and highly efficient BAC recombineering using galK selection. *Nucleic Acids Res*. **33**:e36.
11. de Felipe P, Luke GA, Hughes LE, Gani D, Halpin C, Ryan MD. (2006) E unum pluribus: multiple proteins from a self-processing polyprotein. *Trends Biotechnol*. **24**:68-75.
12. Smith R, Owen LA, Trem DJ, Wong JS, Whangbo JS, Golub TR, Lessnick SL. (2006) Expression profiling of EWS/FLI identifies NKX2.2 as a critical target gene in Ewing's sarcoma. *Cancer Cell*. **9**:405-416.
13. Zhang D, Paley AJ, Childs G. (1998) The transcriptional repressor ZFM1 interacts with and modulates the ability of EWS to activate transcription. *J Biol Chem*. **273**:18086-18091.

14. France KA, Anderson JL, Park A, Denny CT. (2011) Oncogenic fusion protein EWS/FLI1 down-regulates gene expression by both transcriptional and posttranscriptional mechanisms. *J Biol Chem.* **286**:22750-22757.
15. Carroll D. (2008) Progress and prospects: zinc-finger nucleases as gene therapy agents. *Gene Ther.* **15**:1463-1468.
16. Zou J, Maeder ML, Mali P, Pruetz-Miller SM, Thibodeau-Beganny S, Chou BK, Chen G, Ye Z, Park IH, Daley GQ, Porteus MH, Joung JK, Cheng L. (2009) Gene targeting of a disease-related gene in human induced pluripotent stem and embryonic stem cells. *Cell Stem Cell.* **5**:97-110.

CHAPTER 7
CONCLUSIONS AND FUTURE DIRECTIONS

Summary

ESFT is a group of bone and soft tissue neoplasms distinguished by pathognomonic chromosomal translocations. The genetic rearrangement produces an EWS/ETS fusion protein that primarily acts as an aberrant transcription factor. EWS/ETS modulation of gene expression coupled with increased IGF1 signaling promotes tumorigenesis. As this family of malignancies is beset with low survival rates, especially for recurrent and metastatic cases, novel therapeutic strategies are urgently needed. To address this issue, this dissertation investigated the molecular basis of the disease by analyzing modulated signal transduction networks. The study was separated into two components: IGF1 and EWS/FLI1 downstream signaling. A global, unbiased approach revealed novel components of ESFT signaling as well as a paracrine signaling mechanism that may have implications for current treatments.

Chapter 4 describes the results of system-wide phosphotyrosine profiling downstream of IGF1. ESFT cells were treated with IGF1 or the IGF1R inhibitor AMG-479 and changes in global tyrosine phosphorylation levels were measured using quantitative, label-free mass spectrometry. In addition to identifying modulated proteins, this analysis also uncovered phosphopeptides whose intensity remained constant after treatment. A large portion of the group included members of Eph family of receptor tyrosine kinases. Subsequent analysis revealed broad expression of the EphA2 and EphB4 receptors among ESFT cell lines. However, phospho-specific examination showed the receptors were only phosphorylated at low levels. Although ligand-driven forward signaling does not appear to be occurring, this does not mean Eph signaling does not contribute to tumorigenesis. Low levels of Eph phosphorylation have been observed in other neoplasms in which crosstalk with other signaling pathways drives tumor progression. Further investigation is required to ascertain how Eph signaling affects ESFT pathogenesis. Additionally, detection of modulated upstream regulators and enriched residue patterns that are associated with Src substrates suggest a role for Src family kinases

(SFKs). SFK signaling appears to be coupled to that of IGF1, as the receptor tyrosine phosphatase PTRPA displays increased activity in response to IGF1. SFKs also show modulation upon IGF1 treatment, though this response only occurs in a subset of ESFT cell lines.

Chapter 5 describes the results of global phosphoproteomics downstream of EWS/FLI1. The ESFT cell line A673 was transduced with lentivirus containing EWS/FLI1 shRNA or empty vector. After enrichment for either phosphotyrosine or phosphoserine/threonine, peptides were identified and quantified by tandem mass spectrometry. The most dramatic response uncovered by these analyses was a large up regulation of phospho-Stat3 upon EWS/FLI1 knock down. Further investigation revealed this occurs in a subset of cells untransduced by the lentiviral shRNA construct, indicating EWS/FLI1 modulation of Stat3 occurs through a paracrine mechanism. Analysis of secreted factors demonstrated that ESFT cells emit IL-6 upon EWS/FLI1 knock down, which activates Stat3 through binding to the gp130 receptor.

Conclusions and Future Directions

Our investigation began with a system-wide, unbiased experiment to study cell signaling in ESFT. This led to the discovery of previously undescribed regulators that would have been missed if a directed approach had been taken. Furthermore, a high-throughput technique was able to pinpoint a single response that led to the elucidation of a paracrine signaling mechanism. These results affirm the benefits of using quantitative mass spectrometry to study oncogenic signaling.

Our analyses of the IGF1 and EWS/FLI1 phosphoproteomics data sets have so far focused on individual components. We have presented evidence supporting the involvement of Eph kinases, Src family kinases, and Stat3 in ESFT biology. However, a network analysis is necessary to fully extract all the information contained in the data. Preliminary efforts have been made with initial IGF1 phosphotyrosine profiling data set, but components still need to be

added that were identified as being modulated by AMG-479. The large size of the EWS/FLI1 phosphoserine/threonine profiling data set has made it difficult to construct a network that connects all of the components, so future plans include overlaying nodes with enriched pathways identified by the DAVID analysis. Starting with members of known signaling networks will allow for the construction of a core network that can then be built upon by assessing individual connections with databases such as STRING [1] and NetworKIN [2]. Complete networks of modulated components downstream of IGF1 and EWS/FLI1 can aid in classifying elements that are restricted to one network or are regulated by both proteins. Additionally, a system view of ESFT signaling can provide further insight into the biology of the tumor.

Although we have uncovered a paracrine signaling pathway that activates Stat3 in ESFT, we have yet to elucidate the biological consequences of this activation. As Stat3 is known to increase cell survival and proliferation, we hypothesize the population of ESFT that displays increased phosphorylation possesses a growth advantage over the remaining cells. This can be tested in multiple ways. The simplest approach entails analysis of GFP positive and negative populations at multiple time points after lentiviral shRNA transduction. If the untransduced cells, which contain higher levels of phospho-Stat3, are proliferating at a faster rate, we would expect to see an increase in the GFP negative population over time. However, this population shift may not be due to the increase in proliferation of the untransduced cells but the decrease in growth rate from cells affected by EWS/FLI1 inhibition. EWS/FLI1 knock down typically results in growth arrest of ESFT cells [3], except for the A673 cell line. But although this cell line continues to proliferate with decreased EWS/FLI1 expression, its growth rate is slowed compared to cells transduced with empty vector. An alternative strategy would be to treat cells with conditioned media obtained from knock down cells and compare their growth to untreated cells. Measurement of growth in culture as well as anchorage independent growth can assess both proliferation and tumorigenic potential. Additionally, wound healing assays can be performed to measure cell migration as well as proliferation.

We have shown that Stat3 can be activated through a paracrine mechanism, but we have not ruled out that autocrine activation can also occur. Our phospho-flow data demonstrated that A673 cells that have undergone EWS/FLI1 knock down do display an increase in phospho-Stat3 levels, just not to the extent of the untransduced cells. Preliminary immunoblot analysis showed a decrease in phospho-Jak2 and phospho-Src family kinases after EWS/FLI1 knock down, which suggests autocrine Stat3 activation may be diminished due to decreased activity of the upstream kinase. However, stimulating ESFT cells with U6 818 conditioned media or IL-6 only caused a minor increase in phospho-Jak2 and did not modulate phospho-Src. This data argues against the involvement of these proteins in paracrine Stat3 activation, so it is unclear whether their decreased phosphorylation levels after EWS/FLI1 knock down affect autocrine activation of Stat3. Before experiments can be performed to ascertain the reason EWS/FLI1 knock down prevents autocrine Stat3 activation, more work needs to be done to uncover the kinase upstream of Stat3. Targeting potential kinases either with small molecular inhibitors or siRNA and measuring subsequent Stat3 activation can provide more definitive evidence on which protein phosphorylates Stat3.

A more clinically relevant question is whether IL-6 secretion upon EWS/FLI1 knock down is specific to this targeting or is a general stress response observed in ESFT. One study demonstrated siRNA targeting of IGF1R in a murine breast cancer cell line results in the production of TNF- α (tumor necrosis factor alpha) and INF- γ (interferon gamma) [4]. This provides an additional example of the secretion of pro-inflammatory cytokines as a response to siRNA therapy. In ESFT, treatment with a Stat3 inhibitor mainly decreased cytokine secretion, except for IL-8, another factor that contributes to inflammation [5]. Additionally, we have observed IL-6 secretion in serum starved A673 cells transduced only with empty vector. This evidence suggests stressing ESFT cells by methods other than inhibiting EWS/FLI1 may also result in cytokine production. We are particularly interested in response to chemotherapeutic agents and IGF1R inhibitors and plan to investigate IL-6 secretion after treatment with these

drugs in the near future. If we do see an increase in IL-6 levels due to these therapies, our next step will be to investigate the possible benefit of combination therapy with Stat3 inhibitors. Furthermore, measurement of IL-6 levels in patient tumor samples can aid in ascertaining the clinical relevance of cytokine secretion in ESFT.

Another point of interest is the mechanism in which down regulation of EWS/FLI1 results in the secretion of inflammatory cytokines. There is a large body of data linking cancer and inflammation [6-8]. In particular, dominant oncogenes such as RAS [9] and MYC [10] induce the production of inflammatory chemokines and cytokines. However, to our knowledge, there is no evidence of activating this response by inhibiting an oncogene.

One of the key proteins involved in cancer-related inflammation is NF- κ B [6,8,11]. NF- κ B regulates the expression of many inflammatory cytokines, such as IL-6 and IL-8 [8]. If EWS/FLI1 represses NF- κ B, then siRNA-mediated release of this inhibition may result in higher IL-6 levels. Investigation of the relationship between EWS/FLI1 and NF- κ B is warranted to further elucidate the mechanism in which ESFT cells secrete inflammatory cytokines.

Additionally, we would like to ascertain if IL-6 secretion in response to oncogene inhibition is specific to ESFT. If other neoplasms such as Ras-driven tumors or other fusion-associated sarcomas possess a similar response, this may provide a novel connection between cancer and inflammation.

Of the results presented in this dissertation, paracrine activation of Stat3 appears to be the most clinically relevant. The future studies described here will aid in characterizing this mechanism in ESFT and potentially other malignancies, allowing for the development of new therapeutic strategies.

References

1. Jensen LJ, Kuhn M, Stark M, Chaffron S, Creevey C, Muller J, Doerks T, Julien P, Roth A, Simonovic M, Bork P, von Mering C. (2009) STRING 8--a global view on proteins and their functional interactions in 630 organisms. *Nucleic Acids Res.* **37**:D412-416.
2. Linding R, Jensen LJ, Pasculescu A, Olhovsky M, Colwill K, Bork P, Yaffe MB, Pawson T. (2008) NetworKIN: a resource for exploring cellular phosphorylation networks. *Nucleic Acids Res.* **36**:D695-699.
3. Potikyan G, France KA, Carlson MR, Dong J, Nelson SF, Denny CT. (2008) Genetically defined EWS/FLI1 model system suggests mesenchymal origin of Ewing's family tumors. *Lab Invest.* **88**:1291-1302.
4. Durfort T, Tkach M, Meschaninova MI, Rivas MA, Elizalde PV, Venyaminova AG, Schillaci R, Francois JC. (2012) Small interfering RNA targeted to IGF-IR delays tumor growth and induces proinflammatory cytokines in a mouse breast cancer model. *PLoS ONE.* **7**:e29213.
5. Behjati S, Basu BP, Wallace R, Bier N, Sebire N, Hasan F, Anderson J. (2012) STAT3 Regulates Proliferation and Immunogenicity of the Ewing Family of Tumors In Vitro. *Sarcoma.* **2012**:987239.
6. Mantovani A, Allavena P, Sica A, Balkwill F. (2008) Cancer-related inflammation. *Nature.* **454**:436-444.
7. Yu H, Kortylewski M, Pardoll D. (2007) Crosstalk between cancer and immune cells: role of STAT3 in the tumour microenvironment. *Nat Rev Immunol.* **7**:41-51.
8. Yu H, Pardoll D, Jove R. (2009) STATs in cancer inflammation and immunity: a leading role for STAT3. *Nat Rev Cancer.* **9**:798-809.
9. Sparmann A, Bar-Sagi D. (2004) Ras-induced interleukin-8 expression plays a critical role in tumor growth and angiogenesis. *Cancer Cell.* **6**:447-458.
10. Shchors K, Shchors E, Rostker F, Lawlor ER, Brown-Swigart L, Evan GI. (2006) The Myc-dependent angiogenic switch in tumors is mediated by interleukin 1beta. *Genes Dev.* **20**:2527-2538.
11. Bollrath J, Greten FR. (2009) IKK/NF-kappaB and STAT3 pathways: central signalling hubs in inflammation-mediated tumour promotion and metastasis. *EMBO Rep.* **10**:1314-1319.